

Supporting Information  
for

**Synthesis of Heteroleptic Phosphine-copper(I) Complexes: Fluorescent Sensing  
and Catalytic Properties**

Chen-Lin Luo,<sup>a,#</sup> Chu-Xing Hu,<sup>a,#</sup> Ping Shang,<sup>a,\*</sup> Guan-Zhao, Wen,<sup>d</sup> Jia-Jun Zhu,<sup>a</sup>  
Ya-Hui Xuan,<sup>a</sup> Bang-Lian Xia,<sup>a</sup> Yu-Chen Liu,<sup>a</sup> Zi-Hao Jiang,<sup>a</sup> Geng, Dong,<sup>c</sup> Liu-  
Cheng Gui,<sup>b,\*</sup> Xuan-Feng Jiang<sup>a,e,\*</sup>

<sup>a</sup> Key Laboratory of Green Preparation and Application for Functional Materials,  
Ministry of Education, Hubei Key Laboratory of Polymer Science, School of Materials  
Science and Engineering, Hubei University, Wuhan, Hubei, 430062, P. R. China

<sup>b</sup> State Key Laboratory for the Chemistry and Molecular Engineering of Medicinal  
Resources, School of Chemistry & Pharmaceutical Sciences, Guangxi Normal  
University, Guilin, Guangxi, 541004, P. R. China.

<sup>c</sup> Medical Informatics Research Center, Shantou University Medical College, Shantou  
515041, China.

<sup>d</sup> School of Physics and Materials Science, Guangzhou University, GuangZhou,  
510006, China.

<sup>e</sup> Hubei Key Laboratory of Processing and Application of Catalytic materials,  
Huanggang Normal University, Huanggang, Hubei, 438000, P. R. China

*To whom correspondence should be addressed.*

*E-mail:* pingshang02@126.com; guiliucheng2000@163.com;  
[xuanfengjiang@hubu.edu.cn](mailto:xuanfengjiang@hubu.edu.cn)

## Table of Contents

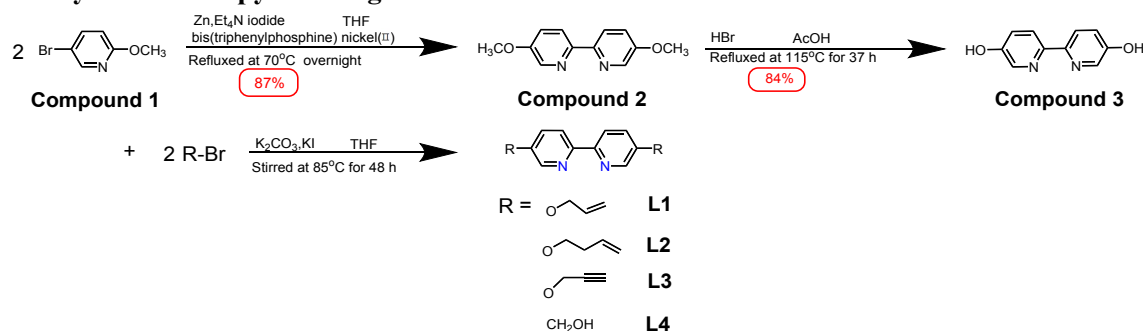
<b>S1. General Information .....</b>	<b>2</b>
<b>S2. Synthesis of bipyridine ligands.....</b>	<b>2</b>
<b>S3. The synthesis pathway of heteroleptic Cu(I) complexes C1-C10.....</b>	<b>11</b>
<b>S4. X-ray crystallography of clusters C1, C2, C5, C6, C9 and C10.....</b>	<b>30</b>
<b>S5. Photophysical Characterizations of Cu(I) Complexes C1-C10.....</b>	<b>45</b>

<b>S6. Luminescent sensing experiments for silver ions of Cu(I)-POP Complexes C1-C4 in solution. ....</b>	<b>62</b>
<b>S7. The experimental procedures and catalytical performance of C1-C10 for CuAAC reaction in water solution.....</b>	<b>65</b>

## S1. General Information

All reactions and manipulations were performed under an atmosphere of prepurified nitrogen using Schlenk techniques. All the organic solvents were obtained from commercial chemical company and used here were distilled over 4 Å molecular sieves under an argon atmosphere. All other chemicals were used as received without any further purification. NMR spectra were recorded on either a Bruker AVIII 400 MHz spectrometer or a Bruker AVIII 500 MHz Spectrometer and referenced to residual solvent peaks. The working frequencies are 400 or 500 MHz for  $^1\text{H}$  and 100 MHz for  $^{13}\text{C}$ . The Fluorescence spectral analyses were carried out on an Edinburgh FLS980 spectrometer. The X-ray diffraction single-crystal data of Cu(I)-POP complexes **C1-C4** and Cu(I)-DPPM complexes **C7-C8** were collected on a Bruker D8 Venture APEX II CCD single crystal diffractometer.

## S2. Synthesis of bipyridine ligands



**Scheme S1.** The Synthesis procedures of compounds **2**, **3** and bipyridine ligands **L1-L4**

**Synthesis of Compound 2.** The 2-bromo-5-methoxypyridine (100 mg, 0.53 mmol), zinc dust (100 mg, 1.53 mmol), bis(triphenylphosphine) nickel(II) (150 mg, 0.20 mmol) and  $\text{Et}_4\text{N}$  iodide (200 mg, 0.79 mmol) were dissolved into dry THF (40 mL) in a clean 100 mL round flask. The mixture was refluxed at  $70^\circ\text{C}$  under an  $\text{N}_2$  atmosphere for 24 hours. The solution was concentrated under reduced pressure, the residue dissolved in  $\text{CH}_2\text{Cl}_2$  and washed with a 3M aqueous ammonia ( $2 \times 100$  mL), then brine, dried ( $\text{Na}_2\text{SO}_4$ ) and the solvent was removed under reduced pressure. Flash chromatography ( $\text{SiO}_2$ , AcOEt: light petroleum) afforded compounds **2** as a pale-yellow solid (50 mg, 0.23 mmol, 87%).  $^1\text{H}$  NMR (500 MHz, Chloroform- $d$ )  $\delta$  8.33 (s, 2H,  $\text{H}^b$ ), 8.25 (d,  $J = 8.9$  Hz, 2H,  $\text{H}^d$ ), 7.32 (d,  $J = 8.9$  Hz, 2H,  $\text{H}^c$ ), 7.26 (s, 1H), 3.91 (s, 6H,  $\text{H}^a$ ).  $^{13}\text{C}$  NMR (100 MHz, Chloroform- $d$ )  $\delta$  155.5, 149.0, 136.6, 121.1, 120.9, 55.7. ESI-MS ( $\text{CH}_3\text{CN}$ ,  $m/z$ ): [**2** + **H**] $^+$ , calcd  $m/z = 217.09$ . found  $m/z = 217.1$ . This compound was directly subjected to next step synthesis without further purification.

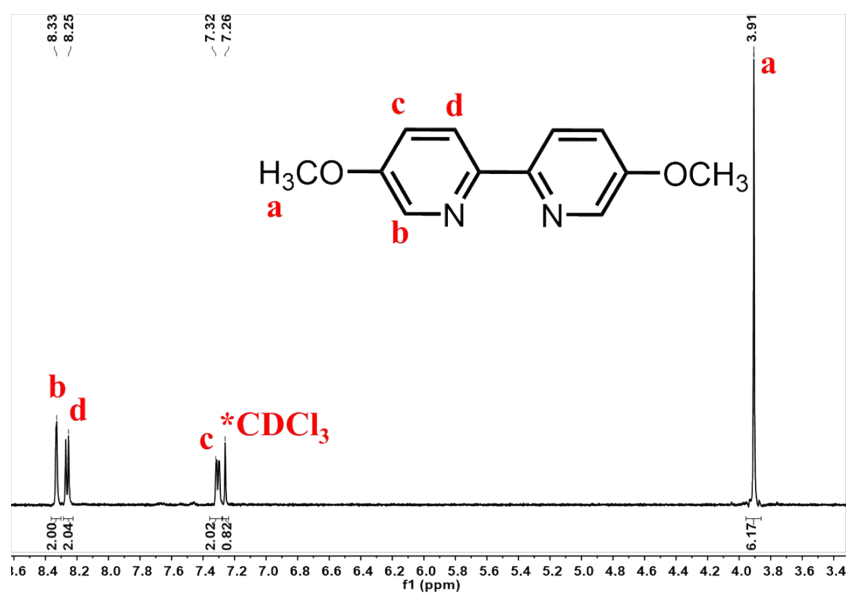


**Figure S1.** <sup>1</sup>H NMR spectrum (500 MHz, Chloroform-d) of compound **2** recorded at 298 K.

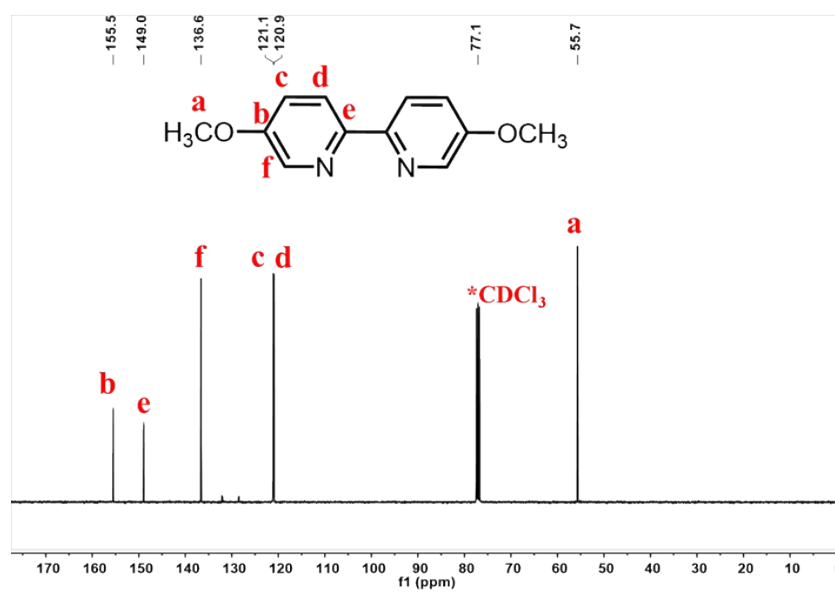


**Figure S2.** <sup>13</sup>C NMR spectrum (100 MHz, Chloroform-d) of compound **2** recorded at 298 K.

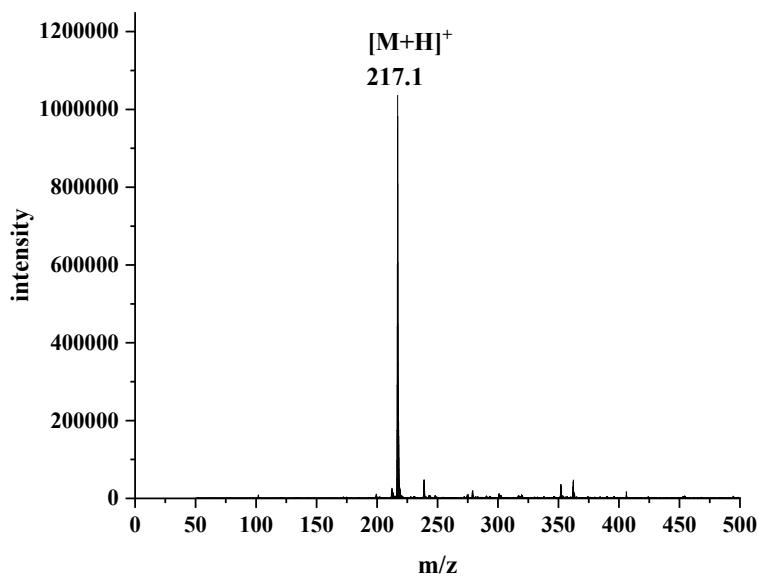


**Figure S3.** ESI-MS spectrum of compound **2** in CH<sub>3</sub>CN at 298 K.

**Synthesis of compound 3.** Compound **2** (200 mg, 0.92 mmol) was dissolved in hydrogen bromide 33 wt% solution in acetic acid (20 mL) in a sealed tube was heated 115°C for 37 h. after cooling, the resulting precipitates were collected by filtration and dried in air. The obtained crystalline samples were dissolved in water, and the *pH* value of aqueous solution was adjusted to *ca.* 7 by dropwise addition of 10% NaOH solution. The resulting precipitates were collected by filtration and dried under vacuum to give compound **3** as a pale-yellow powder (130 mg, 0.69mmol, 84%).

<sup>1</sup>H NMR (500 MHz, DMSO-d<sub>6</sub>) δ 10.04 (s, 2H, H<sup>a</sup>), δ 8.14 (d, *J* = 2.4 Hz, 2H, H<sup>b</sup>), 8.07 (d, *J* = 8.8 Hz, 2H, H<sup>d</sup>), 7.24 (brs, 2H, H<sup>c</sup>). <sup>13</sup>C NMR (100 MHz, DMSO-d<sub>6</sub>) δ 153.6, 147.1, 137.1, 123.1, 120.4. ESI-MS (CH<sub>3</sub>CN, *m/z*): [**3**+H]<sup>+</sup>, calcd *m/z* =188.06. found *m/z* =188.40. This compound was directly subjected to next step synthesis without further purification.

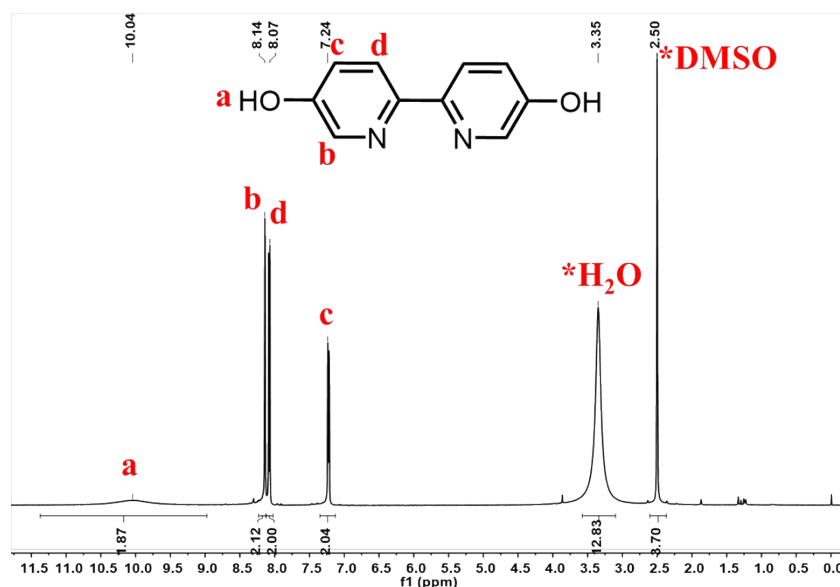


**Figure S4.** <sup>1</sup>H NMR spectrum (500 MHz, DMSO-d<sub>6</sub>) of compound **3** recorded at 298 K

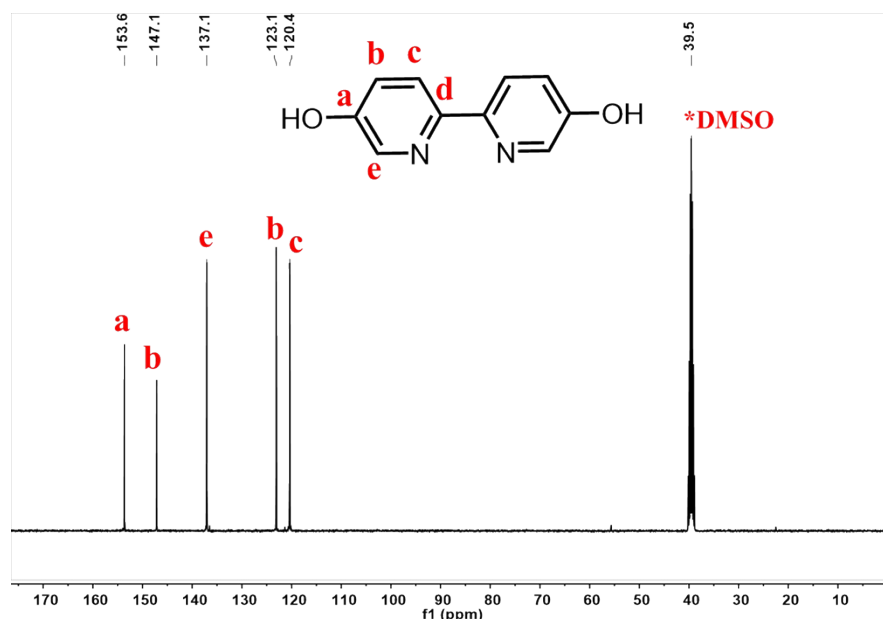


**Figure S5.**  $^{13}\text{C}$  NMR spectrum (100 MHz,  $\text{DMSO-d}_6$ ) of compound **3** recorded at 298 K.

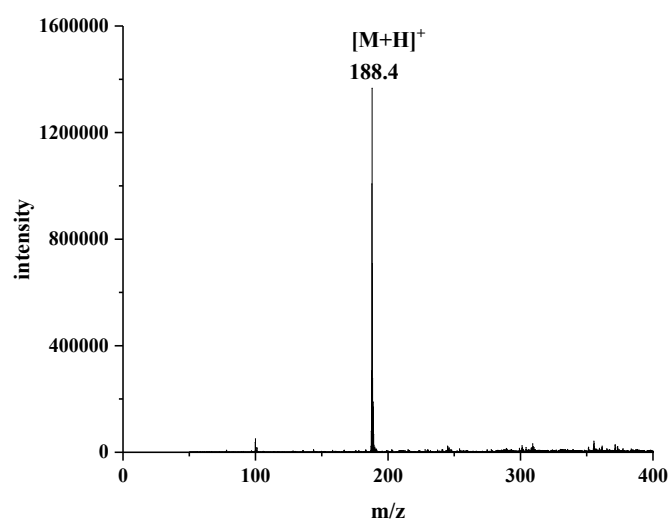


**Figure S6.** ESI-MS spectrum of compound **3** in  $\text{CH}_3\text{CN}$  at 298 K.

**Synthesis of ligand L1.** Compound **3** (100 mg, 0.53 mmol),  $\text{K}_2\text{CO}_3$  (2.50 g, 18.12 mmol), KI (20 mg, 0.12 mmol) and allyl bromide (0.8 mL, 9.26 mmol) were dissolved into dry THF (20 mL) in a sealed tube. The mixture was stirred at 85 °C for 48 hours. Next, the solution was concentrated under reduced pressure. The afforded solid was dissolved in  $\text{CH}_2\text{Cl}_2$  and washed with water, then brine, dried ( $\text{Na}_2\text{SO}_4$ ) and the solvent was evaporated in the vacuum. Flash chromatography ( $\text{SiO}_2$ , AcOEt: light petroleum) afforded **L1** as a pale-yellow solid (80.50 mg, 0.30 mmol, 57%).  $^1\text{H}$  NMR (500 MHz, Chloroform-*d*)  $\delta$  8.33 (d,  $J = 3.0$  Hz, 2H,  $\text{H}^{\text{e}}$ ), 8.22 (d,  $J = 8.8$  Hz, 2H,  $\text{H}^{\text{f}}$ ), 7.30 (d,  $J = 3.0$  Hz, 2H,  $\text{H}^{\text{e}}$ ), 6.07 (brs, 2H,  $\text{H}^{\text{c}}$ ), 5.47 (d,  $J = 18.4$  Hz, 2H,  $\text{H}^{\text{b}}$ ), 5.35 (d,  $J = 11.4$  Hz, 2H,  $\text{H}^{\text{a}}$ ), 4.62 (d,  $J = 5.0$  Hz, 4H,  $\text{H}^{\text{d}}$ ).  $^{13}\text{C}$  NMR (100 MHz, Chloroform-*d*)  $\delta$  154.70, 149.22, 137.33, 132.65, 122.26, 121.09, 118.49, 69.33.  $[\mathbf{3}+\mathbf{H}]^+$ , calcd  $m/z = 269.12$ . found  $m/z = 269.12$ . This compound was directly subjected to next step synthesis without further purification.

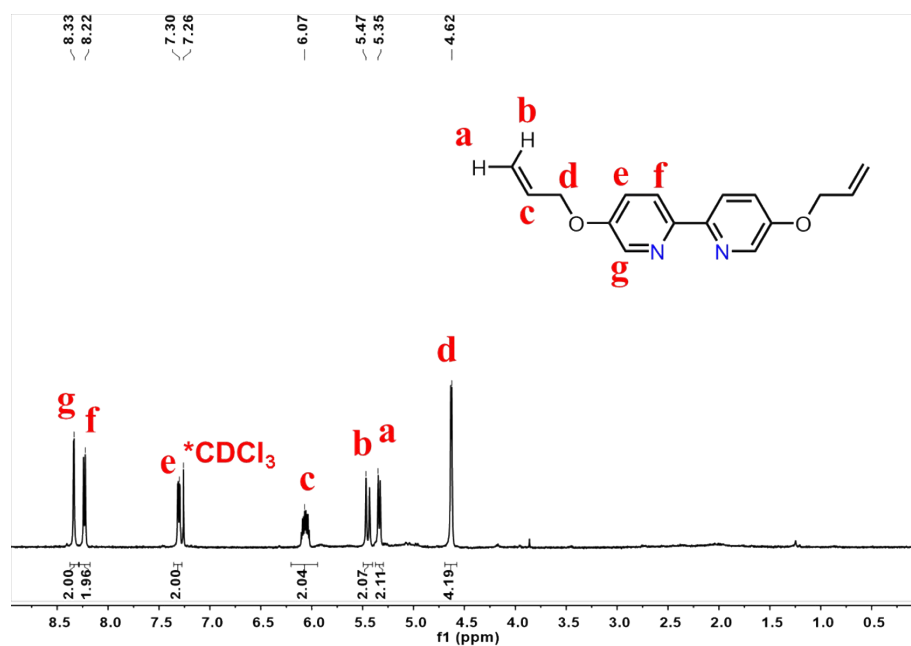


Figure S7.  $^1\text{H}$  NMR spectrum (500 MHz, Chloroform-d) of **L1** recorded at 298 K.

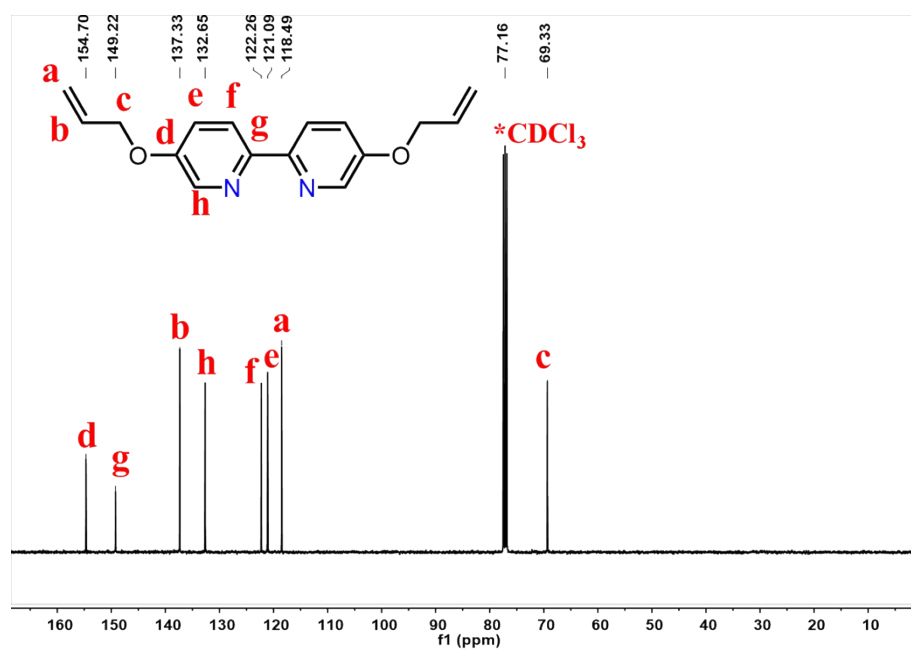
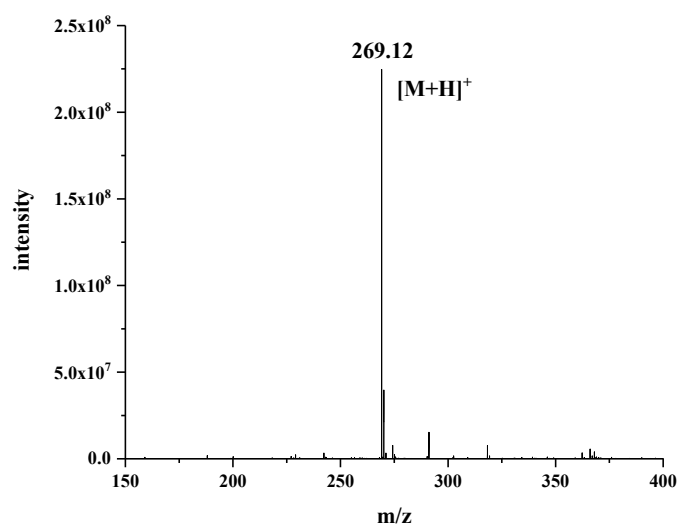
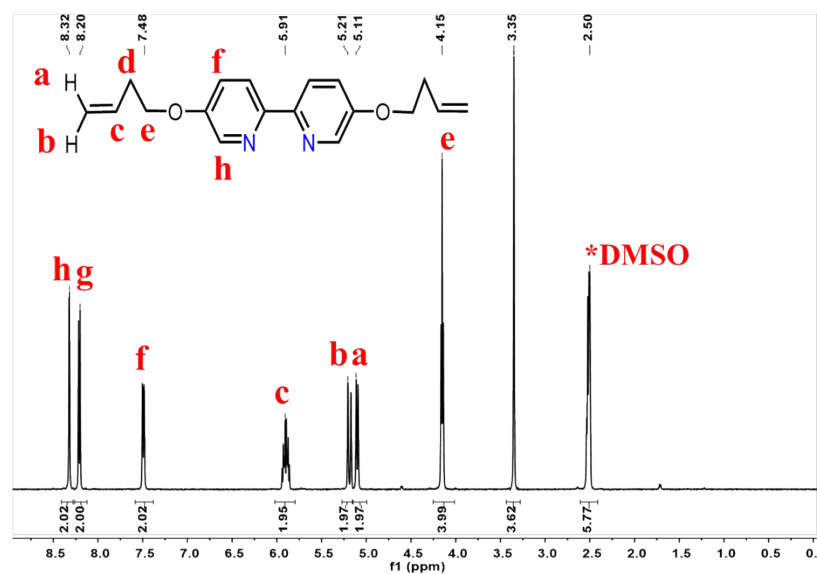


Figure S8.  $^{13}\text{C}$  NMR spectrum (100 MHz, Chloroform-d) of **L1** recorded at 298 K.



**Figure S9.** ESI-MS spectrum of **L1** in  $\text{CH}_3\text{CN}$  at 298 K.

**Synthesis of ligand L2.** Compound **3** (100 mg, 0.53 mmol),  $\text{K}_2\text{CO}_3$  (2.50 g, 18.12 mmol), KI (20 mg, 0.12 mmol) and 4-Bromo-1-butene (0.9 mL, 9.0 mmol) were dissolved into dry THF (20 mL) in a sealed tube. The mixture was stirred at 85 °C for 48 hours. The solution was concentrated under reduced pressure, the residue dissolved in  $\text{CH}_2\text{Cl}_2$  and washed with water, then brine, dried ( $\text{Na}_2\text{SO}_4$ ) and the solvent removed. Flash chromatography ( $\text{SiO}_2$ , AcOEt: light petroleum) afforded ligand **L2** as a yellow solid (80.00 mg, 0.27 mmol, 51%).  $^1\text{H}$  NMR (500 MHz,  $\text{DMSO}-d_6$ )  $\delta$  8.32 (d,  $J = 2.8$  Hz, 2H,  $\text{H}^h$ ), 8.20 (d,  $J = 8.8$  Hz, 2H,  $\text{H}^g$ ), 7.48 (d,  $J = 11.6$  Hz, 2H,  $\text{H}^f$ ), 5.91 (brs, 2H,  $\text{H}^c$ ), 5.21 (d,  $J = 17.2$  Hz, 2H,  $\text{H}^b$ ), 5.11 (d,  $J = 10.2$  Hz, 2H,  $\text{H}^a$ ), 4.15 (t,  $J = 6.6$  Hz, 4H,  $\text{H}^e$ ), 3.35 (s, 4H,  $\text{H}^d$ ).  $^{13}\text{C}$  NMR (100 MHz, Chloroform- $d$ )  $\delta$  149.11, 137.17, 134.09, 121.99, 121.08, 117.55, 67.81, 33.66.  $[\text{L2}+\text{H}]^+$ , calcd  $m/z = 297.15$ . found  $m/z = 297.10$ . This compound was directly subjected to next step synthesis without further purification.



**Figure S10.**  $^1\text{H}$  NMR spectrum (500 MHz,  $\text{DMSO-d}_6$ ) of **L2** recorded at 298 K.

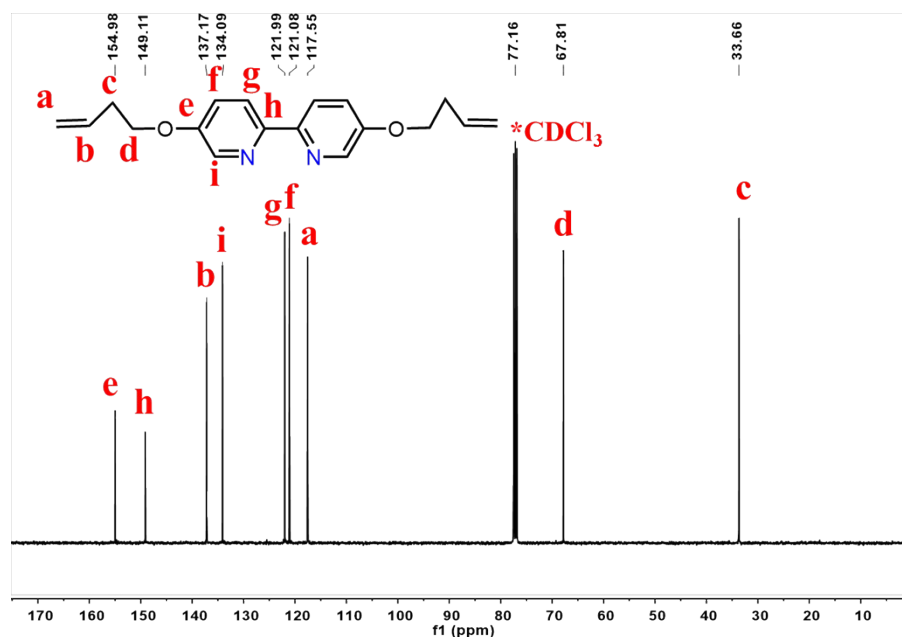


**Figure S11.**  $^{13}\text{C}$  NMR spectrum (100 MHz,  $\text{DMSO-d}_6$ ) of **L2** recorded at 298 K.

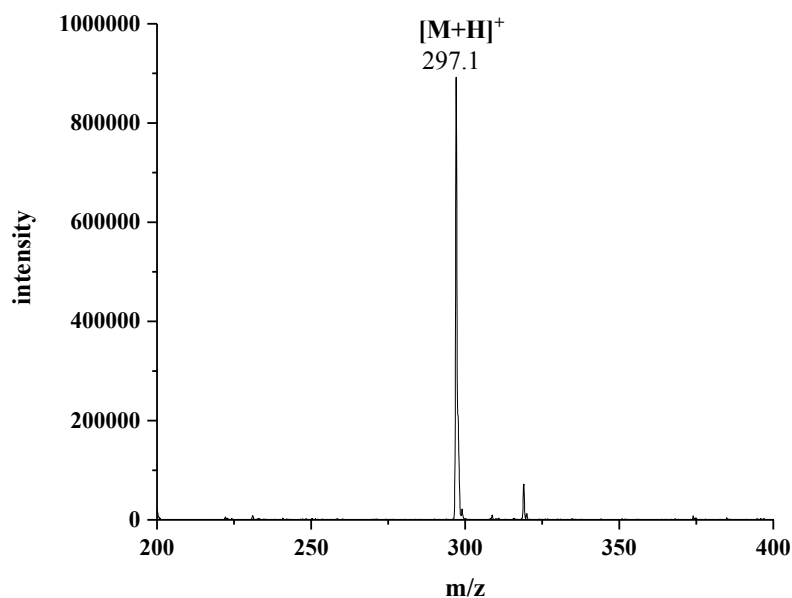


**Figure S12.** ESI-MS spectrum of **L2** in  $\text{CH}_3\text{CN}$  at 298 K.

**Synthesis of ligand L3.** Compound **3** (100 mg, 0.53 mmol),  $\text{K}_2\text{CO}_3$  (2.50 g, 18.12 mmol), KI (20 mg, 0.12 mmol) and propargyl bromide (0.8 mL, 9.0 mmol) were dissolved into dry THF (20 mL) in a sealed tube. The mixture was stirred at 85 °C for 48 h. The solution was concentrated under reduced pressure, the residue dissolved in  $\text{CH}_2\text{Cl}_2$  and washed with water, then brine, dried ( $\text{Na}_2\text{SO}_4$ ) and the solvent removed. Flash chromatography ( $\text{SiO}_2$ , AcOEt: light petroleum) afforded ligand **L3** as a brown solid (100 mg, 0.34 mmol, 64%).  $^1\text{H}$  NMR (500 MHz, Chloroform- $d$ )  $\delta$  8.39 (s, 2H, H<sup>e</sup>), 8.27 (d,  $J$  = 8.8 Hz, 2H, H<sup>d</sup>), 7.40 (d,  $J$  = 8.7 Hz, 2H, H<sup>c</sup>), 7.4.78



(s, 4H, H<sup>b</sup>), 2.57 (s, 2H, H<sup>a</sup>). <sup>13</sup>C NMR (100 MHz, Chloroform-d) δ 153.63 , 149.63 , 137.41 , 122.47 , 121.06 , 77.80 , 76.60 , 56.26 . [L<sub>3</sub>+H]<sup>+</sup>, calcd *m/z* =265.28. found *m/z* =265.10. This compound was directly subjected to next step synthesis without further purification.

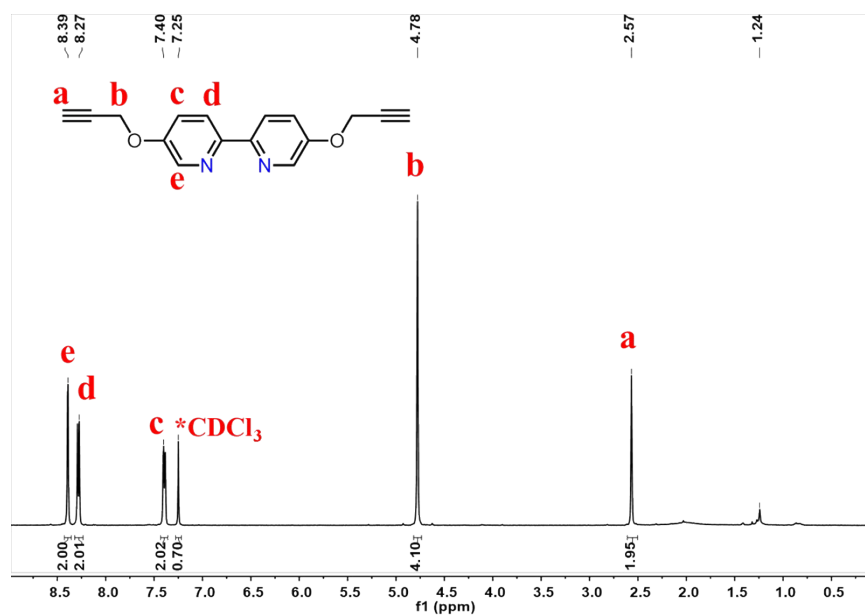


**Figure S13.** <sup>1</sup>H NMR spectrum (500 MHz, Chloroform-d) of L<sub>3</sub> recorded at 298 K

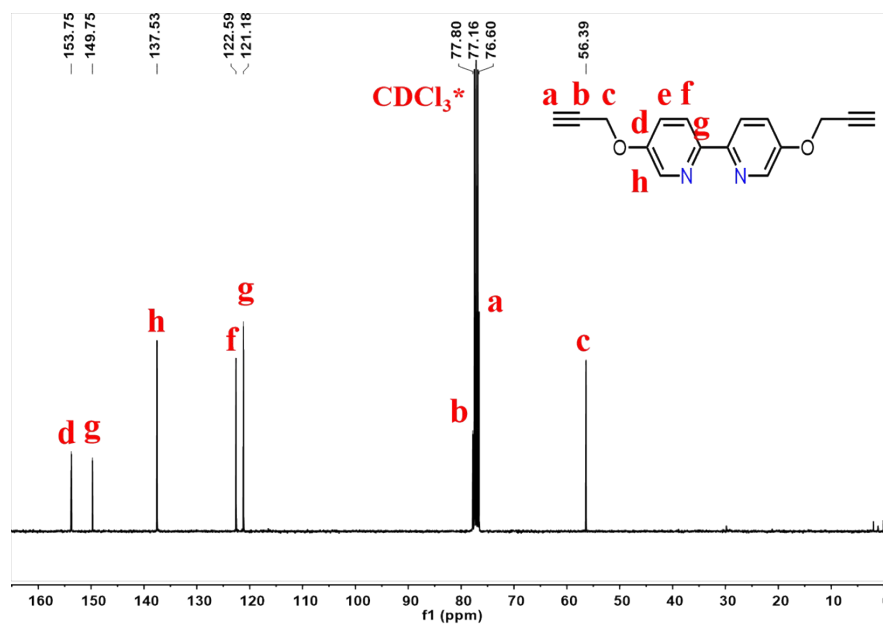


**Figure S14.** <sup>13</sup>C NMR spectrum (100 MHz, Chloroform-d) of L<sub>3</sub> recorded at 298 K.

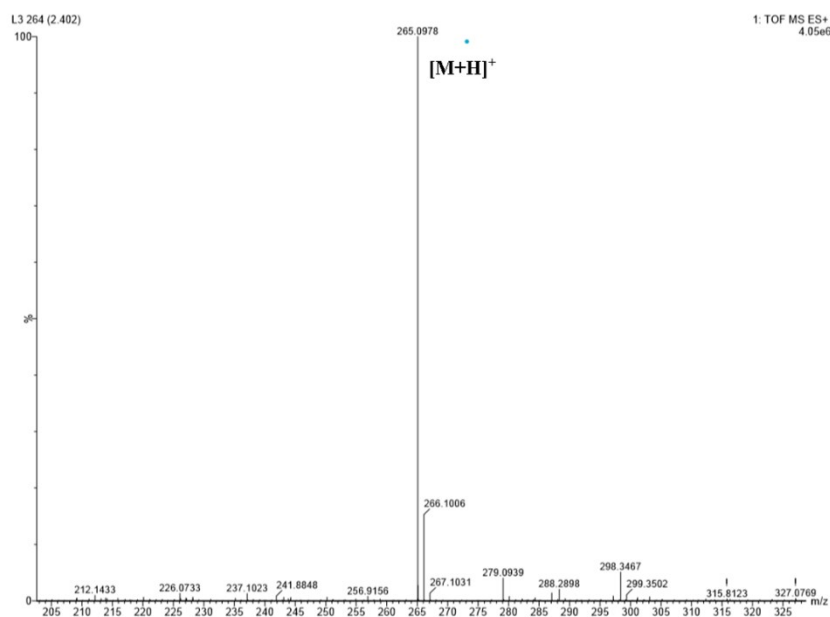


**Figure S15.** ESI-MS spectrum of **L3** in  $\text{CH}_3\text{CN}$  at 298 K.

**Synthesis of ligand L4.** The compound was synthesized according to reference.  $^1\text{H}$  NMR (400 MHz,  $\text{DMSO}-d_6$ )  $\delta$  8.60 (s, 2H,  $\text{H}^e$ ), 8.34 (d,  $J = 8.1$  Hz, 2H,  $\text{H}^d$ ), 7.86 (d,  $J = 8.2$  Hz, 2H,  $\text{H}^c$ ), 5.40 (t,  $J = 5.7$  Hz, 2H,  $\text{H}^a$ ), 4.59 (d,  $J = 5.5$  Hz, 4H,  $\text{H}^b$ ).

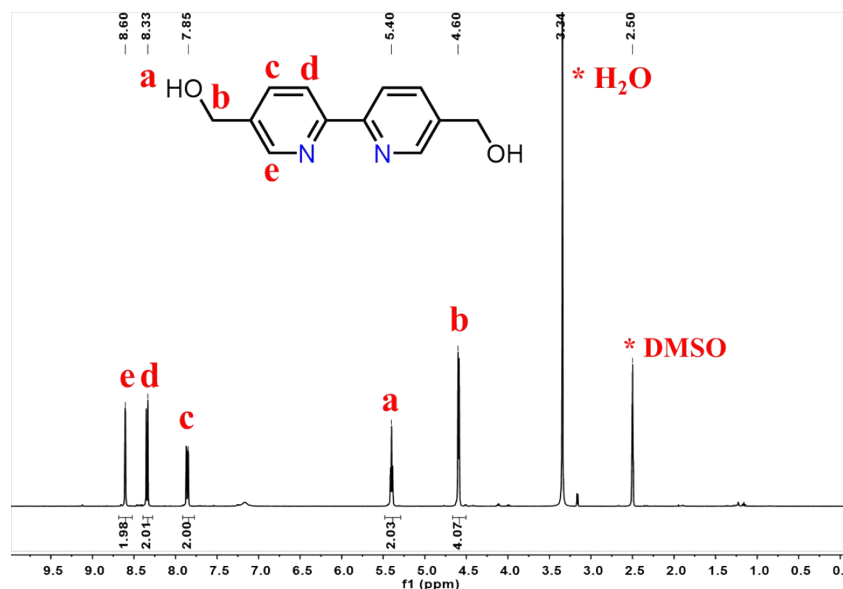
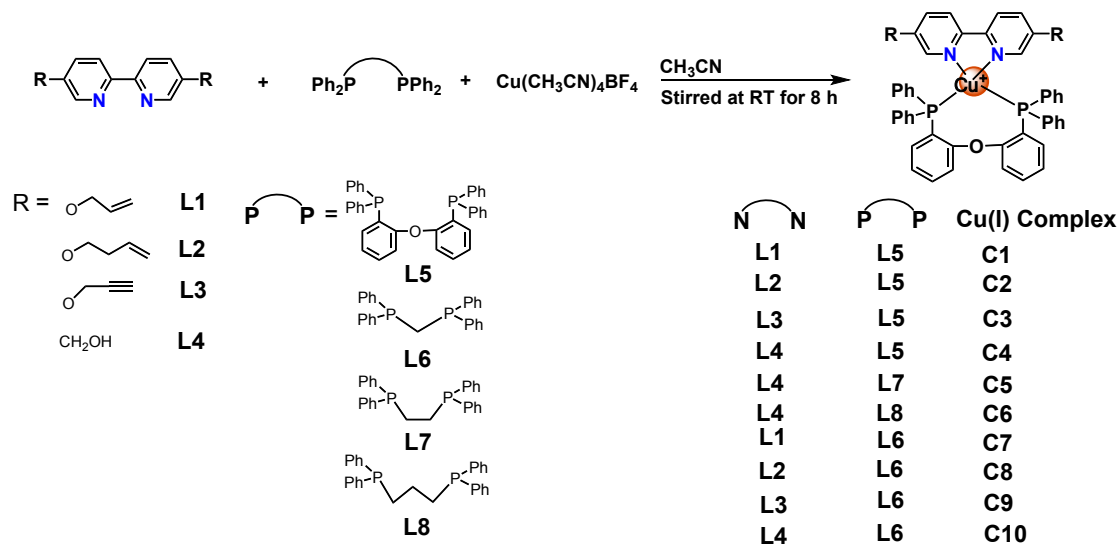


**Figure S16.**  $^1\text{H}$  NMR spectrum (500 MHz,  $\text{DMSO}-d_6$ ) of **L4** recorded at 298 K.

### S3. The synthesis pathway of heteroleptic Cu(I) complexes C1-C10.



**Scheme S2.** Synthesis routes of mononuclear Cu(I) complexes **C1-C6** and dinuclear Cu(I) complexes **C7-C10**.

**Synthesis of Cu(I)-POP complex C1.** Ligand **L1** (20 mg, 0.074 mmol) and Tetrafluoro-borate tetra (acetonitrile) copper (23 mg, 0.074 mmol) were dissolved into acetonitrile (3 mL) in an assembly tube, stirred at room temperature for 2 hours. Then added the **L5** Bis(2-diphenylphosphino)phenyl ether (40 mg, 0.074 mmol) stirred at room temperature for 8 hours. The solution was divided into three parts. It was grown by solvent diffusion method with Ethyl ether as diffusion agent. A week later, the Cu(I)-POP complex **C1** was obtained.  $^1\text{H}$  NMR (400 MHz, Chloroform-*d*)  $\delta$  8.24 (d,  $J = 9.0$  Hz, 2H, H<sup>e</sup>), 7.82 (s, 2H, H<sup>f</sup>), 7.46 (d,  $J = 11.7$  Hz, 2H, H<sup>d</sup>), 7.24 (m, 6H, H<sup>j/k/m</sup>), 7.13 (m, 8H, H<sup>i</sup>), 6.91 (m, 12H, H<sup>g/h</sup>), 6.68 (m, 2H, H<sup>l</sup>), 5.82 (m, 2H, H<sup>b</sup>), 5.19 (m, 4H, H<sup>a</sup>), 4.26 (d,  $J = 5.3$  Hz, 4H, H<sup>c</sup>).  $^{13}\text{C}$  NMR (100 MHz, Chloroform-*d*)  $\delta$  155.67, 144.88, 136.97, 134.38, 133.11, 132.08, 131.70, 130.71, 130.20, 128.83, 125.30, 124.09, 122.87, 120.41, 118.78, 69.39.  $[\text{M}]^+$ , calcd  $m/z = 868.93$ . found  $m/z = 868.90$ .

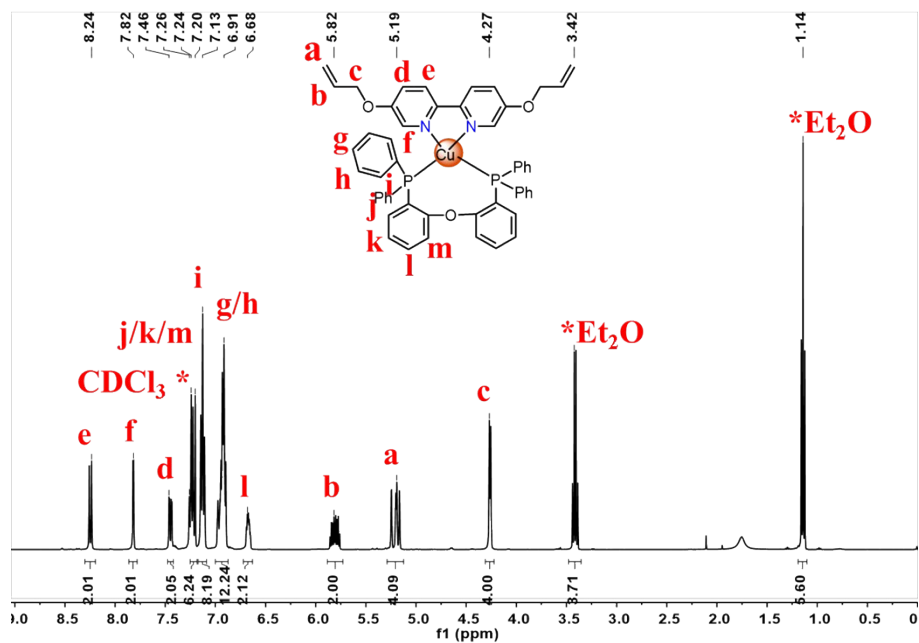


Figure S17. <sup>1</sup>H NMR spectrum (400 MHz, Chloroform-*d*) of C1 recorded at 298 K.

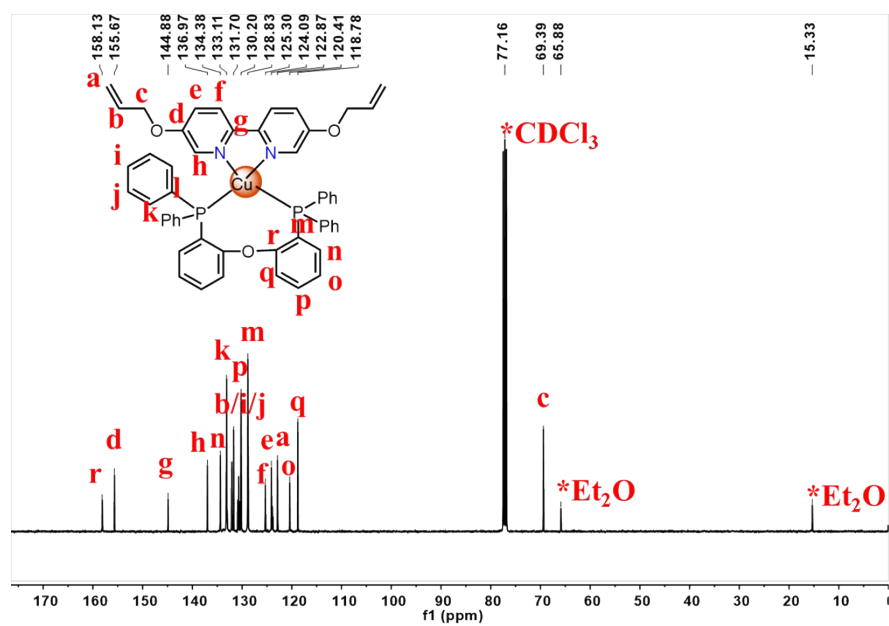
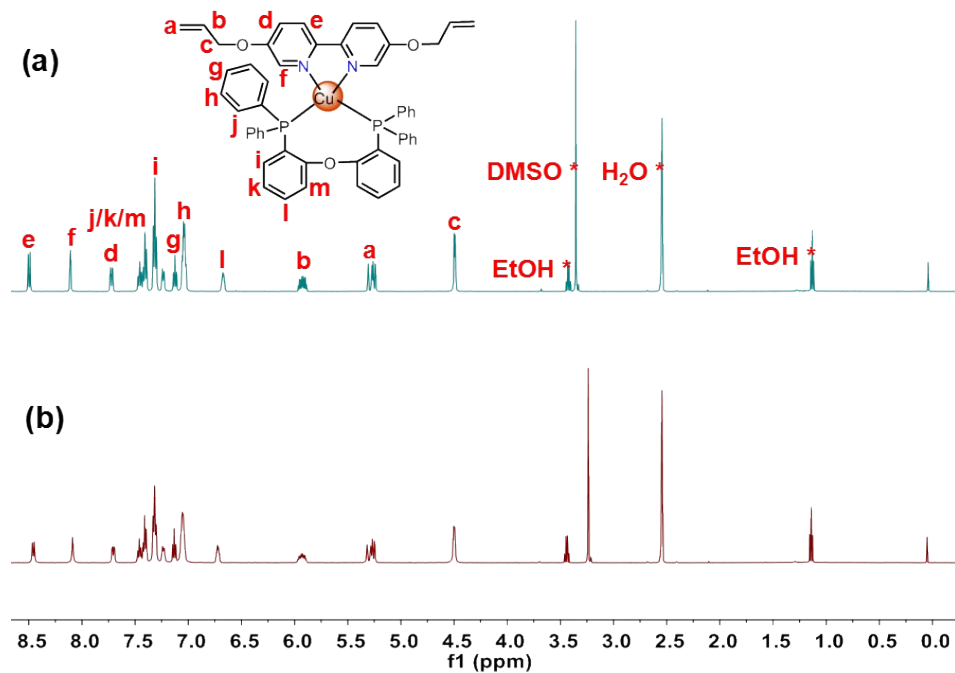
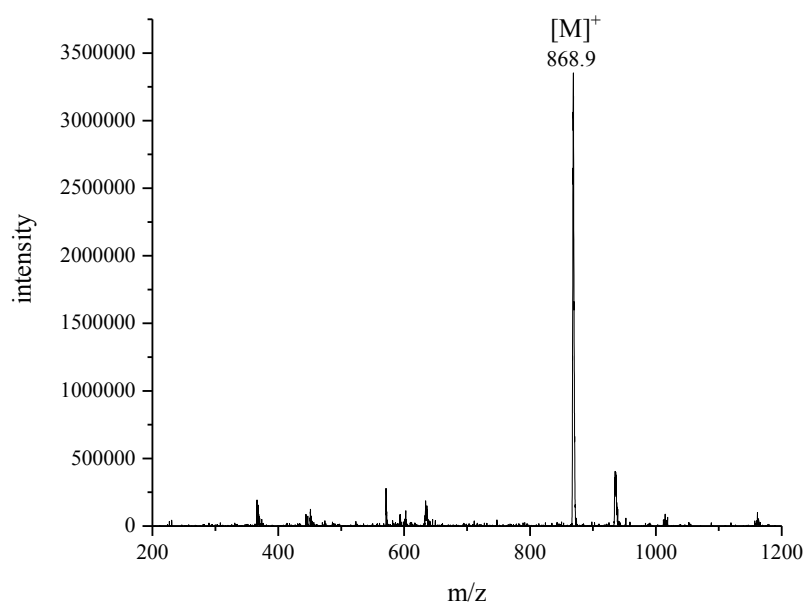


Figure S18. <sup>13</sup>C NMR spectrum (100 MHz, Chloroform-*d*) of C1 recorded at 298 K.



**Figure S19.** Temperature-dependent  $^1\text{H}$  NMR spectrum (500 MHz,  $\text{DMSO-}d_6$ ) of **C1** recorded at (a) 298K, (b) 323K.



**Figure S20.** ESI-MS spectrum of complex **C1** in  $\text{CH}_3\text{CN}$  at 298 K.

**Synthesis of Cu(I)-POP Complex C2.** Ligand **L2** (20 mg, 0.067 mmol) and Tetrafluoroborate tetra (acetonitrile) copper (21 mg, 0.067 mmol) were dissolved into acetonitrile (3 mL) in an assembly tube, stirred at room temperature for 2 hours. Then added the **L5** Bis(2-diphenylphosphinophenyl)ether (36 mg, 0.067 mmol) stirred at room temperature for 8 hours. The solution was

divided into three parts. The single crystal was grown by solvent diffusion method with Ethyl ether as diffusion agent. A week later, the Cu(I)-POP complex **C2** was obtained. <sup>1</sup>H NMR (400 MHz, Chloroform-*d*) δ 8.24 (d, *J* = 9.0 Hz, 2H, H<sup>f</sup>), 7.79 (s, 2H, H<sup>g</sup>), 7.43 (d, *J* = 8.9 Hz, 2H, H<sup>e</sup>), 7.24 (m, 6H, H<sup>k/l/n</sup>), 7.13 (m, 8H, H<sup>i</sup>), 6.94 (m, 12H, H<sup>h/i</sup>), 6.67 (s, 2H, H<sup>m</sup>), 5.69 (m, 2H, H<sup>b</sup>), 5.05 (m, 4H, H<sup>a</sup>), 3.72 (t, *J* = 6.6 Hz, 4H, H<sup>d</sup>), 2.37 (m, 4H, H<sup>c</sup>). <sup>13</sup>C NMR (100 MHz, Chloroform-*d*) δ 158.10, 155.98, 144.84, 136.72, 134.41, 133.71, 133.17, 132.08, 130.72, 130.23, 128.85, 125.35, 123.97, 122.92, 120.39, 117.60, 68.00, 33.14. [**C2**-BF<sub>4</sub>]<sup>+</sup>, calcd *m/z* = 896.91. found *m/z* = 896.90.

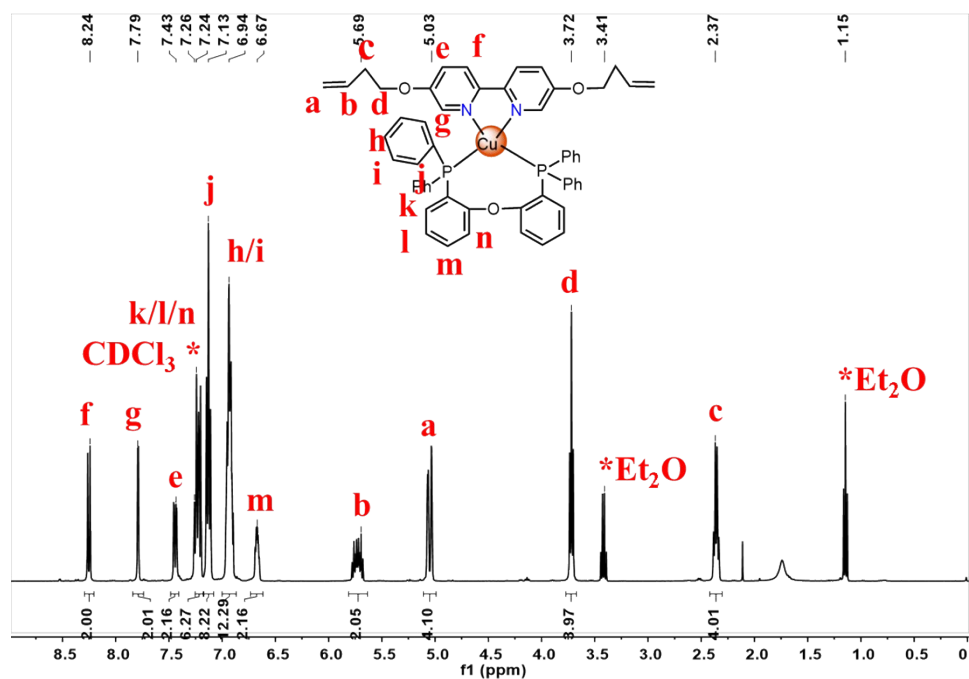
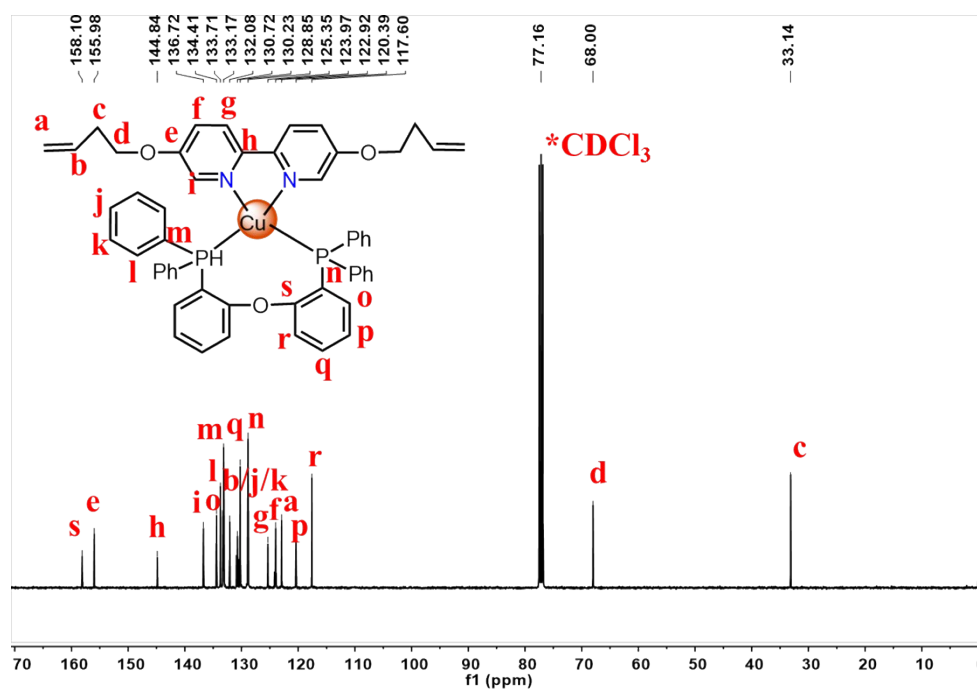
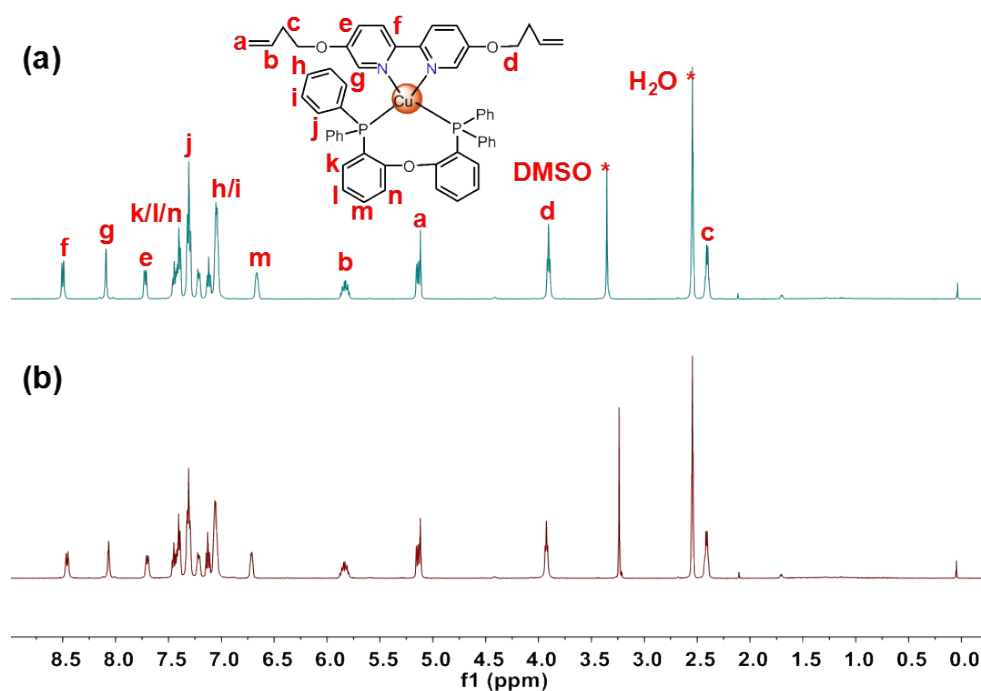


Figure S21. <sup>1</sup>H NMR spectrum (400 MHz, Chloroform-*d*) of **C2** recorded at 298 K.



**Figure S22.**  $^{13}\text{C}$  NMR spectrum (100 MHz, Chloroform- $d$ ) of **C2** recorded at 298 K.



**Figure S23.** Temperature-dependent  $^1\text{H}$  NMR spectrum (500 MHz, DMSO- $d$ ) of **C2** recorded at (a) 298K, (b) 323K.

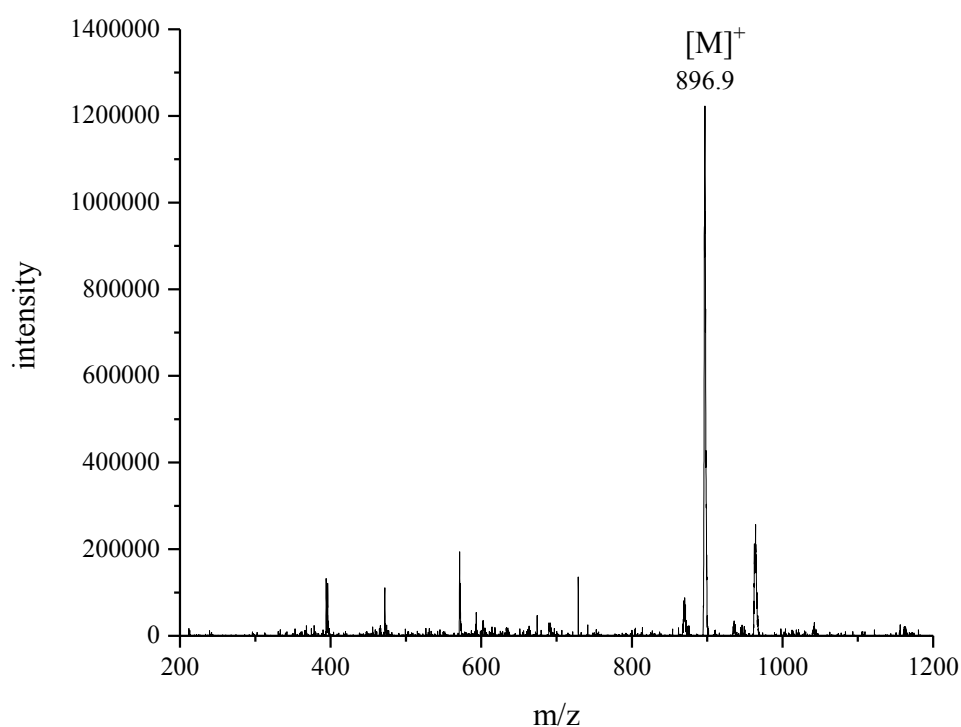


**Figure S24.** ESI-MS spectrum of **C2** in  $\text{CH}_3\text{CN}$  at 298 K.

**Synthesis of Cu(I)-POP Complex C3.** Ligand **L3** (18 mg, 0.067 mmol) and Tetrafluoroborate tetra (acetonitrile) copper (21 mg, 0.067 mmol) were dissolved into acetonitrile (3 mL) in a

assembly tube, stirred at room temperature for 2 hours. Then added the **L5** Bis(2-diphenylphosphinophenyl)ether (36 mg, 0.067 mmol) stirred at room temperature for 8 hours. The solution was divided into three parts. The single crystal was grown by solvent diffusion method with Ethyl ether as diffusion agent. A week later, the Cu(I)-POP complex **C3** was obtained.  $^1\text{H}$  NMR (400 MHz, Chloroform-*d*)  $\delta$  8.32 (d,  $J = 9.0$  Hz, 2H, H<sup>d</sup>), 7.98 (s, 2H, H<sup>e</sup>), 7.60 (d,  $J = 14.7$  Hz, 2H, H<sup>c</sup>), 7.30 (m, 6H, H<sup>i/k/l</sup>), 7.18 (m, 8H, H<sup>h</sup>), 7.02 (m, 12H, H<sup>f/g</sup>), 6.72 (m, 2H, H<sup>j</sup>), 4.49 (s, 2H, H<sup>b</sup>), 2.42 (s, 2H, H<sup>a</sup>).  $^{13}\text{C}$  NMR (100 MHz, Chloroform-*d*)  $\delta$  158.21, 154.78, 145.38, 137.17, 134.39, 133.07, 132.12, 130.26, 128.87, 125.28, 124.40, 123.06, 120.53, 78.48, 76.84, 56.57. [**C3**-BF<sub>4</sub>]<sup>+</sup>, *calcd*  $m/z = 865.28$ . *found*  $m/z = 865.17$ .

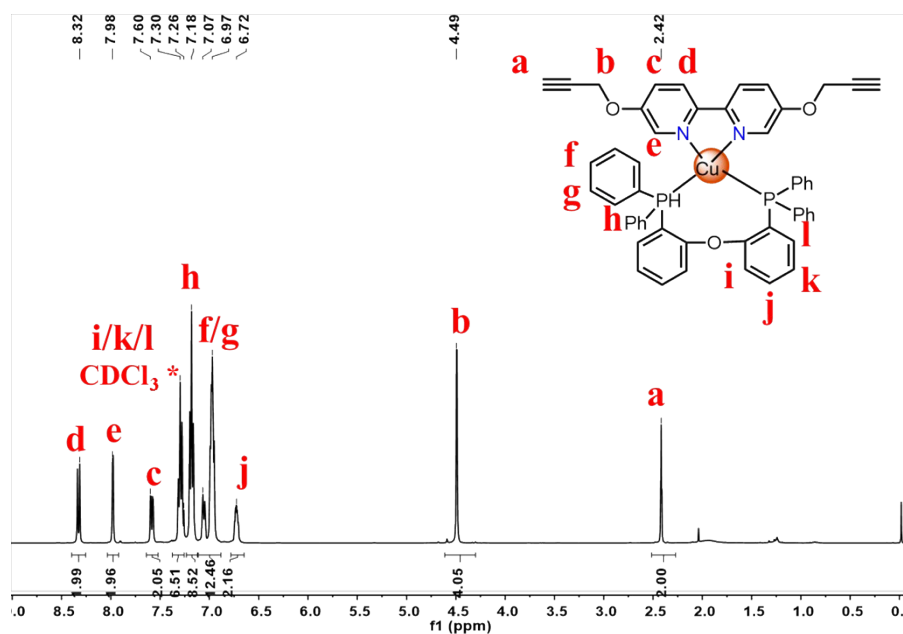


**Figure S25.**  $^1\text{H}$  NMR spectrum (400 MHz, Chloroform-*d*) of **C3** recorded at 298 K.



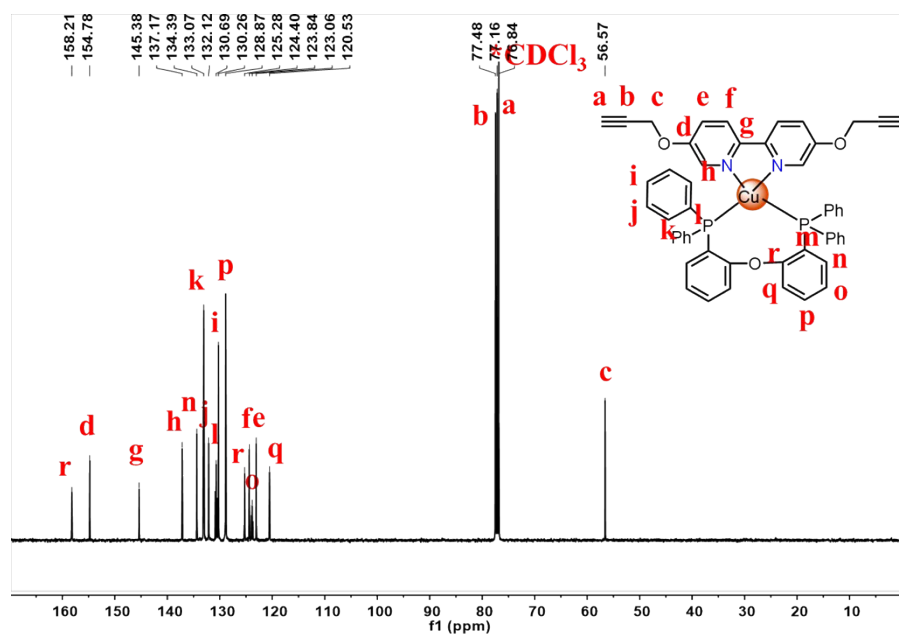


**Figure S26.** <sup>13</sup>C NMR spectrum (100 MHz, Chloroform-*d*) of **C3** recorded at 298 K

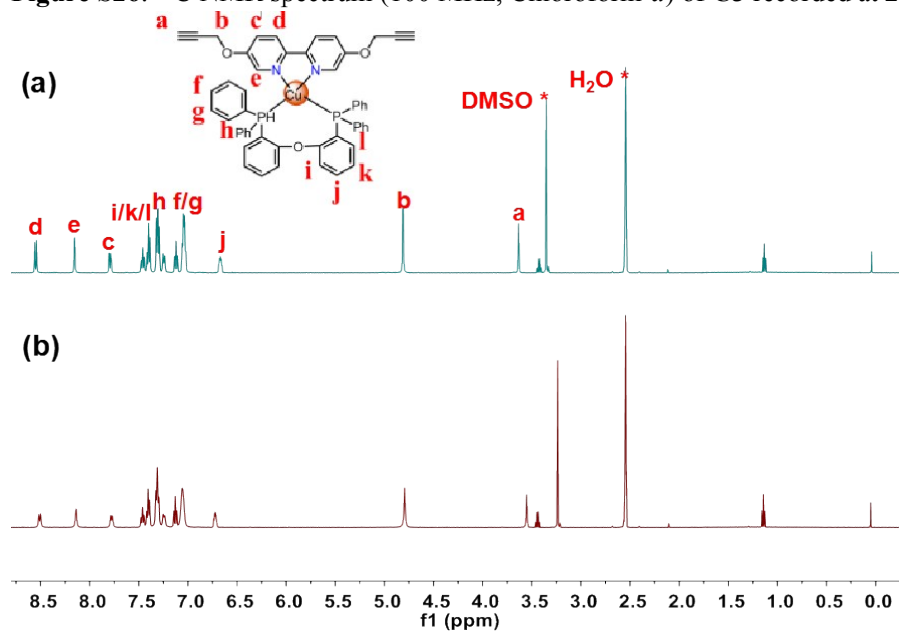


**Figure S27.** Temperature-dependent <sup>1</sup>H NMR spectrum (500 MHz, DMSO-*d*) of **C3** recorded at (a) 298K, (b) 323K.

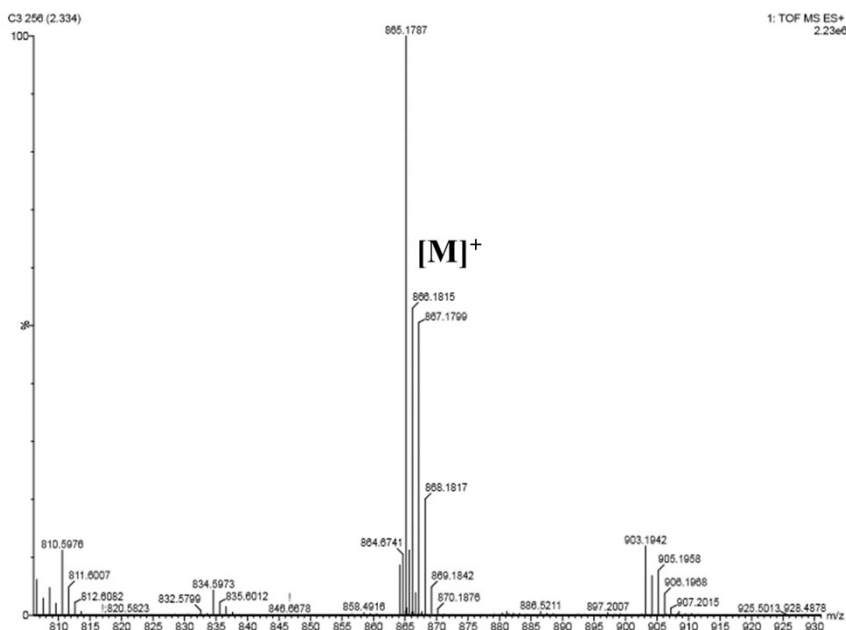


**Figure S28.** ESI-MS spectrum of **C3** in  $\text{CH}_3\text{CN}$  at 298 K.

**Synthesis of Cu(I)-POP Complex C4.** Ligand **L4** (14 mg, 0.067 mmol) and Tetrafluoroborate tetra (acetonitrile) copper (21 mg, 0.067 mmol) were dissolved into acetonitrile (3 mL) in an assembly tube, stirred at room temperature for 2 hours. Then added the **L5** Bis(2-diphenylphosphinophenyl)ether (36 mg, 0.067 mmol) stirred at room temperature for 8 hours. The solution was divided into three parts. The single crystal was grown by solvent diffusion method with Ethyl ether as diffusion agent. A week later, the Cu(I)-POP complex **C4** was obtained.  $^1\text{H}$  NMR (400 MHz, Acetonitrile- $d_3$ )  $\delta$  8.26 (d,  $J = 8.0$  Hz, 2H,  $\text{H}^d$ ), 8.18 (s, 2H,  $\text{H}^e$ ), 7.88 (d,  $J = 11.5$  Hz, 2H,  $\text{H}^c$ ), 7.26 (m, 6H,  $\text{H}^{i/k/l}$ ), 7.14 (d,  $J = 9.4$  Hz, 8H,  $\text{H}^h$ ), 6.95 (m, 12H,  $\text{H}^{f/g}$ ), 6.67 (m, 2H,  $\text{H}^j$ ), 4.38 (d,  $J = 14.5$  Hz, 4H,  $\text{H}^b$ ), 3.48 (s, 2H,  $\text{H}^a$ ).  $^{13}\text{C}$  NMR (100 MHz, Acetonitrile- $d_3$ )  $\delta$  157.49, 149.79, 147.06, 139.19, 135.75, 133.46, 132.43, 131.47, 130.15, 129.40, 128.07, 124.45, 123.01, 121.14, 119.81, 116.40, 59.98. TOF-MS: fragment of **C4** with a formula of  $[\text{C4-L4-BF}_4]^+$ , calcd  $m/z = 601.09$ . found  $m/z = 601.34$ .

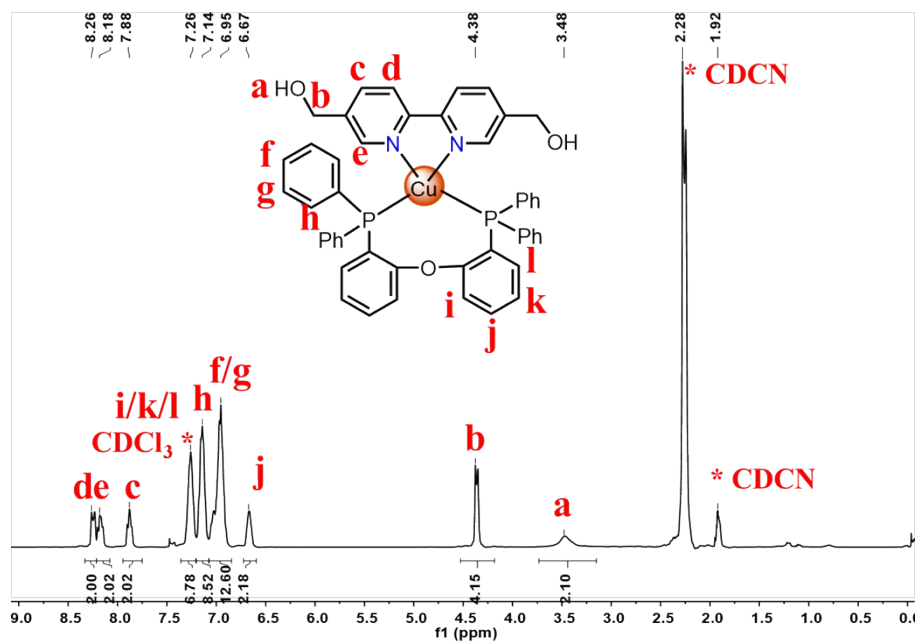


Figure S29.  $^1\text{H}$  NMR spectrum (400 MHz, Acetonitrile- $d_3$ ) of **C4** recorded at 298 K.

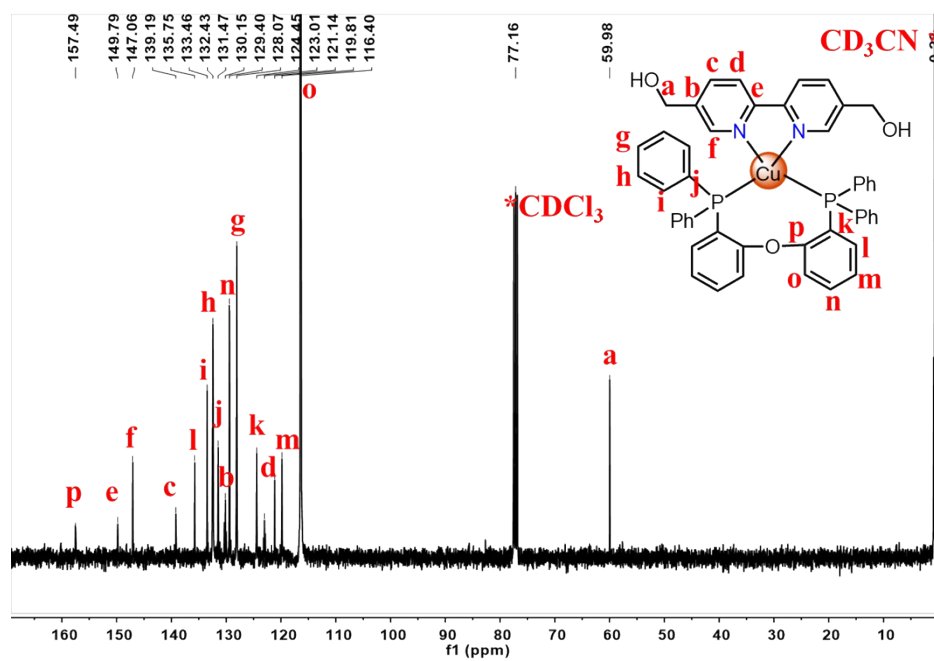
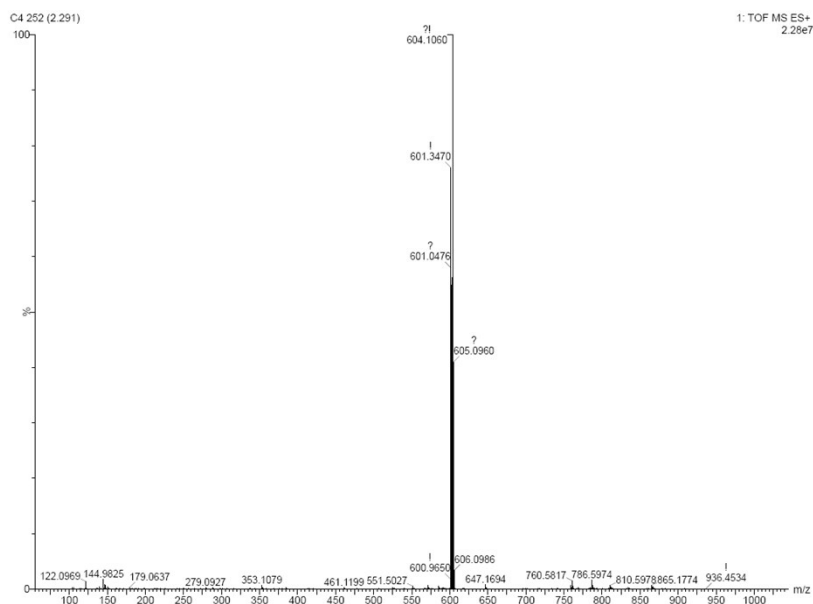


Figure S30.  $^{13}\text{C}$  NMR spectrum (100 MHz, Acetonitrile- $d_3$ ) of **C4** recorded at 298 K.



**Figure S31.** ESI-MS spectrum of **C4** in  $\text{CH}_3\text{CN}$  at 298 K.

**Synthesis of Cu(I)-DPPE Complex C5.** Ligand **L4** (34 mg, 0.12 mmol) and Tetrafluoroborate tetra (acetonitrile) copper (38 mg, 0.12 mmol) were dissolved into acetonitrile (3 mL) in an assembly tube, stirred at room temperature for 2 hours. Next, diphosphine ligand **L7** (1, 2-Bis(diphenylphosphino)ethane, 48 mg, 0.12 mmol) was added into above mixture and stirred at room temperature for 8 hours. The solution was filtrated and divided into three parts. The single crystal was grown by solvent diffusion method with Ethyl ether as diffusion agent. A week later, the Cu(I)-DPPE complex **C5** was obtained.  $^1\text{H}$  NMR (500 MHz,  $\text{DMSO}-d_6$ )  $\delta$  8.76 (s, 2H), 8.46 (s, 2H), 8.21 (s, 2H), 7.46 (s, 20H), 5.56 (s, 2H), 4.61 (s, 4H), 2.77 (s, 4H).  $^{13}\text{C}$  NMR (126 MHz,  $\text{DMSO}-d_6$ )  $\delta$  150.86, 148.69, 137.37, 132.70, 130.87, 129.61, 129.36, 122.76, 60.43, 25.16.

$[\text{C5}-\text{BF}_4]^{+}$ , calcd  $m/z = 678.21$ . found  $m/z = 678.1$ .

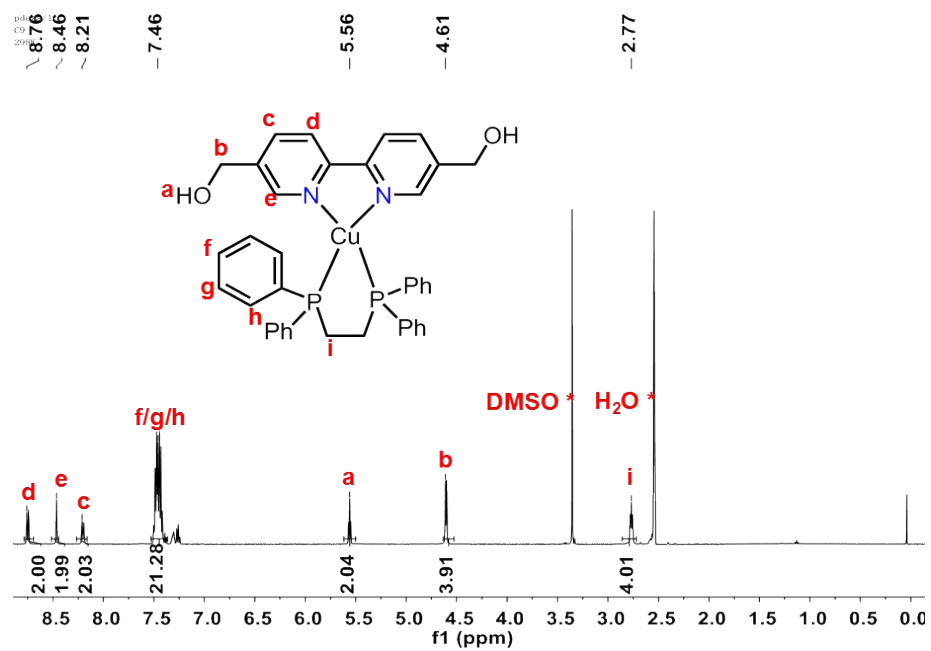


**Figure S32.** <sup>1</sup>H NMR spectrum (500 MHz, Acetonitrile-*d*<sub>6</sub>) of **C5** recorded at 298 K.

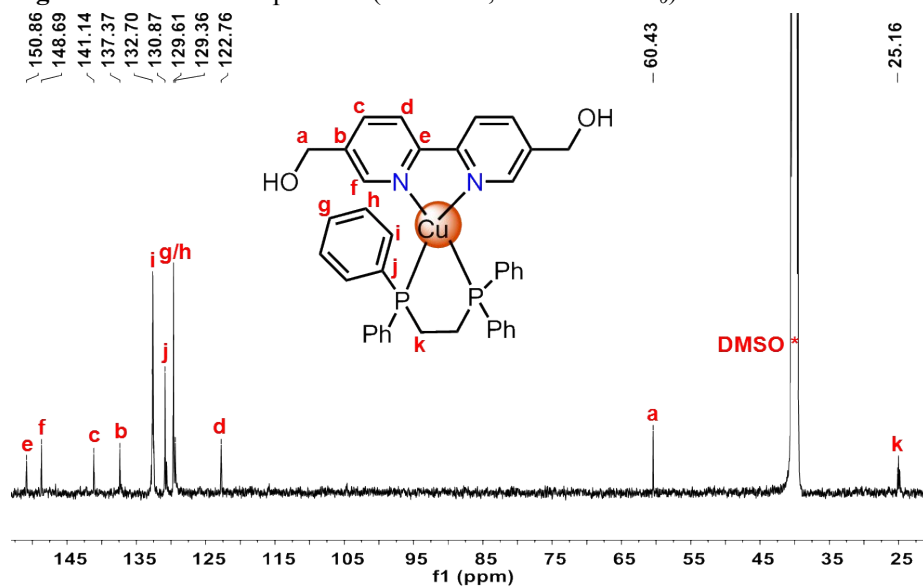


**Figure S33.** <sup>13</sup>C NMR spectrum (100 MHz, DMSO-*d*<sub>3</sub>) of **C5** recorded at 298 K.

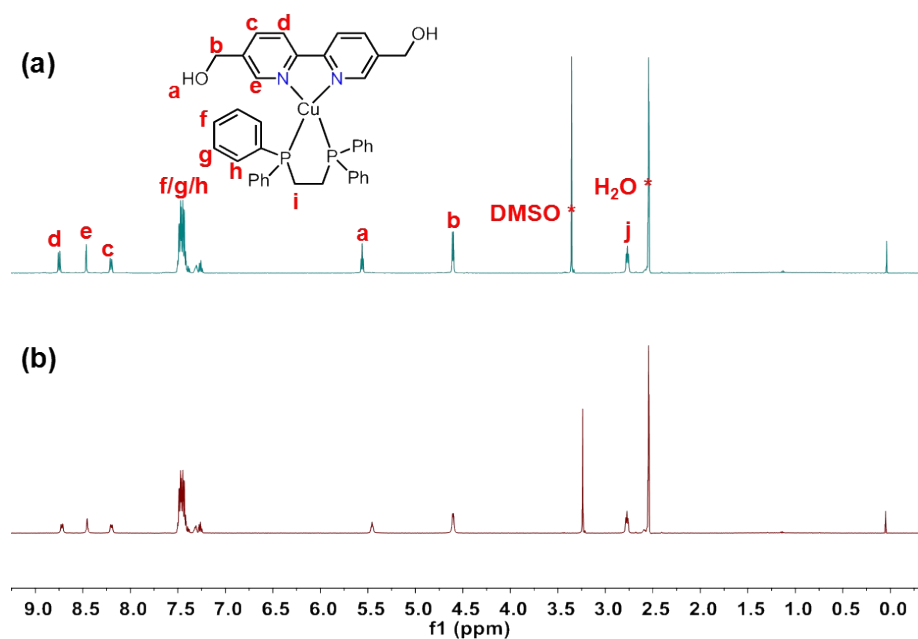


**Figure S34.** Temperature-dependent  $^1\text{H}$  NMR spectrum (500 MHz,  $\text{DMSO-}d_6$ ) of **C5** recorded at (a) 298K, (b) 323K.

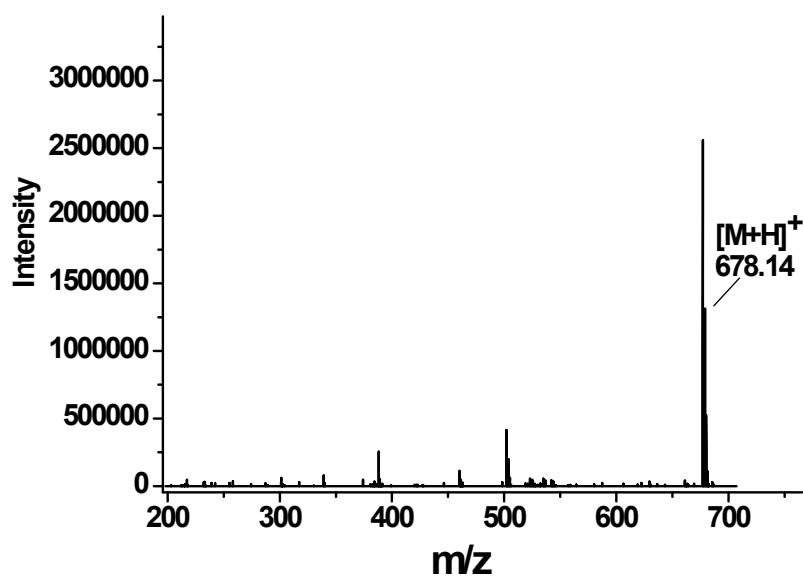


**Figure S35.** ESI-MS spectrum of **C5** in  $\text{CH}_3\text{CN}$  at 298 K.

**Synthesis of Cu(I)-DPPP Complex C6.** Ligand **L4** (34 mg, 0.12 mmol) and Tetrafluoroborate tetra (acetonitrile) copper (38 mg, 0.12 mmol) were dissolved into acetonitrile (3 mL) in an assembly tube, stirred at room temperature for 2 hours. Diphosphine ligands **L8** (1, 3-Bis(diphenylphosphino)propane, 51 mg, 0.12 mmol) was added into mixture and stirred at room temperature for 8 hours. The yellow solution was slowly filtrated. The single crystal was grown by solvent diffusion method with Ethyl ether as diffusion agent. A week later, the Cu(I)-DPPP

complex **C6** was obtained.  $^1\text{H NMR}$  (500 MHz,  $\text{DMSO-}d_6$ )  $\delta$  8.66 (s, 4H), 8.15 (s, 2H), 7.41 (s, 4H), 7.32 (s, 16H), 5.57 (s, 2H), 4.61 (s, 4H), 2.84 (s, 4H), 2.20 – 1.99 (m, 2H).  $^{13}\text{C NMR}$  (126 MHz,  $\text{DMSO-}d_6$ )  $\delta$  150.60, 148.53, 140.93, 137.14, 130.45, 129.29, 122.61, 60.44, 27.24, 19.48.

$[\text{C6-BF}_4]^+$ , calcd  $m/z$  =692.24. found  $m/z$  =692.1.

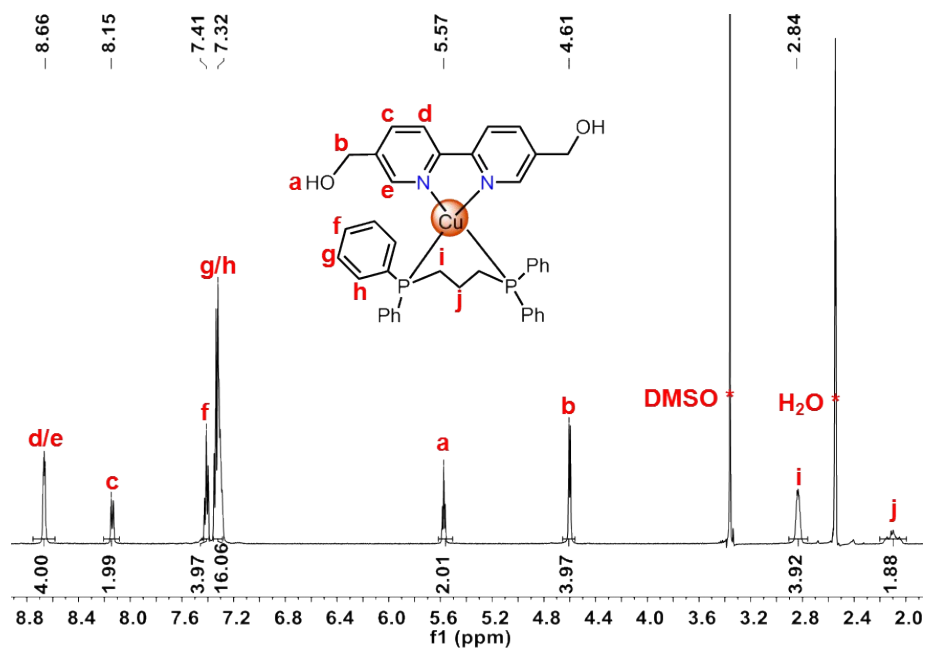


**Figure S36.**  $^1\text{H NMR}$  spectrum (500 MHz,  $\text{Acetonitrile-}d_3$ ) of **C6** recorded at 298 K.

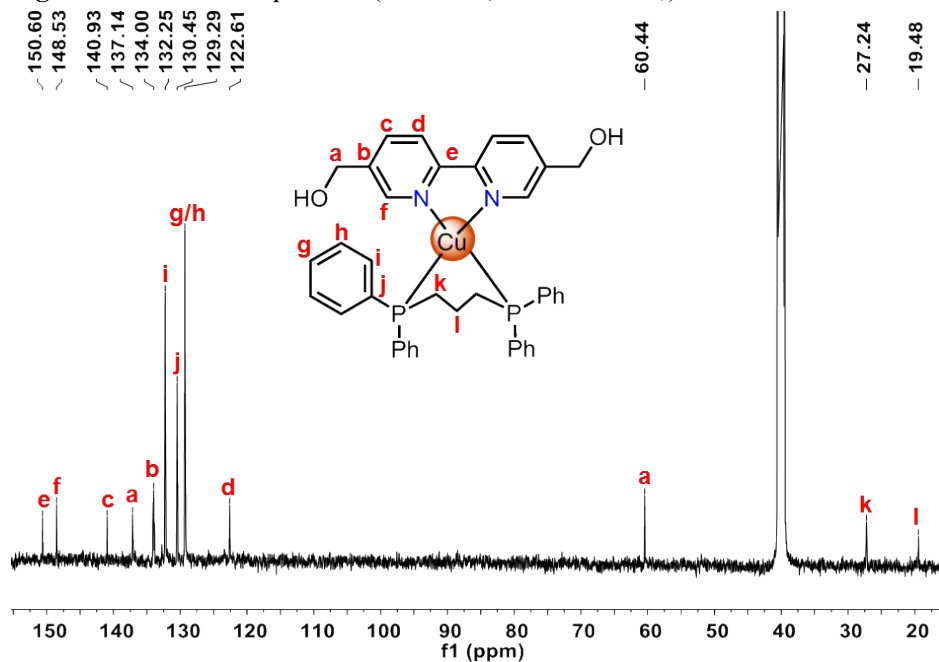


**Figure S37.**  $^{13}\text{C NMR}$  spectrum (500 MHz,  $\text{DMSO-}d_6$ ) of **C6** recorded at 298 K.

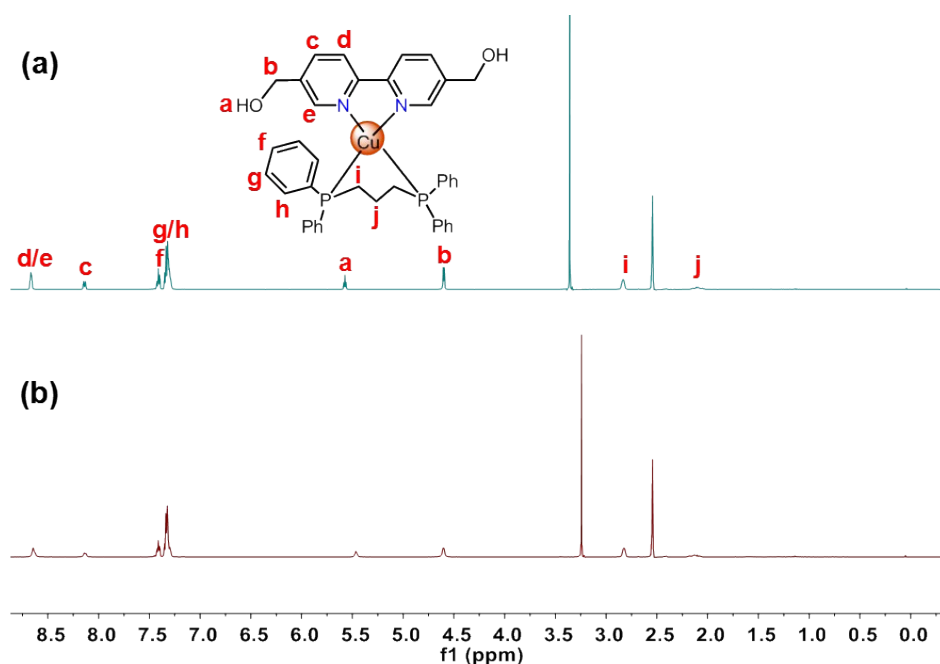


**Figure S38.** Temperature-dependent  $^1\text{H}$  NMR spectrum (500 MHz,  $\text{DMSO-}d_6$ ) of **C6** recorded at (a) 298K, (b) 323K.

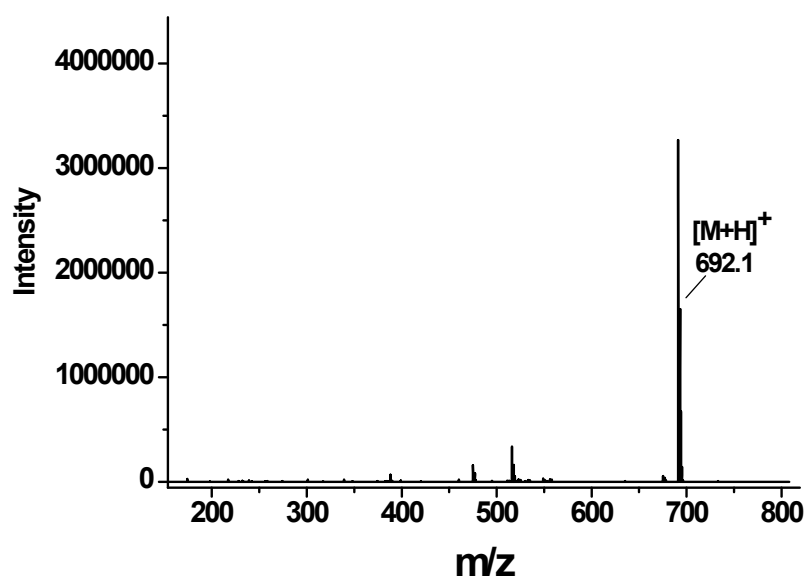


**Figure S39.** ESI-MS spectrum of **C6** in  $\text{CH}_3\text{CN}$  at 298 K.

**Synthesis of Cu(I)-DPPM Complex C7.** Ligand **L1** (20 mg, 0.074 mmol) and Tetrafluoroborate tetra (acetonitrile) copper (23 mg, 0.074 mmol) were dissolved into acetonitrile (3 mL) in an assembly tube, stirred at room temperature for 2 hours. Then added the **L6** Bis(diphenylphosphino)methane (28 mg, 0.074 mmol) stirred at room temperature for 8 hours. The solution was divided into three parts. It was grown by solvent diffusion method with Ethyl ether as diffusion agent. A week later, the Cu(I)-DPPM complex **C7** was obtained.  $^1\text{H}$  NMR (400 MHz, Acetonitrile- $d_3$ )  $\delta$  7.82 (brs, 8H,  $\text{H}^{f/g}$ ), 7.42 (d,  $J = 9.7$  Hz, 4H,  $\text{H}^e$ ), 7.23 (brs, 8H,  $\text{H}^h$ ), 7.05 (brs, 32H,  $\text{H}^{i/j}$ ), 6.01 (m, 4H,  $\text{H}^c$ ), 5.31 (m, 8H,  $\text{H}^{a/b}$ ), 4.55 (d,  $J = 7.5$  Hz, 8H,  $\text{H}^d$ ), 3.65 (s, 4H,



H<sup>k</sup>). <sup>13</sup>C NMR (100 MHz, Chloroform-*d*) δ 155.52 , 138.06 , 132.42 , 132.10 , 130.04 , 128.71 , 123.79 , 122.36 , 118.52 , 69.56 . TOF-ESI-MS: fragment of **C7** with a formula of [L1+Cu+Dppm]<sup>+</sup>, calcd m/z =715.17. found m/z =715.17.

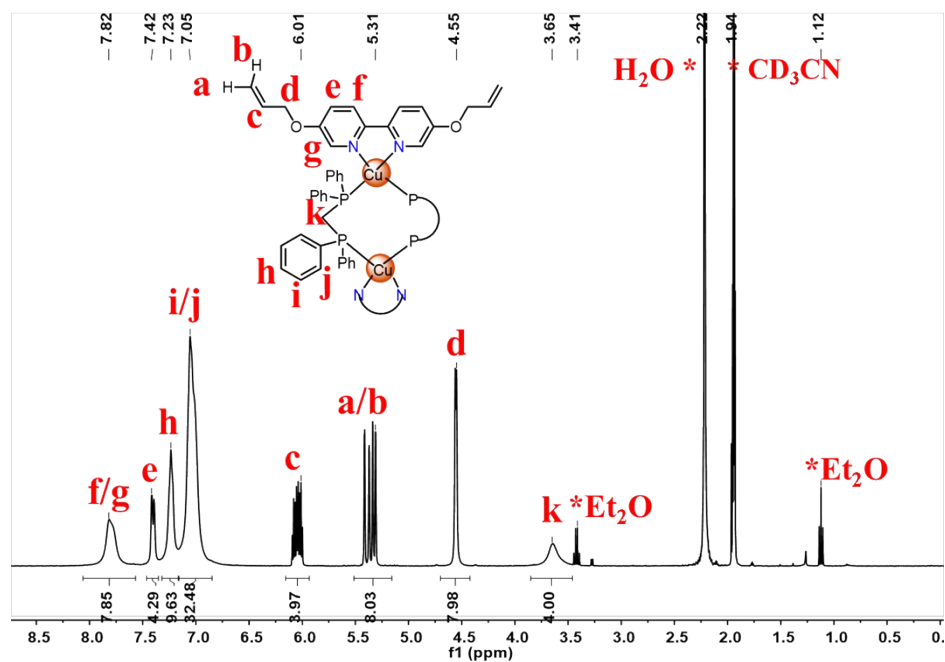


**Figure S40.** <sup>1</sup>H NMR spectrum (400 MHz, Acetonitrile-*d*<sub>3</sub>) of **C7** recorded at 298 K.

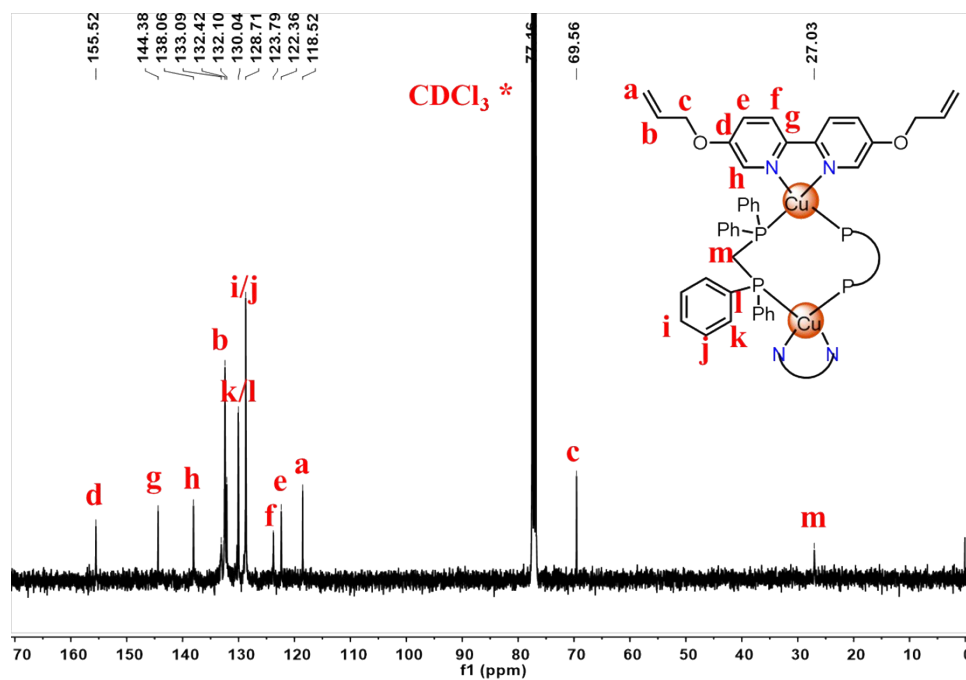


**Figure S41.** <sup>13</sup>C NMR spectrum (100 MHz, Chloroform-*d*) of **C7** recorded at 298 K.

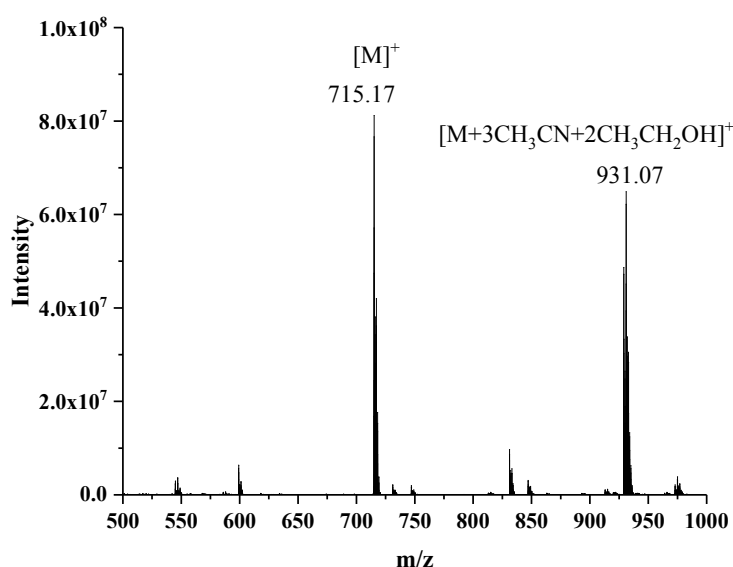


**Figure S42.** ESI-MS spectrum of **C7** in CH<sub>3</sub>CN at 298 K.

**Synthesis of Cu(I)-DPPM Complex C8** Ligand **L2** (20 mg, 0.067 mmol) and Tetrafluoroborate tetra (acetonitrile) copper (21 mg, 0.067 mmol) were dissolved into acetonitrile (3 mL) in an assembly tube, stirred at room temperature for 2 hours. Then added the **L6** Bis(diphenylphosphino)methane (26 mg, 0.067 mmol) stirred at room temperature for 8 hours. The solution was divided into three parts. The single crystal was grown by solvent diffusion method with Ethyl ether as diffusion agent. A week later, the Cu(I)-DPPM complex **C8** was obtained. <sup>1</sup>H NMR (400 MHz, Acetonitrile-*d*<sub>3</sub>) δ 7.79 (brs, 4H, H<sup>g</sup>), 7.69 (s, 4H, H<sup>h</sup>), 7.39 (d, J = 6.3 Hz, 4H, H<sup>f</sup>), 7.24 (brs, 8H, H<sup>i</sup>), 7.06 (brs, 32H, H<sup>g/k</sup>), 5.93 (m, 4H, H<sup>c</sup>), 5.19 (m, 8H, H<sup>a/b</sup>), 4.00 (t, J = 9.5 Hz, 8H, H<sup>e</sup>), 3.66 (s, 4H, H<sup>l</sup>), 2.56 (m, 8H, H<sup>d</sup>). <sup>13</sup>C NMR (100 MHz, Acetonitrile-*d*<sub>3</sub>) δ 156.76, 145.33, 138.73, 135.22, 133.22, 131.05, 123.79, 123.13, 117.88, 69.03, 33.93, 26.79. TOF-ESI-MS: Fragment of **C8** with a formula [**L2**+Cu+Dppm]<sup>+</sup>, calcd m/z = 743.20. found m/z = 743.19.

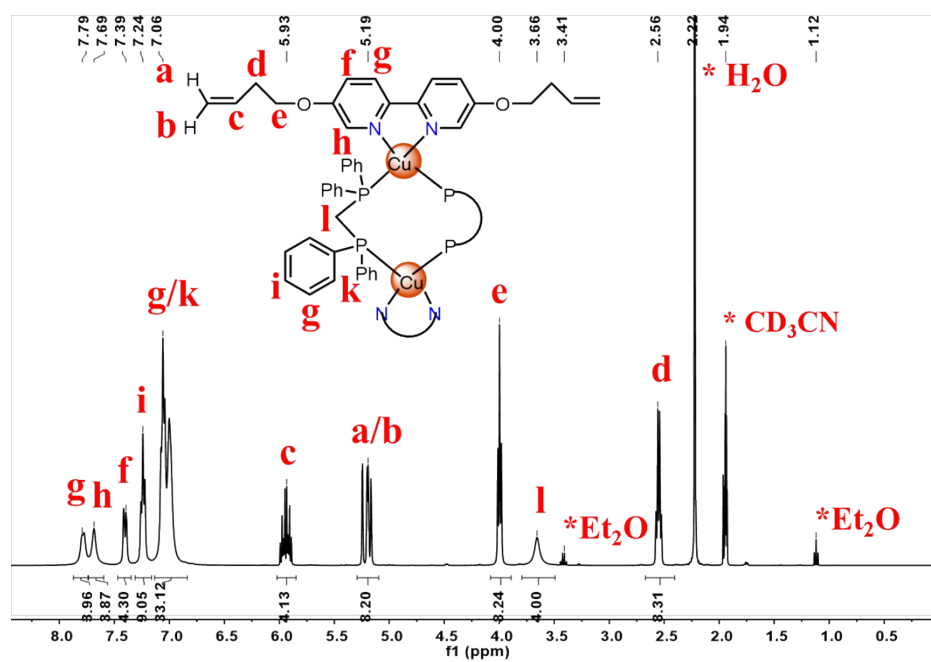


**Figure S43.**  $^1\text{H}$  NMR spectrum (400 MHz,  $\text{Acetonitrile-}d_3$ ) of **C8** recorded at 298 K.

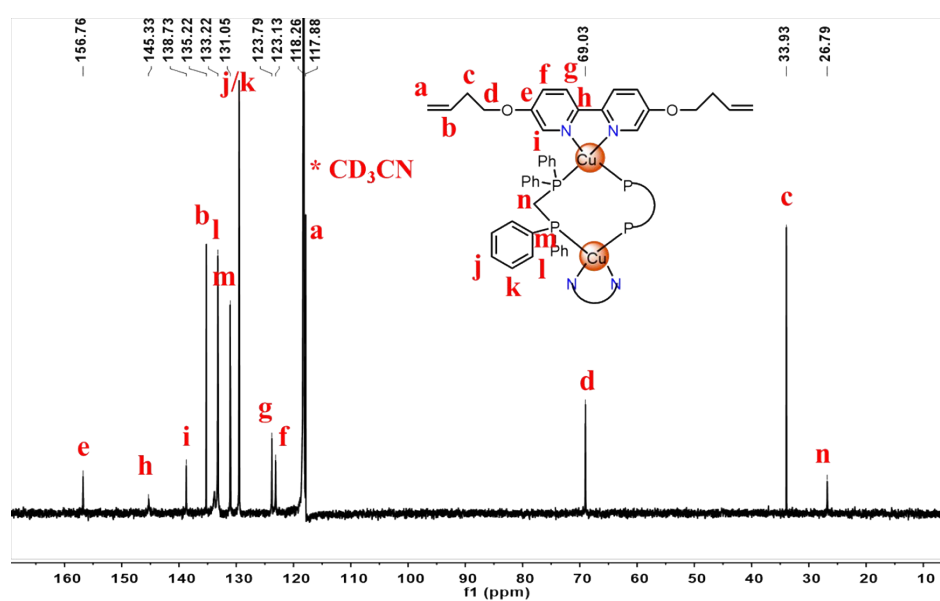


**Figure S44.**  $^{13}\text{C}$  NMR spectrum (100 MHz,  $\text{Acetonitrile-}d_3$ ) of **C8** recorded at 298 K.

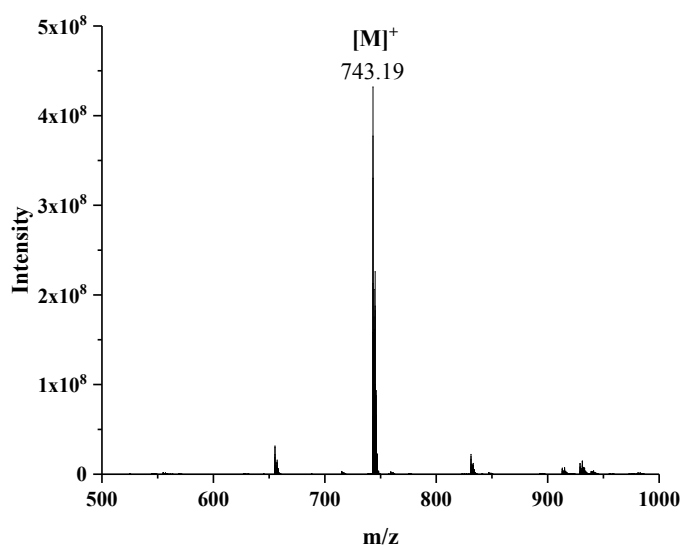


**Figure S45.** TOF-MS spectrum of **C8** in CH<sub>3</sub>CN at 298 K.

**Synthesis of Cu(I)-Dppm Complex C9.** Ligand **L3** (18 mg, 0.067 mmol) and Tetrafluoroborate tetra (acetonitrile) copper (21 mg, 0.067 mmol) were dissolved into acetonitrile (3 mL) in an assembly tube, stirred at room temperature for 2 hours. Then added the **L6** Bis(diphenylphosphino)methane (26 mg, 0.067 mmol) stirred at room temperature for 8 hours. The solution was divided into three parts. The single crystal was grown by solvent diffusion method with Ethyl ether as diffusion agent. A week later, the Cu(I)-Dppm complex **C9** was obtained. <sup>1</sup>H NMR (400 MHz, Acetonitrile-*d*<sub>3</sub>) δ 7.93 (brs, 2H, H<sup>d</sup>), 7.79 (s, 2H, H<sup>e</sup>), 7.50 (d, J = 13.4 Hz, 2H, H<sup>c</sup>), 7.22 (brs, 4H, H<sup>f</sup>), 7.03 (brs, 16H, H<sup>g/h</sup>), 4.81 (s, 4H, H<sup>b</sup>), 3.66 (s, 2H, H<sup>a</sup>), 2.90 (s, 2H, H<sup>i</sup>). <sup>13</sup>C NMR (100 MHz, Acetonitrile-*d*<sub>3</sub>) δ 155.47, 139.22, 133.20, 131.03, 129.46, 124.06, 123.13, 78.25, 57.44, 26.45. [**C9**-BF<sub>4</sub><sup>-</sup>+H<sub>2</sub>O]<sup>+</sup>, calcd m/z = 1528.32. found m/z = 1528.13.

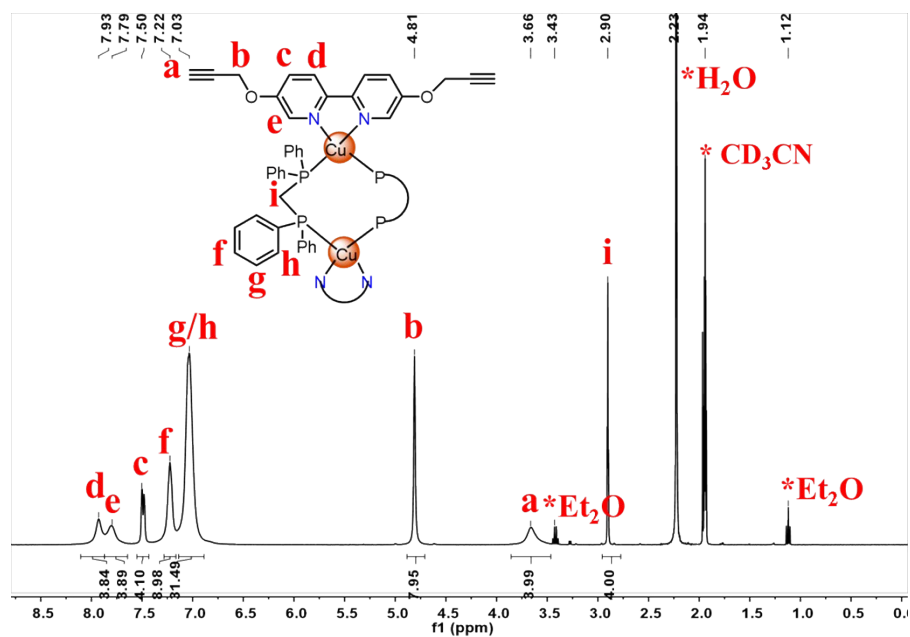


Figure S46.  $^1\text{H}$  NMR spectrum (400 MHz, Acetonitrile- $d_3$ ) of **C9** recorded at 298 K.

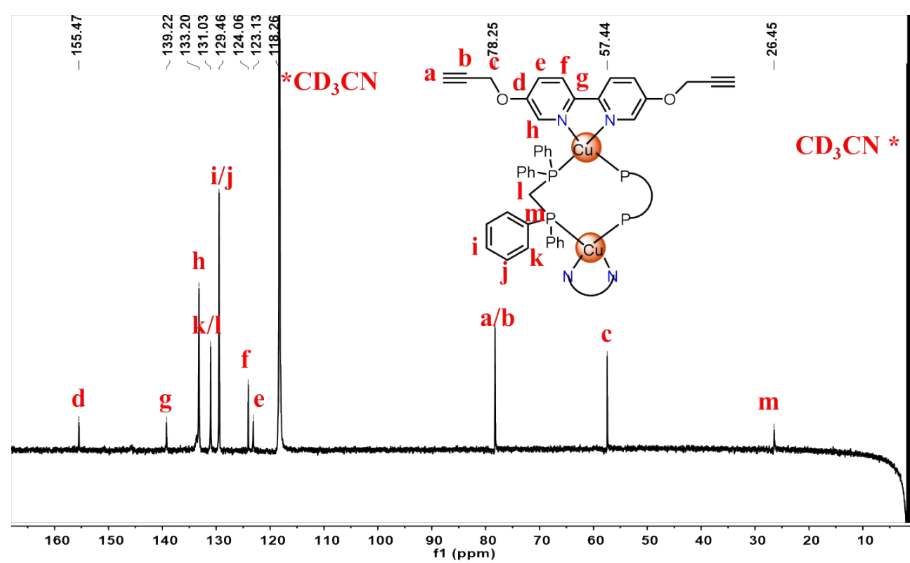
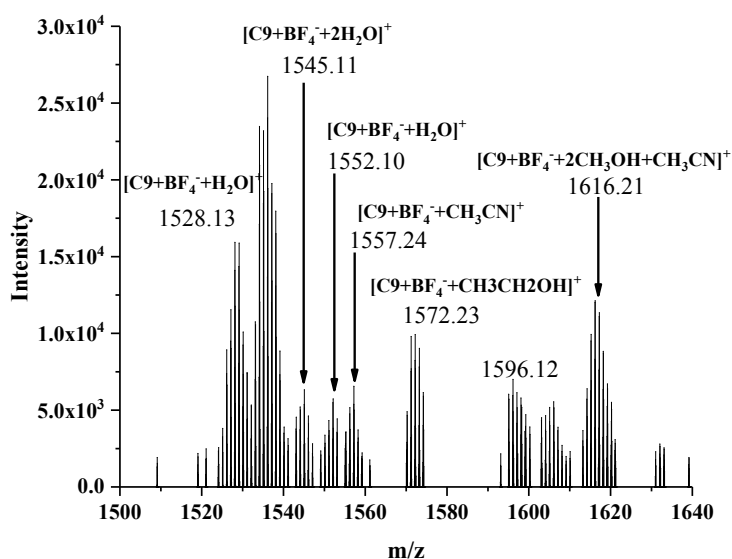
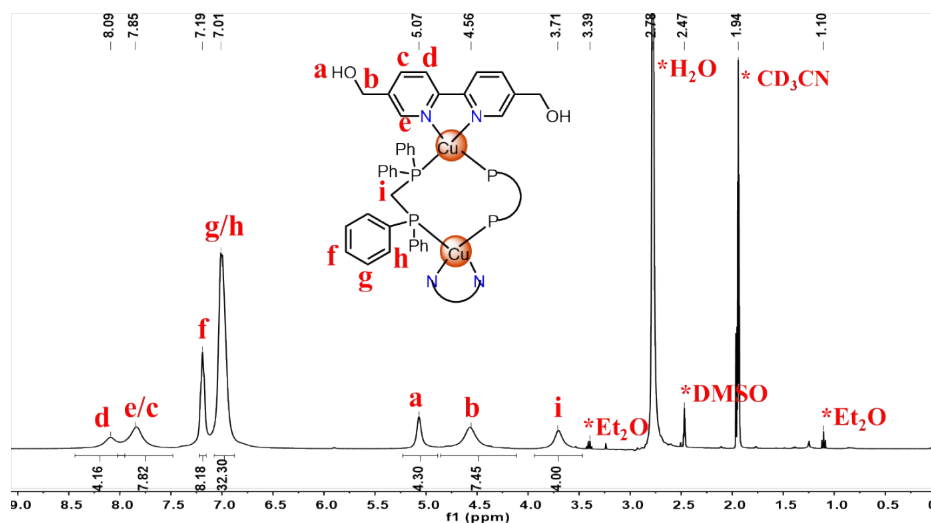


Figure S47.  $^{13}\text{C}$  NMR spectrum (100 MHz, Acetonitrile- $d_3$ ) of **C9** recorded at 298 K.



**Figure S48.** TOF-MS spectrum of **C9** in  $\text{CH}_3\text{CN}$  at 298 K.

**Synthesis of Cu(I)-Dppm Complex C10.** Ligand **L4** (14 mg, 0.067 mmol) and Tetrafluoroborate tetra (acetonitrile) copper (21 mg, 0.067 mmol) were dissolved into acetonitrile (3 mL) in an assembly tube, stirred at room temperature for 2 hours. Then added the **L6** Bis(diphenylphosphino)methane (26 mg, 0.067 mmol) stirred at room temperature for 8 hours. The solution was divided into three parts. The single crystal was grown by solvent diffusion method with Ethyl ether as diffusion agent. A week later, the Cu(I)-DPPM complex **C10** was obtained.  $^1\text{H}$  NMR (400 MHz, Acetonitrile- $d_3$ )  $\delta$  8.09 (brs, 2H,  $\text{H}^d$ ), 7.85 (brs, 4H,  $\text{H}^{e/c}$ ), 7.19 (brs, 4H,  $\text{H}^f$ ), 7.01 (brs, 16H,  $\text{H}^{g/h}$ ), 5.07 (s, 2H,  $\text{H}^a$ ), 4.56 (s, 4H,  $\text{H}^b$ ), 3.71 (s, 2H,  $\text{H}^i$ ).  $^{13}\text{C}$  NMR (100 MHz, Acetonitrile- $d_3$ )  $\delta$  150.69, 139.13, 133.13, 130.53, 129.18, 62.23, 26.40. TOF-ESI-MS:  $[\text{C10}-\text{BF}_4]^-$ , calcd  $m/z$  = 1413.28 found  $m/z$  = 1413.07.  $[\text{C10}+\text{BF}_4+\text{CH}_3\text{CH}_2\text{OH}]^+$ , calcd  $m/z$  = 1459.32 found  $m/z$  = 1459.03.



**Figure S49.**  $^1\text{H}$  NMR spectrum (400 MHz, Acetonitrile- $d_3$ ) of **C10** recorded at 298 K.

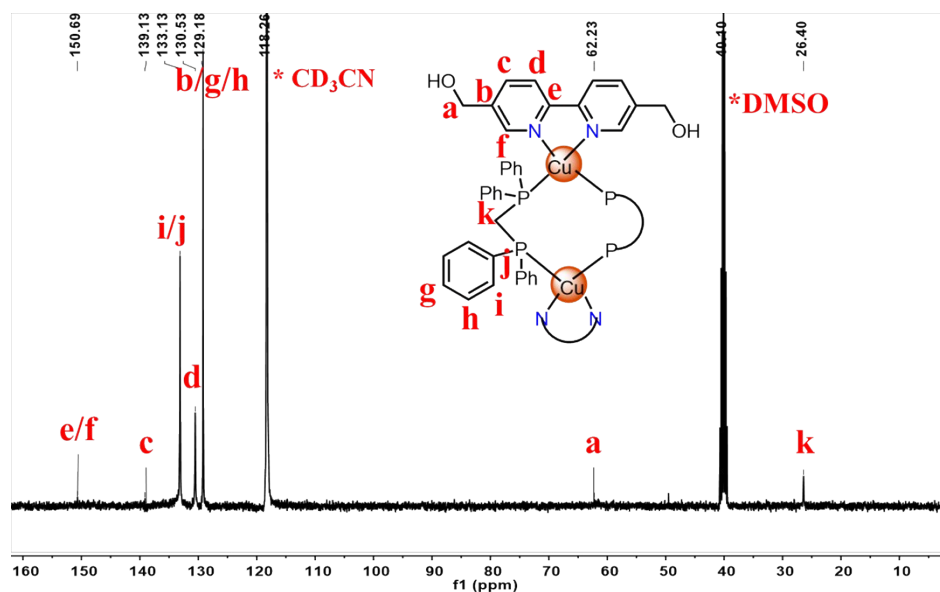


**Figure S50.**  $^{13}\text{C}$  NMR spectrum (100 MHz, Acetonitrile- $d_3$ ) of **C10** recorded at 298 K.

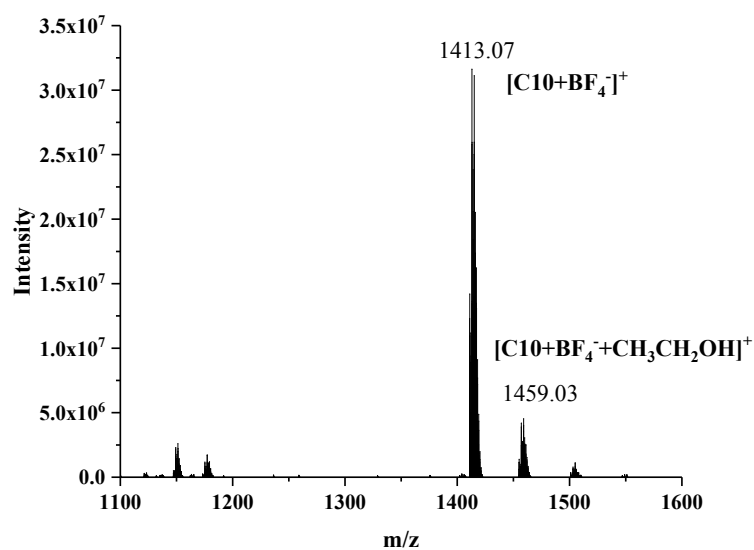


**Figure S51.** TOF-MS spectrum of **C10** in  $\text{CH}_3\text{CN}$  at 298 K.

#### **S4. X-ray crystallography of clusters **C1**, **C2**, **C5**, **C6**, **C9** and **C10**.**

X-ray diffraction data of the crystals of complexes **C1**, **C2**, **C5**, **C6**, **C9** and **C10** were collected using Bruker D8 Venture spectrometer. The diffraction data reduction and integration were performed by the Bruker SAINT software. Positions of the Cu atoms and most of the non-hydrogen atoms were found using the direct methods program in the Bruker SHELXTL software package.<sup>[2-3]</sup> Crystal structure refinement data are given in Table S1. The selected geometric parameters are

shown in Tables S2-S3. These data can be achieved via the Cambridge Crystallographic Data Centre deposit @ ccdc. cam.Ac.uk, <http://www.ccdc.cam.ac.uk/deposit>(CCDC Number: **2050236-2050238, 2050240, 2070930, 2070931**).

**Table S1.** Crystallographic data for Cu(I)-phosphine complexes **C1, C2, C5, C6, C9** and **C10**.

	<b>C1</b>	<b>C2</b>	<b>C5</b>	<b>C6</b>	<b>C9</b>	<b>C10</b>
formula	C <sub>52</sub> H <sub>44</sub> CuBF <sub>4</sub> N <sub>2</sub> O <sub>3</sub> P <sub>2</sub>	C <sub>54</sub> H <sub>48</sub> CuBF <sub>4</sub> N <sub>2</sub> O <sub>3</sub> P <sub>2</sub>	C <sub>40</sub> H <sub>40</sub> BCuF <sub>4</sub> N <sub>2</sub> O <sub>2</sub> P <sub>2</sub>	C <sub>39</sub> H <sub>37</sub> BCuF <sub>4</sub> N <sub>2</sub> O <sub>2</sub> P <sub>2</sub>	C <sub>82</sub> H <sub>68</sub> Cu <sub>2</sub> B <sub>2</sub> F <sub>8</sub> N <sub>4</sub> O <sub>4</sub> P <sub>4</sub>	C <sub>74</sub> H <sub>68</sub> Cu <sub>2</sub> B <sub>2</sub> F <sub>8</sub> N <sub>4</sub> O <sub>4</sub> P <sub>4</sub>
FW	957.23	985.23	892.5	778.01	1598.06	1501.96
crystal size [mm]	0.15, 0.11, 0.10	0.18, 0.14, 0.11	0.14, 0.13, 0.11	0.14, 0.12, 0.09	0.27, 0.23, 0.19	0.26, 0.22, 0.18
crystal system	monoclinic	monoclinic	triclinic	triclinic	monoclinic	monoclinic
space group	P2 <sub>1</sub> /c	P2 <sub>1</sub> /c	P-1	P-1	P2 <sub>1</sub> /c	P2 <sub>1</sub> /c
<i>a</i> [Å]	14.4327(13)	14.5351(5)	11.6111(4)	11.4331(7)	14.3863(16)	12.5434(8)
<i>b</i> [Å]	16.4636(15)	16.4982(6)	14.5775(4)	13.4144(11)	16.3399(11)	12.2727(7)
<i>c</i> [Å]	21.6414(18)	21.4505(8)	23.4859(7)	14.0165(10)	16.536(2)	22.3019(13)
$\alpha$ [°]	90	90	80.009(2)	63.396(8)	90	90
$\beta$ [°]	99.865(3)	99.200(3)	88.285(3)	81.393(6)	111.132(14)	99.668(6)
$\gamma$ [°]	90	90	84.684(3)	67.809(7)	90	90
<i>V</i> [Å <sup>3</sup> ]	5066.3(8)	5077.7(3)	3897.7(2)	1779.2(3)	3625.7(7)	3384.4(4)
<i>Z</i>	38	4	2	2	2	2
$\rho_{\text{calcd}}$ , [g/cm <sup>-3</sup> ]	2.084	1.289	1.364	1.452	1.464	1.474
$\mu$ [mm <sup>-1</sup> ]	4.285	0.551	0.697	0.763	0.751	0.799
<i>F</i> (000)	3040.0	2040.0	1654.0	802.0	1640	1544
$2\theta_{\text{max}}$ [°]	50.48	59.09	59.16	59.06	59.2	59.2
no. unique data	9961	12168	18215	8255	8799	8117
parameters	633	605	952	462	478	444
GOF [F <sup>2</sup> ] <sup>a</sup>	1.028	1.030	1.034	0.0591	1.04	1.03
R [F <sup>2</sup> >2 $\sigma$ (F <sup>2</sup> )], wR[F <sup>2</sup> ] <sup>b</sup>	0.0974, 0.1545	0.0846, 0.1779	0.0621, 0.1548	0.0591, 0.1536	0.0677, 0.1257	0.0623, 0.1660



GOF =  $[w(F_o^2 - F_c^2)^2]/(n - p)^{1/2}$ , where  $n$  and  $p$  denote the number of data points and the number of parameters, respectively. [b] R1 =  $(\|F_o\| - \|F_c\|)/\|F_o\|$ ; wR2 =  $[w(F_o^2 - F_c^2)^2]/[w(F_o^2)^2]^{1/2}$ , Where  $w=1/[\sigma^2(F_o^2)+(aP)^2+bP]$  and  $P=[\max(0, F_o^2)+2F_c^2]/3$ .

**Table S2.** Selective bond distance (Å) and angle (°) of C1

Bond	Dist.[Å]	Bond	Dist.[Å]
C(1)-P(1)	1.826(4)	C(40)-O(2)	1.365(4)
C(6)-O(3)	1.397(4)	C(41)-N(2)	1.346(4)
C(7)-P(1)	1.822(3)	C(42)-O(2)	1.443(5)
C(13)-O(3)	1.398(4)	C(45)-O(1)	1.433(4)
C(18)-P(2)	1.833(4)	C(48)-P(1)	1.819(4)
C(19)-P(2)	1.828(4)	C(80)-O(4)	1.447(7)
C(26)-P(2)	1.827(3)	C(82)-O(4)	1.472(8)
C(32)-N(1)	1.357(4)	Cu(1)-N(1)	2.051(3)
C(33)-O(1)	1.360(4)	Cu(1)-N(2)	2.093(3)
C(36)-N(1)	1.346(4)	Cu(1)-P(1)	2.2545(10)
C(37)-N(2)	1.340(4)	Cu(1)-P(2)	2.2460(10)
Bond	Angel[°]	Bond	Angel[°]
C(2)-C(1)-P(1)	123.4(3)	N(1)-Cu(1)-P(2)	130.20(8)
C(6)-C(1)-P(1)	119.5(3)	N(2)-Cu(1)-P(2)	106.92(8)
C(5)-C(6)-O(3)	117.9(3)	N(1)-Cu(1)-P(1)	110.11(8)
C(12)-C(7)-P(1)	117.9(3)	N(2)-Cu(1)-P(1)	111.39(8)
C(8)-C(7)-P(1)	123.3(3)	P(2)-Cu(1)-P(1)	112.34(4)
C(14)-C(13)-O(3)	121.8(3)	C(36)-N(1)-C(32)	119.4(3)
C(18)-C(13)-O(3)	115.4(3)	C(36)-N(1)-Cu(1)	114.7(2)
C(13)-C(18)-P(2)	118.9(3)	C(32)-N(1)-Cu(1)	125.4(2)
C(17)-C(18)-P(2)	123.5(3)	C(37)-N(2)-C(41)	120.1(3)
C(24)-C(19)-P(2)	118.7(3)	C(37)-N(2)-Cu(1)	113.1(2)
C(20)-C(19)-P(2)	121.9(3)	C(41)-N(2)-Cu(1)	126.3(2)
C(27)-C(26)-P(2)	124.5(3)	C(33)-O(1)-C(45)	118.6(3)
C(31)-C(26)-P(2)	116.8(3)	C(40)-O(2)-C(42)	117.2(3)
N(1)-C(32)-C(33)	121.7(3)	C(6)-O(3)-C(13)	118.0(3)
N(1)-C(36)-C(35)	121.0(3)	C(80)-O(4)-C(82)	112.8(5)
N(1)-C(36)-C(37)	115.5(3)	C(48)-P(1)-C(7)	102.86(16)
N(2)-C(37)-C(38)	121.2(3)	C(48)-P(1)-C(1)	102.52(17)
N(2)-C(37)-C(36)	115.9(3)	C(7)-P(1)-C(1)	105.24(17)
O(2)-C(40)-C(39)	117.7(3)	C(48)-P(1)-Cu(1)	115.27(12)
O(2)-C(40)-C(41)	123.9(3)	C(7)-P(1)-Cu(1)	117.16(13)
N(2)-C(41)-C(40)	121.6(3)	C(1)-P(1)-Cu(1)	112.21(11)
O(2)-C(42)-C(43)	108.2(3)	C(26)-P(2)-C(19)	102.63(16)
C(49)-C(48)-P(1)	124.0(3)	C(26)-P(2)-C(18)	104.35(16)
C(52)-C(48)-P(1)	117.9(3)	C(19)-P(2)-C(18)	102.59(16)
O(4)-C(80)-C(84)	103.4(5)	C(26)-P(2)-Cu(1)	109.09(11)
O(4)-C(82)-C(83)	110.8(6)	C(19)-P(2)-Cu(1)	124.58(12)

N(1)-Cu(1)-N(2)	79.92(11)	C(18)-P(2)-Cu(1)	111.61(12)
-----------------	-----------	------------------	------------

**Table S3.** Selective bond distance (Å) and angle (°) of **C2**

Bond	Dist.[Å]	Bond	Dist.[Å]
Cu01-P2	2.2434(9)	O2-C18	1.393(4)
Cu01-P1	2.2496(8)	O2-C19	1.386(4)
Cu01-N1	2.072(3)	O3-C53	1.362(4)
Cu01-N2	2.049(3)	O3-C46	1.432(4)
P2-C7	1.820(3)	N1-C50	1.342(4)
P2-C13	1.835(3)	N1-C54	1.349(4)
P2-C1	1.829(3)	O1-C38	1.361(5)
P1-C31	1.826(3)	O1-C42	1.753(8)
P1-C25	1.818(3)	N2-C41	1.348(4)
P1-C24	1.833(3)	N2-C37	1.346(4)
Bond	Angel[°]	Bond	Angel[°]
P2-Cu01-P1	111.97(3)	C17-C18-O2	122.5(3)
N1-Cu01-P2	106.82(8)	N1-C50-C41	115.4(3)
N1-Cu01-P1	113.05(7)	N1-C50-C51	120.8(3)
N2-Cu01-P2	128.26(8)	C32-C31-P1	123.3(3)
N2-Cu01-P1	111.43(8)	C36-C31-P1	117.6(2)
N2-Cu01-N1	80.19(11)	O3-C53-C54	125.1(3)
C7-P2-Cu01	122.92(11)	O3-C53-C52	116.3(3)
C7-P2-C13	101.54(14)	C8-C7-P2	117.6(3)
C7-P2-C1	103.92(15)	C12-C7-P2	122.6(3)
C13-P2-Cu01	112.66(10)	C30-C25-P1	116.8(2)
C1-P2-Cu01	110.76(10)	C26-C25-P1	124.1(3)
C1-P2-C13	102.88(14)	N1-C54-C53	122.1(3)
C31-P1-Cu01	116.39(11)	O2-C19-C24	119.4(3)
C31-P1-C24	103.91(14)	C20-C19-O2	118.3(3)
C25-P1-Cu01	115.47(11)	C19-C24-P1	118.9(2)
C25-P1-C31	102.47(15)	C23-C24-P1	123.3(3)
C25-P1-C24	104.49(14)	C18-C13-P2	117.8(2)
C24-P1-Cu01	112.64(10)	C14-C13-P2	124.0(2)
C19-O2-C18	118.6(2)	C6-C1-P2	123.5(2)
C53-O3-C46	117.6(3)	C6-C1-C2	118.6(3)
C50-N1-Cu01	113.5(2)	C2-C1-P2	117.8(3)
C50-N1-C54	119.7(3)	N2-C41-C50	116.1(3)
C54-N1-Cu01	126.3(2)	N2-C41-C40	121.0(3)
C38-O1-C42	112.6(3)	N2-C37-C38	121.7(3)
C41-N2-Cu01	113.9(2)	O1-C38-C37	123.4(4)
C37-N2-Cu01	126.1(2)	O1-C38-C39	117.4(3)
C37-N2-C41	119.4(3)	C43-C42-O1	108.2(5)

O2-C18-C13	115.5(3)	
------------	----------	--

**Table S4.** Selective bond distance (Å) and angle (°) of **C5**

Bonds	Dist. [Å]	Bond	Angles[°]
Cu01-P003	2.2503(8)	P15-Cu01-P003	91.29(3)
Cu01-P15	2.2532(9)	N7-Cu01-P003	120.41(8)
Cu01-N7	2.042(3)	N7-Cu01-P15	121.78(8)
Cu01-N6	2.033(3)	N6-Cu01 -P003	125.67(8)
Cu02-P005	2.2449(9)	N6-Cu01 -P15	120.37(8)
Cu02-P006	2.2507(9)	N6-Cu01-N7	81.19(10)
Cu02-N9	2.030(3)	P006-Cu02-P005	91.51(3)
Cu02-N8	2.026(3)	N9-Cu02 -P005	115.81(8)
P003-C00J	1.829(3)	N9-Cu02 -P006	122.40(8)
P003-C00K	1.821(3)	N8-Cu02 -P005	131.25(8)
P003-C01J	1.841(3)	N8-Cu02 -P006	118.99(8)
P15-C00T	1.817(3)	N8-Cu02 -N9	80.67(10)

**Table S5.** Selective bond distance (Å) and angle (°) of **C6**

Bond	Dist. [Å]	Bond	Angles [°]
Cu1-P2	2.2506(9)	P1-Cu1-P2	104.96(3)
Cu1-P1	2.2345(9)	N1-Cu1-P2	115.66(8)
Cu1-N1	2.060(3)	N1-Cu1-P1	125.00(8)
Cu1-N2	2.059(3)	N2-Cu1-P2	107.44(8)
P2-C35	1.824(3)	N2-Cu1-P1	121.58(8)
P2-C26	1.818(3)	N2-Cu1-N1	80.26(10)

**Table S6.** Selective bond distance (Å) and angle (°) of **C9**.

Bond	Dist.[Å]	Bond	Dist.[Å]
Cu1-P2	2.2466(9)	P3-C45	1.841(5)
Cu1-P3	2.2259(10)	O1-C4	1.381(5)
Cu1-N1	2.064(3)	O1-C18	1.432(5)
Cu1-N2	2.105(3)	O2-C10	1.352(5)
P2-C21	1.818(4)	O2-C14	1.439(5)
P2-C27	1.836(5)	N1-C7	1.359(6)
P2-C45	1.846(5)	N1-C11	1.313(6)
P3-C33	1.833(4)	N2-C5	1.336(6)
P3-C39	1.840(5)	N2-C1	1.353(6)
Bond	Angel[°]	Bond	Angel[°]
P2-Cu1-P3	136.39(5)	O2-C10-C11	115.1(4)
P2-Cu1-N1	100.00(8)	Cu1-P3-C45	122.75(13)
P2-Cu1-N2	102.23(8)	C33-P3-C39	103.19(15)

P3-Cu1-N1	118.06(8)	N1-C11-C10	123.2(4)	
O1-C4-C3	126.4(4)	C33-P3-C45	102.21(17)	
P3-Cu1-N2	105.24(8)	O2-C14-C15	107.9(4)	
O1-C4-C5	114.5(4)	C39-P3-C45	103.2(2)	
N1-Cu1-N2	78.72(12)	C4-O1-C18	118.6(3)	O1-
Cu1-P2-C21	119.45(13)	C18-C19	112.0(3)	
N2-C5-C4	123.3(4)	C10-O2-C14	117.4(3)	
Cu1-P2-C27	105.14(12)	Cu1-N1-C7	115.8(3)	P2-
N1-C7-C1	115.5(4)	C21-C22	117.6(3)	
Cu1-P2-C45	117.33(12)	Cu1-N1-C11	124.5(3)	P2-
N1-C7-C8	119.7(4)	C21-C26	124.1(3)	
C21-P2-C27	103.97(19)	C7-N1-C11	119.6(4)	Cu1-
C21-P2-C45	107.1(2)	N2-C1	115.1(3)	Cu1-N2-C5
C27-P2-C45	101.4(2)		126.3(3)	
Cu1-P3-C33	113.36(14)	C1-N2-C5	118.5(4)	
O2-C10-C9	126.8(4)	N2-C1-C2	120.4(4)	
Cu1-P3-C39	110.02(12)	N2-C1-C7	114.8(4)	

**Table S7.** Selective bond distance (Å) and angle (°) of **C10**

Bond	Dist.[Å]	Bond	Dist.[Å]	
Cu1-P1	2.2209(10)	P2-C32	1.835(4)	
Cu1-P2	2.2595(10)	P2-C38	1.839(4)	
Cu1-N1	2.066(3)	O1-C4	1.393(6)	
Cu1-N2	2.099(4)	O2-C56	1.418(5)	
P1-C15	1.831(4)	N1-C9	1.352(5)	
P1-C21	1.837(4)	N1-C13	1.341(5)	
P1-C38_a	1.845(4)	N2-C2	1.339(5)	
P2-C26	1.817(4)	N2-C8	1.348(5)	
Bond	Angel[°]	Bond	Angel[°]	
P1-Cu1-P2	137.29(4)	Cu1-P2-C38	117.22(12)	
P1-Cu1-N1	120.80(10)	C26-P2-C32	104.41(17)	
P1-Cu1-N2	105.75(8)	C26-P2-C38	106.86(17)	
O1-C4-C3	108.6(4)	N1-C13-C12	123.6(3)	
P2-Cu1-N1	96.14(8)	C32-P2-C38	101.90(17)	
P2-Cu1-N2	101.28(9)	Cu1-N1-C9	114.4(2)	P1-
N1-Cu1-N2	79.30(12)	C15-C16	120.5(3)	
Cu1-P1-C15	115.52(12)	Cu1-N1-C13	124.8(3)	P1-
N2-C8-C9	115.3(3)	C15-C20	120.2(3)	
Cu1-P1-C21	106.95(12)	C9-N1-C13	118.9(3)	
N2-C8-C7	121.0(3)	C4-O1-H1	109.00	
Cu1-P1-C38_a	125.55(12)	Cu1-N2-C8	113.8(2)	
N1-C9-C10	120.8(3)	C2-N2-C8	118.7(3)	
C15-P1-C21	101.85(17)	Cu1-N2-C2	127.5(2)	

N1-C9-C8	115.6(3)	P1-C21-C22	122.6(3)
C15-P1-C38_a	101.91(17)	N2-C2-C3	123.6(3)
C21-P1-C38_a	101.98(17)	P1-C21-C57	118.4(3)
Cu1-P2-C26	115.46(12)	P2-C26-C27	124.6(3)
Cu1-P2-C32	109.42(11)	P2-C26-C31	116.6(3)

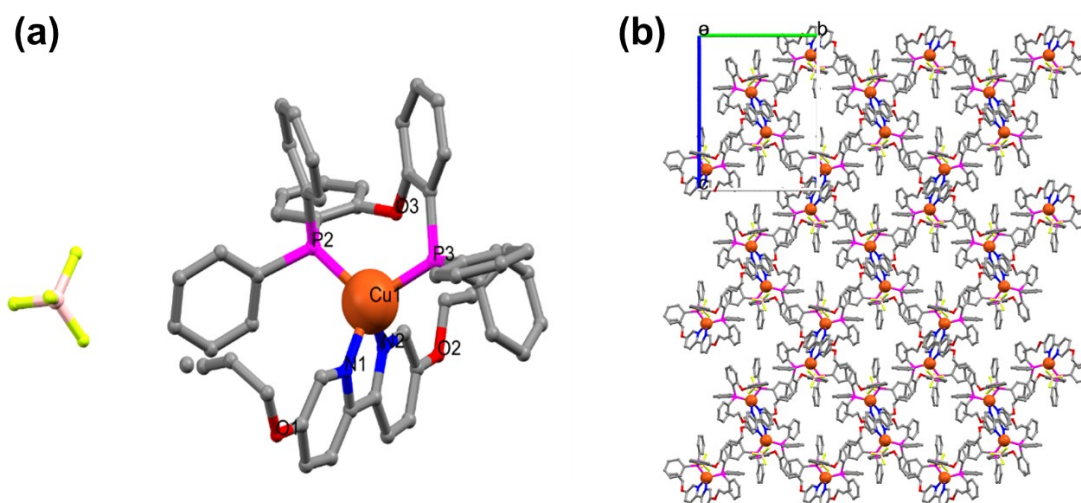


**Figure S52.** The single crystal of complex **C1** (a) and stacking structure(b).

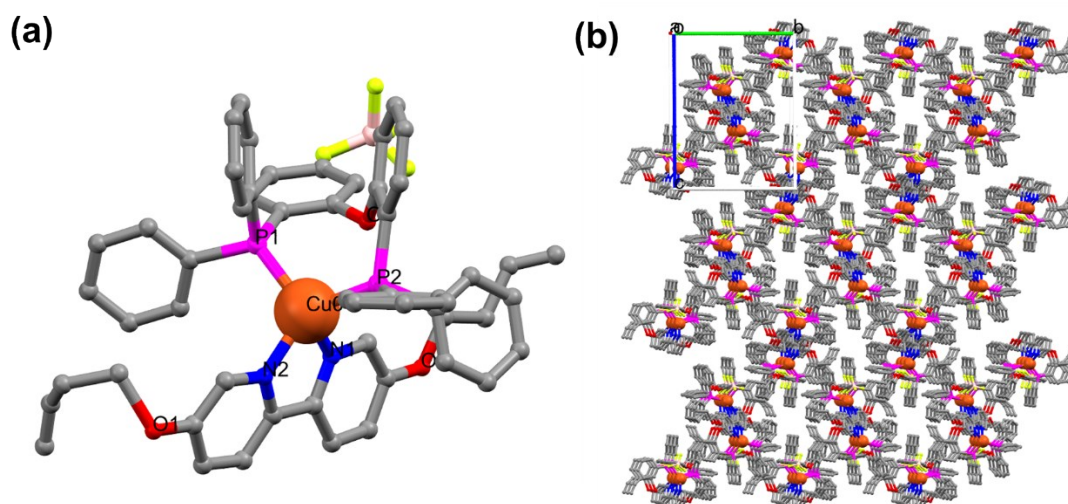


**Figure S53.** The single crystal of complex **C2** (a) and stacking structure(b).

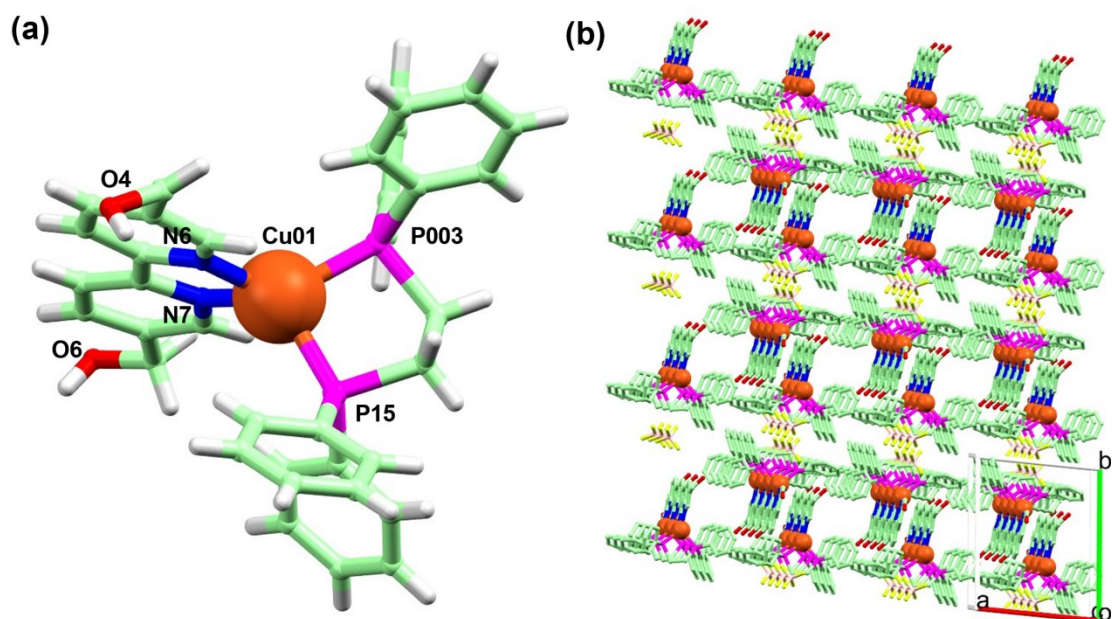


**Figure S54.** The single crystal of complex **C5** (a) and stacking structure(b).

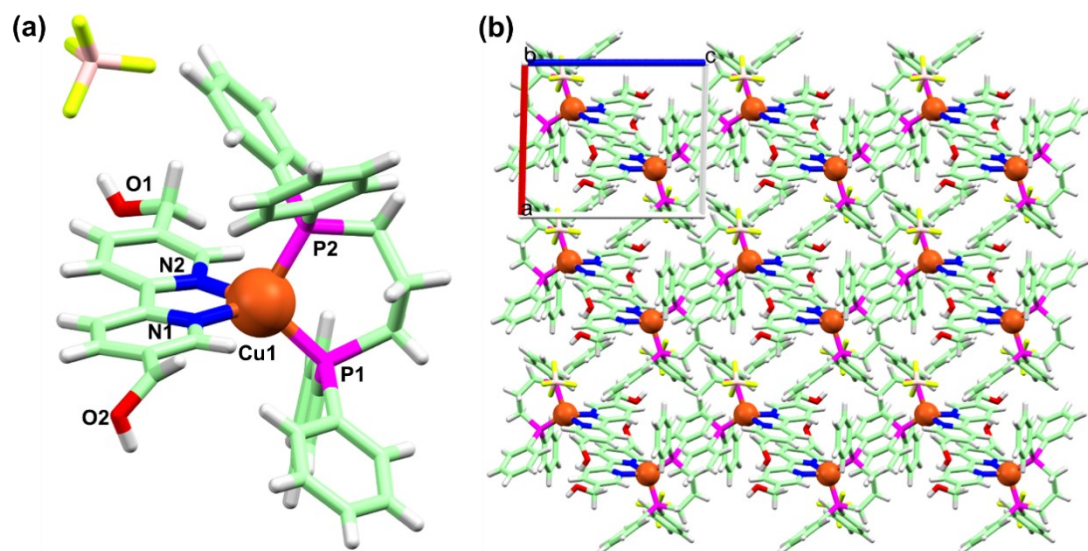


**Figure S55.** The single crystal of complex **C6** (a) and stacking structure(b).

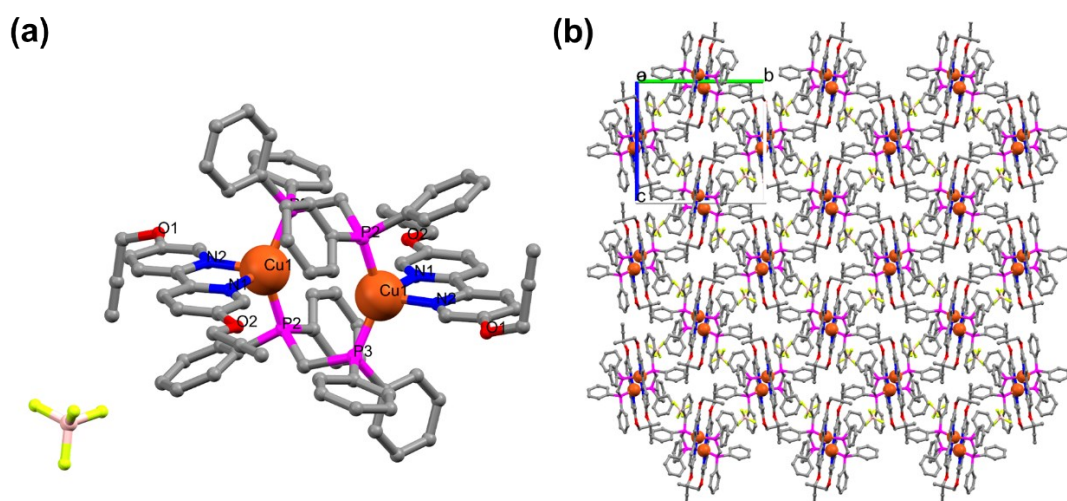


**Figure S56.** The single crystal of complex **C9** (a) and stacking structure(b).

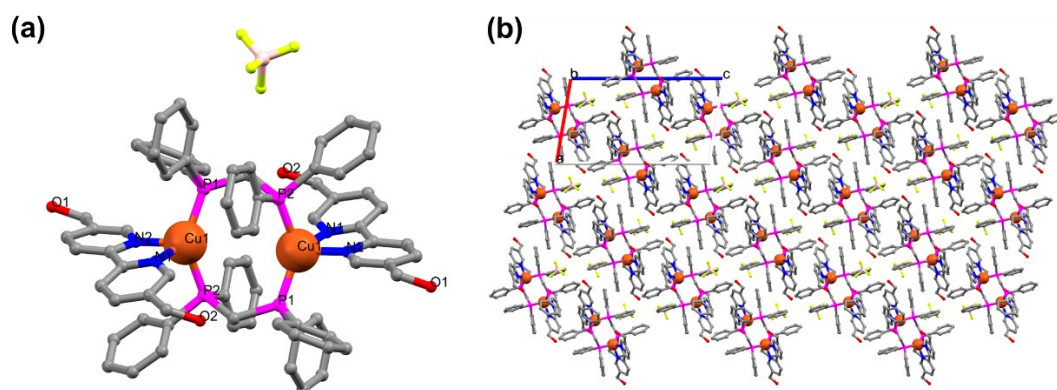


**Figure S57.** The single crystal of complex **C10** (a) and stacking structure(b).

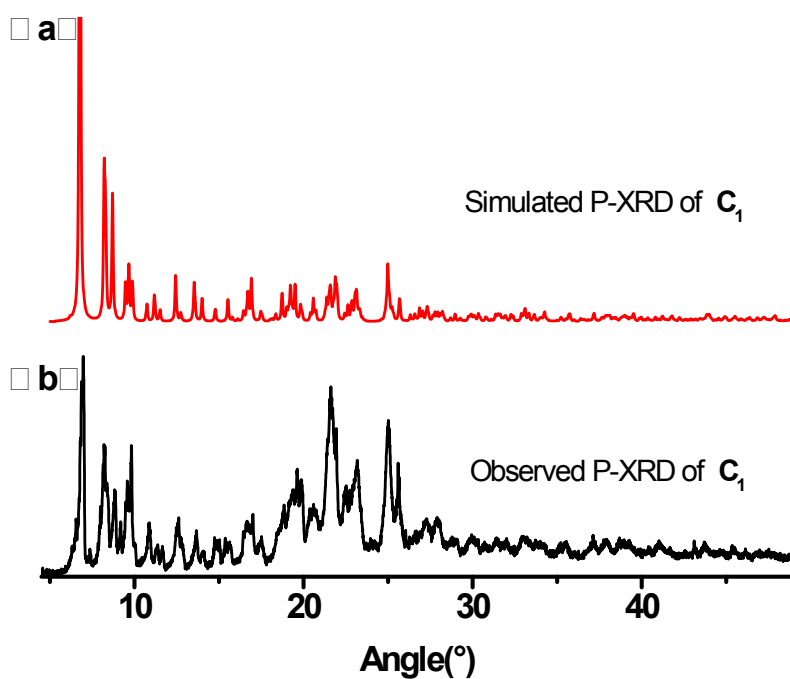


**Figure S58.** PXRD profiles of **C1**, simulated pattern (a) and observed pattern (b).

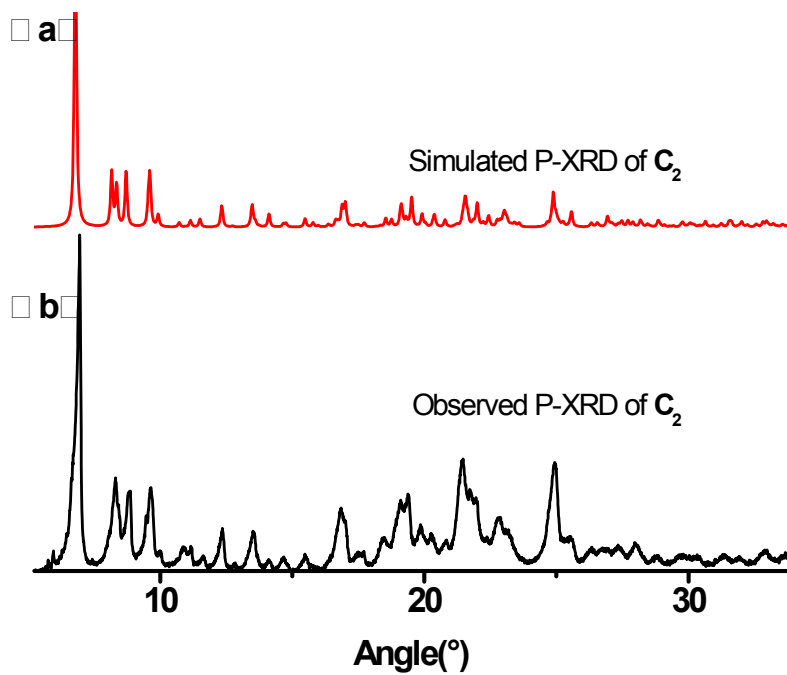


Figure S59. PXR profiles of C<sub>2</sub>, simulated pattern (a) and observed pattern (b).

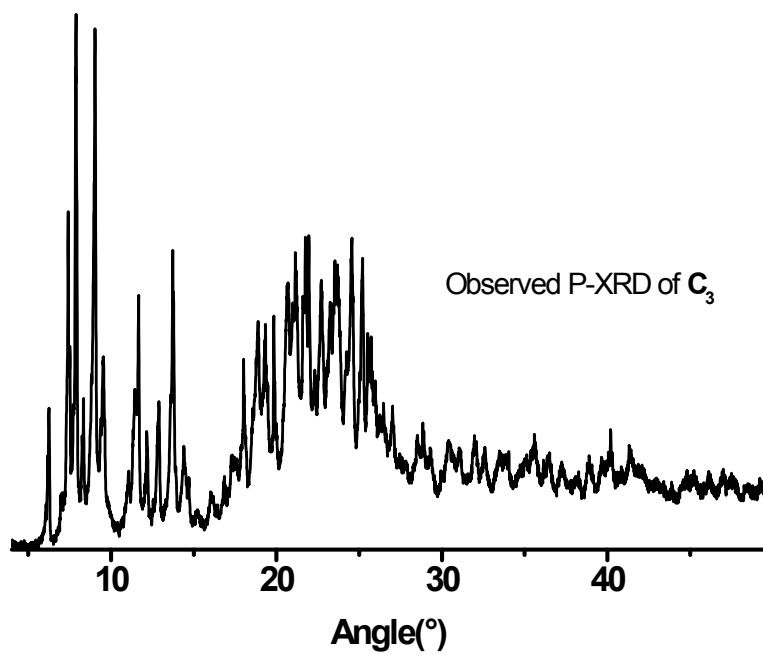


Figure S60. PXR profiles of C<sub>3</sub> observed pattern.



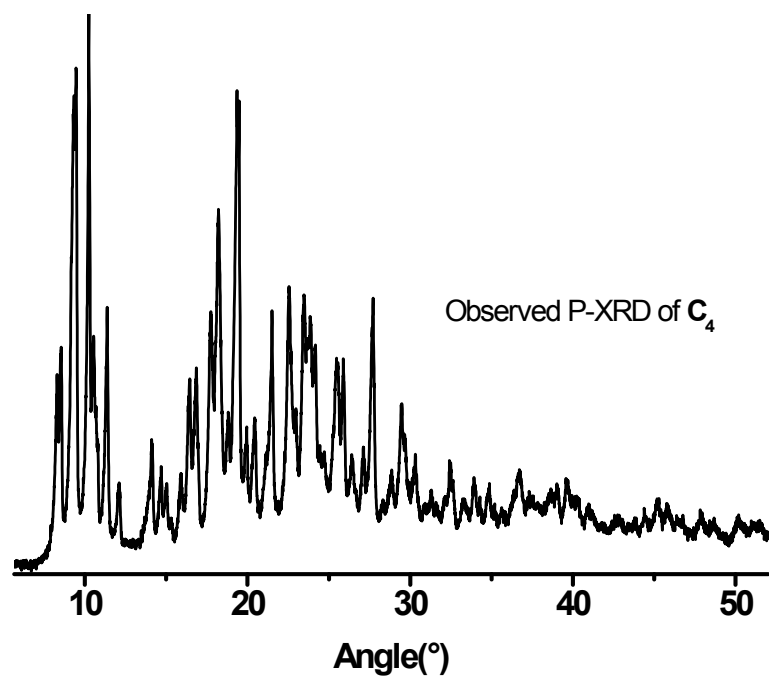


Figure S61. PXRD profiles of  $C_4$  observed pattern.

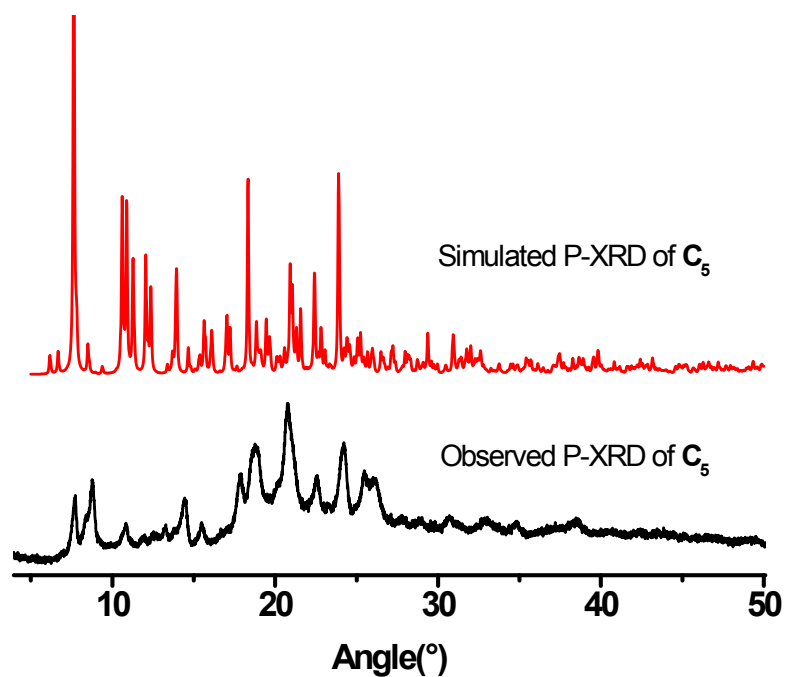
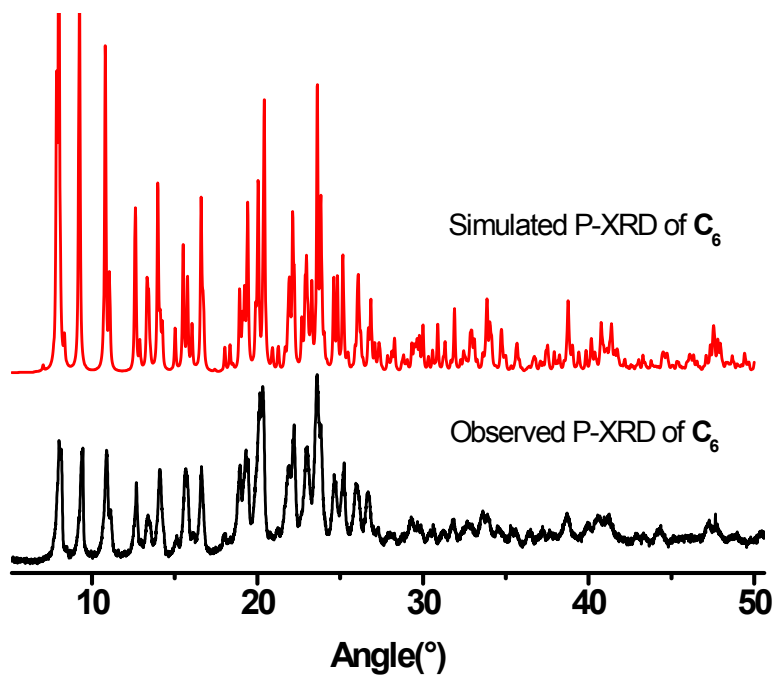
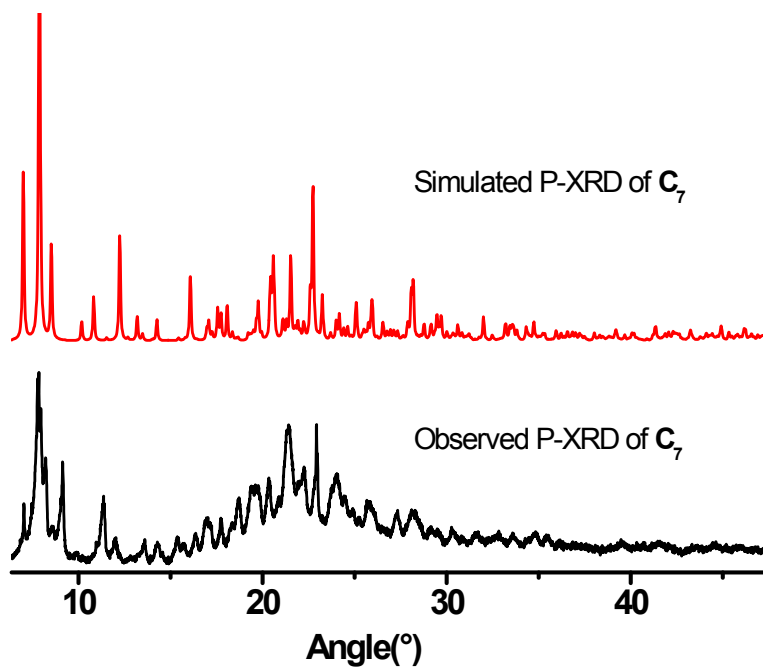


Figure S62. PXRD profiles of  $C_5$ , simulated pattern (a) and observed pattern (b).



**Figure S63.** PXR profiles of C<sub>6</sub>, simulated pattern (a) and observed pattern (b).



**Figure S64.** PXR profiles of C<sub>7</sub>, simulated pattern (a) and observed pattern (b).

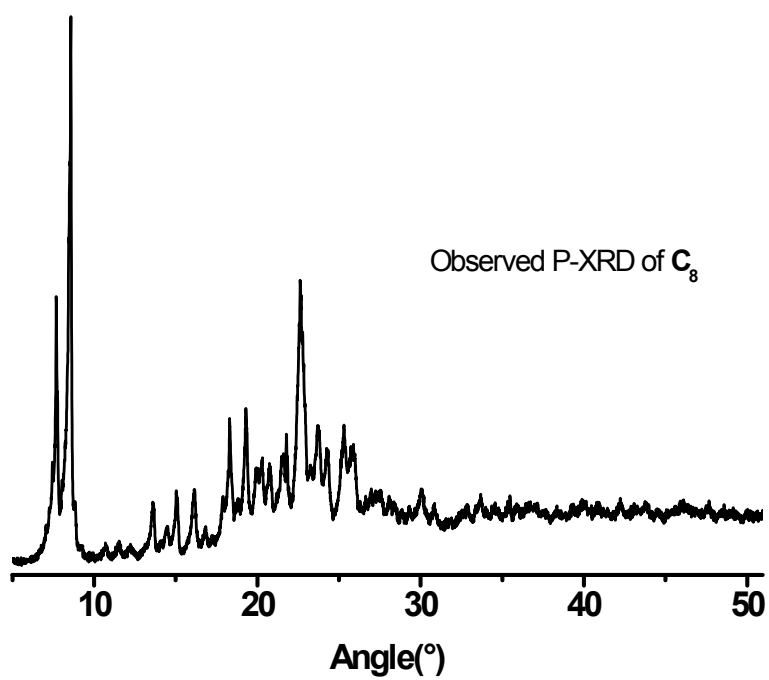


Figure S65. PXRD profiles of  $C_8$  observed pattern.

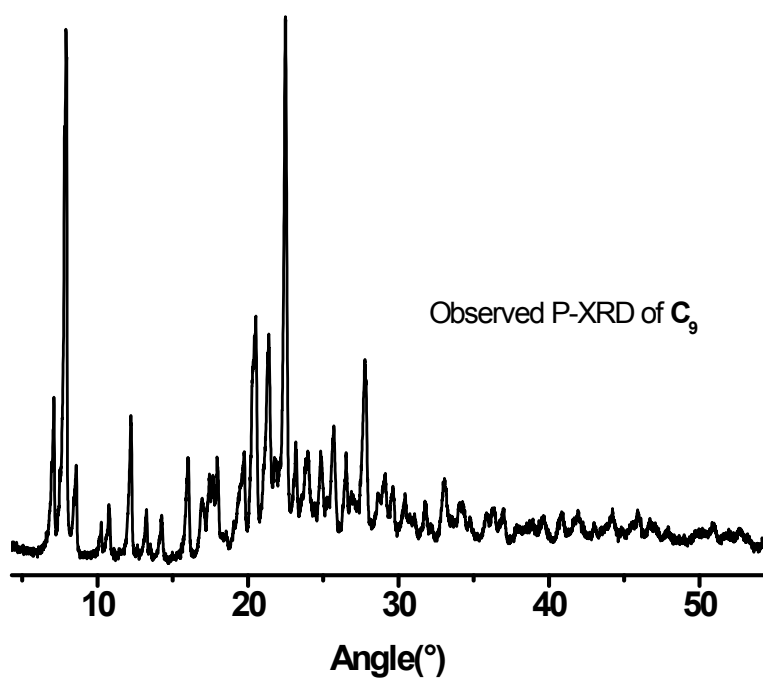
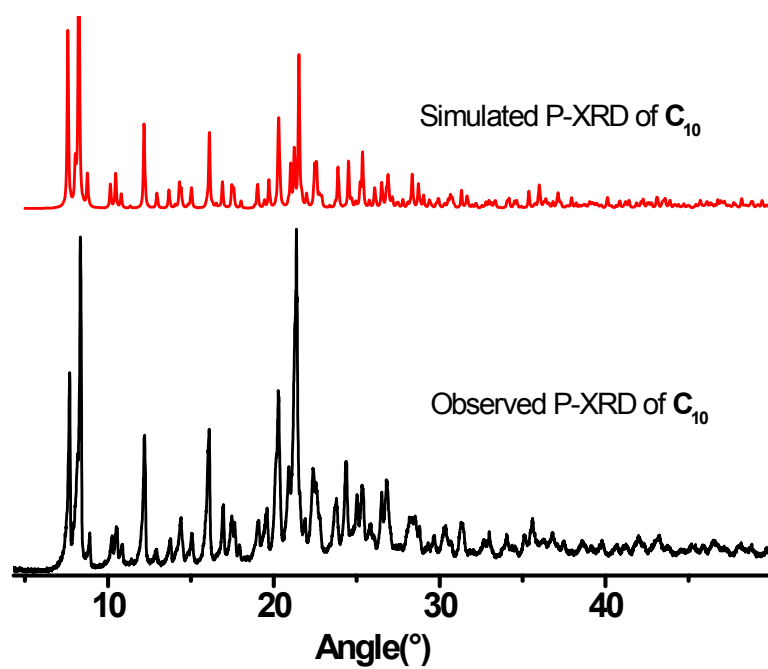


Figure S66. PXRD profiles of  $C_9$  observed pattern.



**Figure S67.** PXR profiles of **C10**, simulated pattern (a) and observed pattern (b).

### **S5. Photophysical Characterizations of Cu(I) Complexes C1-C10.**

**Table S8.** Photophysical data of Cu(I) complexes **C1-C10**.

complexes	Medium (T/K)	Uv-vis Absorbance $\lambda$ /nm( $\epsilon$ /M <sup>-1</sup> cm <sup>-1</sup> )	Excitation $\lambda$ /nm	Emission $\lambda$ /nm	Lifetime (us)	Quantum Yield (%)
C1	CH <sub>2</sub> Cl <sub>2</sub> (298)	334(13280)	421	610	0.827	5.58
	Solid(298)	329	398	559	1.07	
C2	CH <sub>2</sub> Cl <sub>2</sub> (298)	340(14780)	421	610	0.804	5.47
	Solid(298)	336	398	556	13	
C3	CH <sub>2</sub> Cl <sub>2</sub> (298)	332(12840)	415	615	69.8	18.9
	Solid(298)	337	450	557	33.7	
C4	CH <sub>2</sub> Cl <sub>2</sub> (298)	314(14870),376(4870)	389	640	28.9	0.67
	Solid(298)	286	400	596	6.4	
C5	CH <sub>2</sub> Cl <sub>2</sub> (298)	250(9330),288(8126)	468,370	540	7.2	-
	Solid(298)		468	618	1.7	
C6	CH <sub>2</sub> Cl <sub>2</sub> (298)	250(5673),287(5615)	468	544	7.5	0.02
	Solid(298)		468	598	1.3	
C7	CH <sub>2</sub> Cl <sub>2</sub> (298)	260(23160),291(18040)	390	550	3.51	2.03
	Solid(298)	271	387	505	1008	
C8	CH <sub>2</sub> Cl <sub>2</sub> (298)	263(22060),289(17760)	393	560	3.4	7.17
	Solid(298)	275	398	504	702.9	
C9	CH <sub>2</sub> Cl <sub>2</sub> (298)	332(12230),312(15130)	373	500	3.3	24.45
	Solid(298)	276	384	509	728.7	
C10	CH <sub>2</sub> Cl <sub>2</sub> (298)	315(17710)	378	545	4.8	9.47
	Solid(298)	263	390	548	13.8	

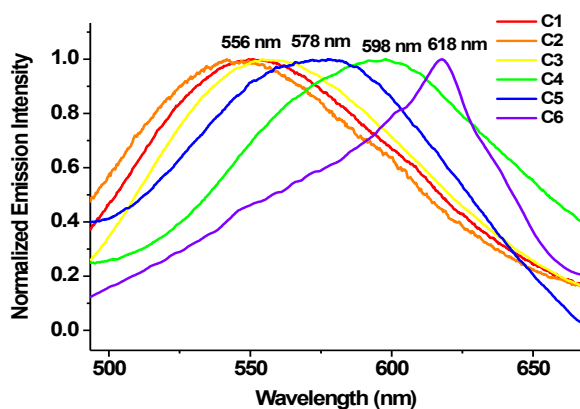


**Figure S68.** Emission spectra of mononuclear complexes **C1-C6** in the solid state at 298k.

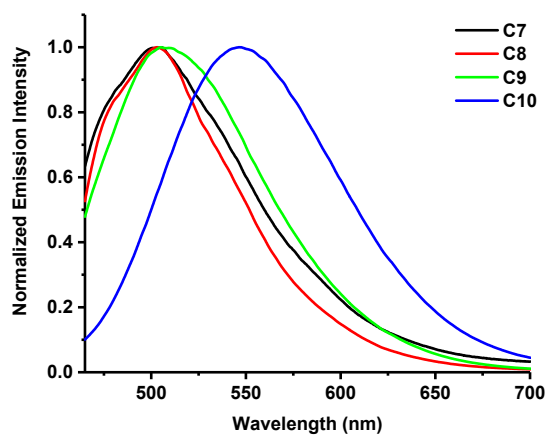


**Figure S69.** Emission spectra of dinuclear complexes **C7-C10** at the solid state at 298k.

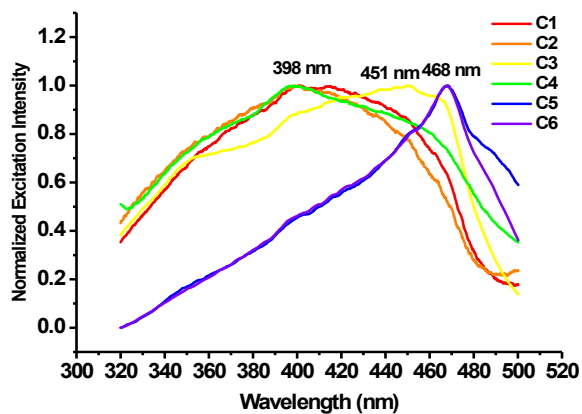


**Figure S70.** Excitation spectra of mononuclear complexes **C1-C6** in the solid state at 298k.

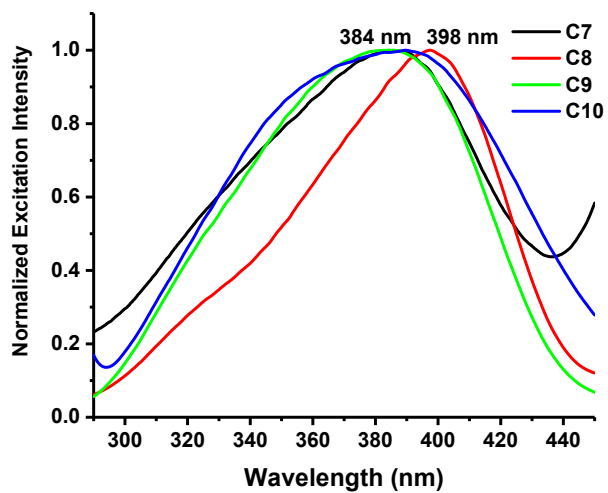


**Figure S71.** Excitation spectra of complexes **C5-C8** in the solid state at 298k.

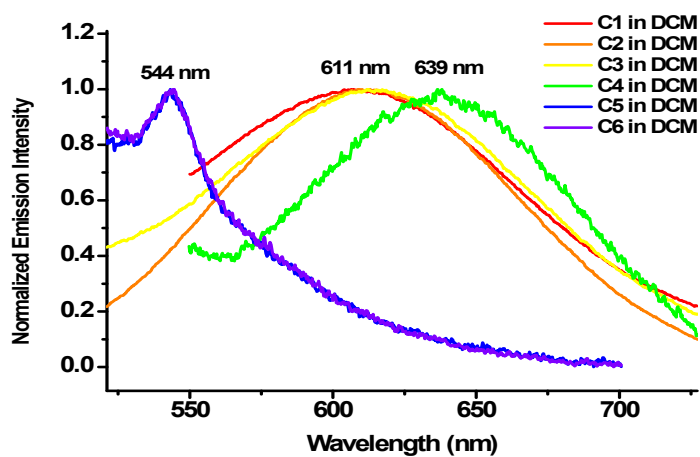


**Figure S72.** Emission spectra of mononuclear complexes **C1- C6** in  $\text{CH}_2\text{Cl}_2$  solution ( $1 \times 10^{-6}\text{M}$ ) at 298k.

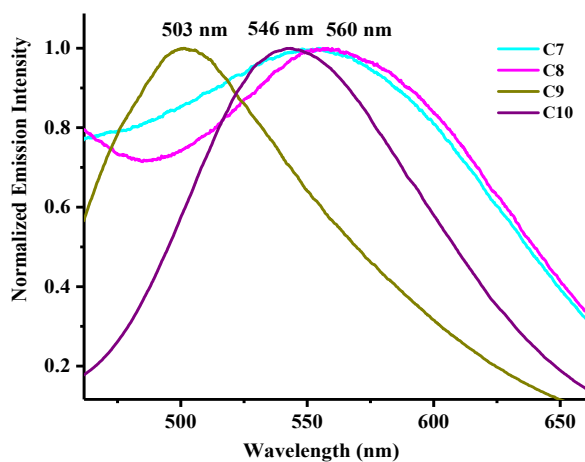


**Figure S73.** Emission spectra of complexes **C5-C8** in  $\text{CH}_2\text{Cl}_2$  solution ( $1 \times 10^{-6}\text{M}$ ) at 298k.

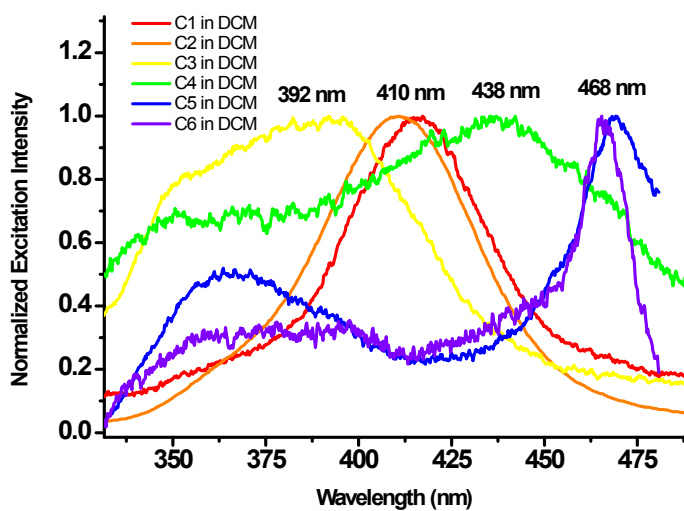


**Figure S74.** Excitation spectra of complexes **C1-C6** in  $\text{CH}_2\text{Cl}_2$  solution ( $1 \times 10^{-6}\text{M}$ ) at 298K.

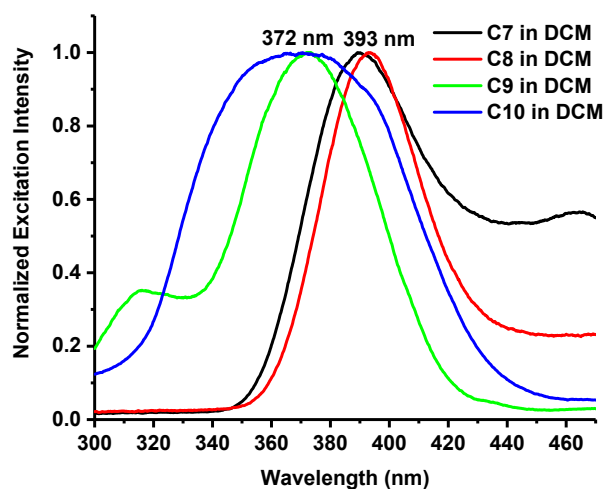


**Figure S75.** Excitation spectra of complexes **C7-C10** in  $\text{CH}_2\text{Cl}_2$  solution ( $1 \times 10^{-6}\text{M}$ ) at 298K.

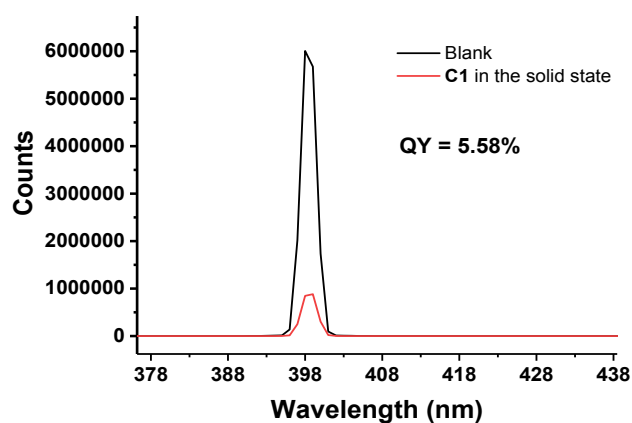


**Figure S76.** Phosphorescence decay profiles (a) and quantum yield spectra (b) of **C1** in the solid state at 298K.

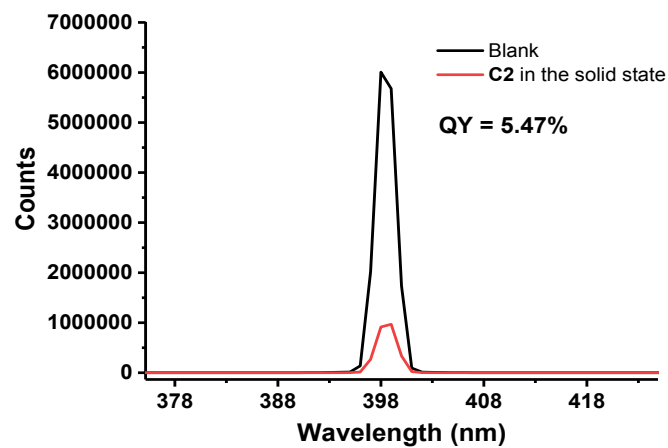




**Figure S77.** Phosphorescence decay profiles (a) and quantum yield spectra (b) of **C2** in the solid state at 298K.

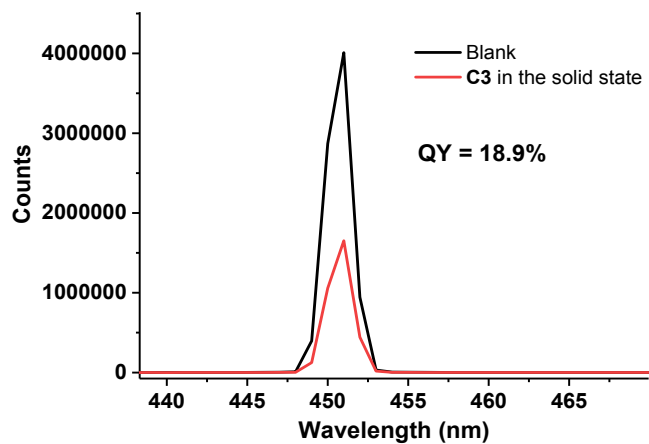


**Figure S78.** Phosphorescence decay profiles (a) and quantum yield spectra (b) of **C3** in the solid state at 298K.

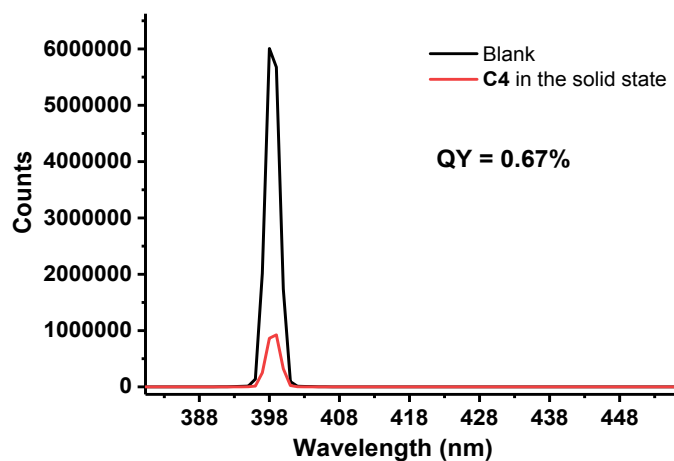


**Figure S79.** Phosphorescence decay profiles (a) and quantum yield spectra (b) of **C4** in the solid state at 298K.

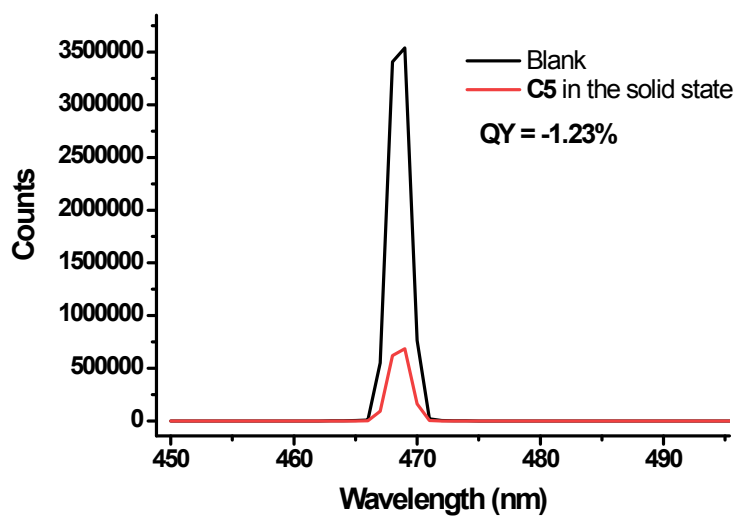


**Figure S80.** Phosphorescence decay profiles (a) and quantum yield spectra (b) of **C5** in the solid state at 298K.

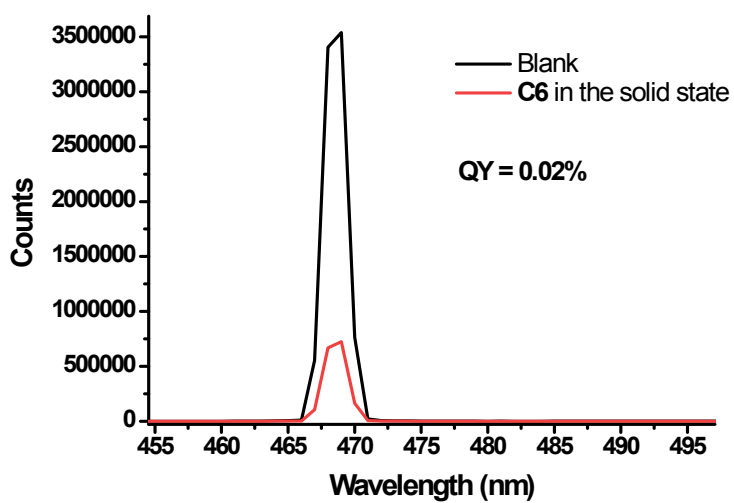


**Figure S81.** Phosphorescence decay profiles (a) and quantum yield spectra (b) of **C6** in the solid state at 298K.

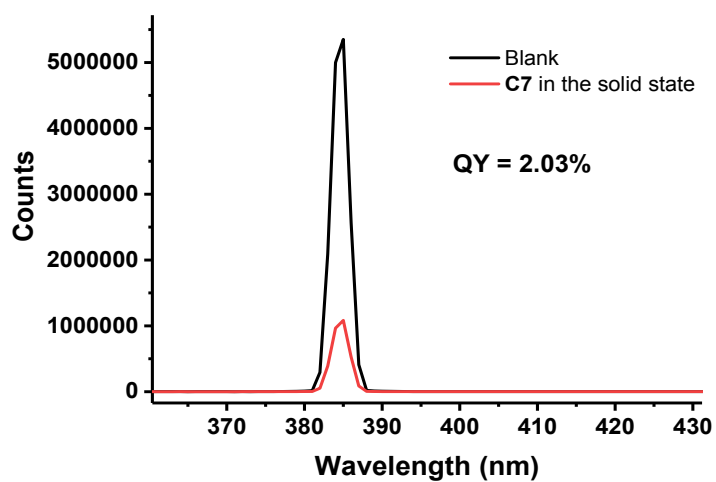


**Figure S82.** Phosphorescence decay profiles (a) and quantum yield spectra (b) of **C7** in the solid state at 298K.

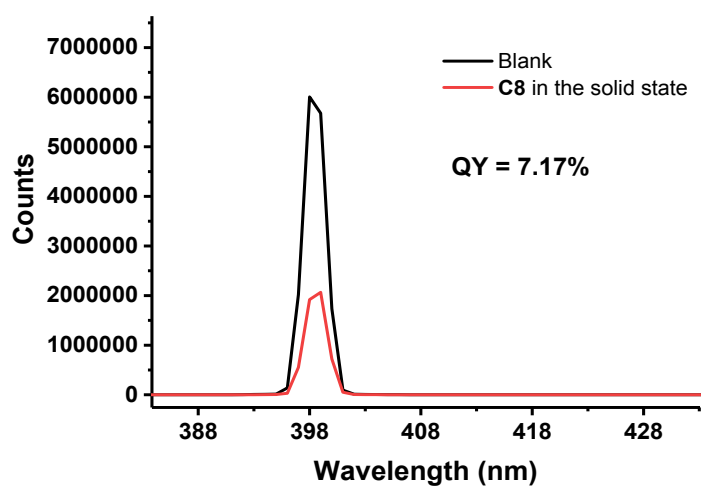


**Figure S83.** Phosphorescence decay profiles (a) and quantum yield spectra (b) of **C8** in the solid state at 298K.

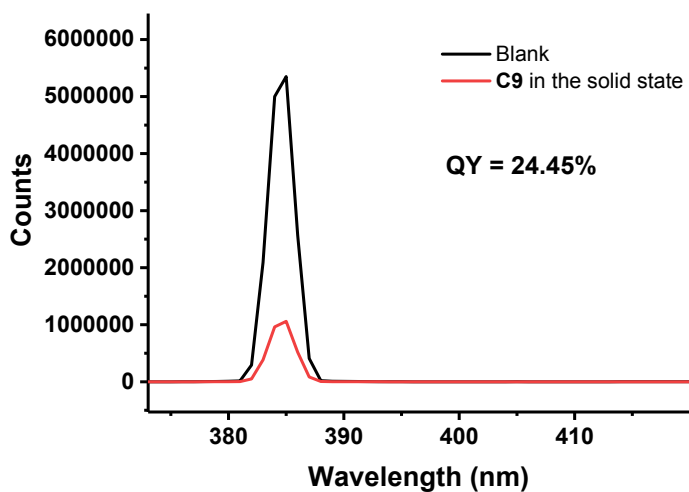


Figure S84. Phosphorescence decay profiles (a) and quantum yield spectra (b) of C9 in the solid state at 298K.

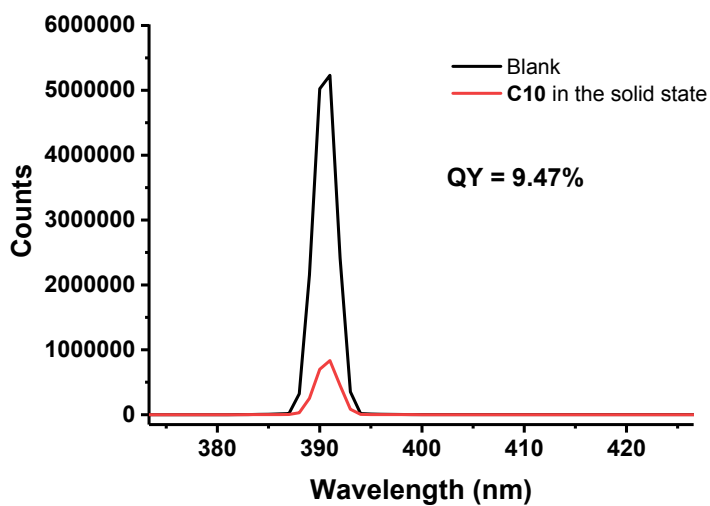


Figure S85. Phosphorescence decay profiles (a) and quantum yield spectra (b) of C10 in the solid state at 298K.

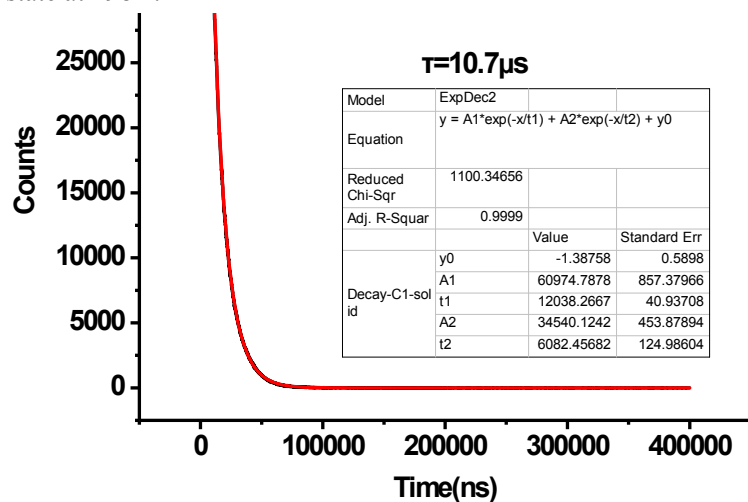


Figure S86. Phosphorescence decay profiles of C1 in the solid state at 298K.

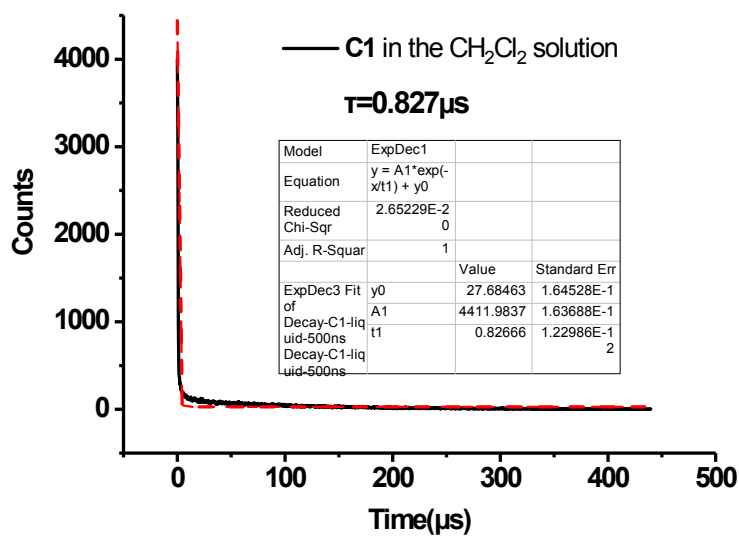


Figure S87. Phosphorescence decay profiles of C1 in CH<sub>3</sub>CN solution (1×10<sup>-5</sup> mol/L).

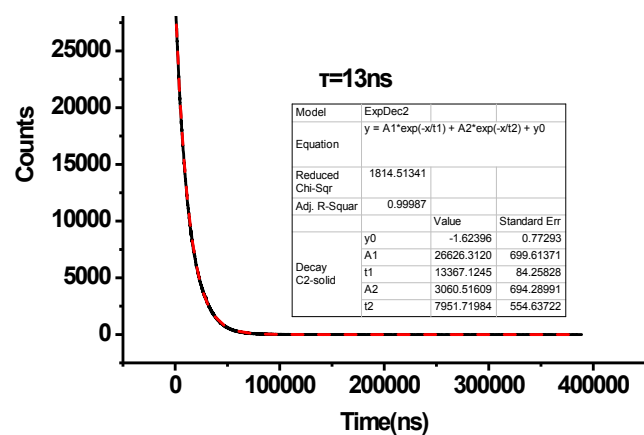


Figure S88. Phosphorescence decay profiles of C2 in the solid state at 298K.

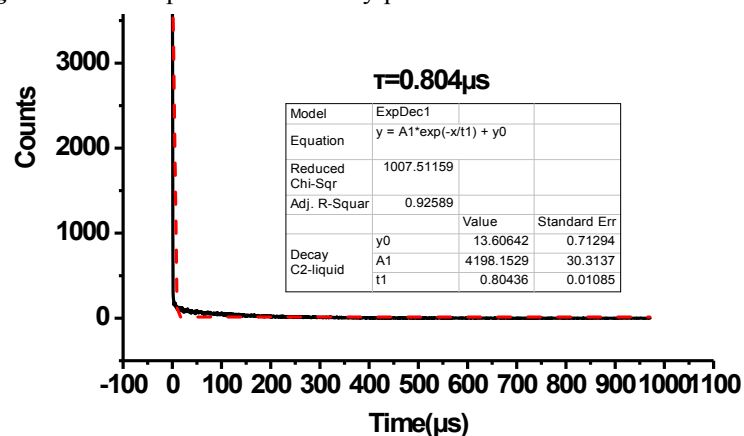


Figure S89. Phosphorescence decay profiles of C2 in CH<sub>3</sub>CN solution (1×10<sup>-5</sup> mol/L).

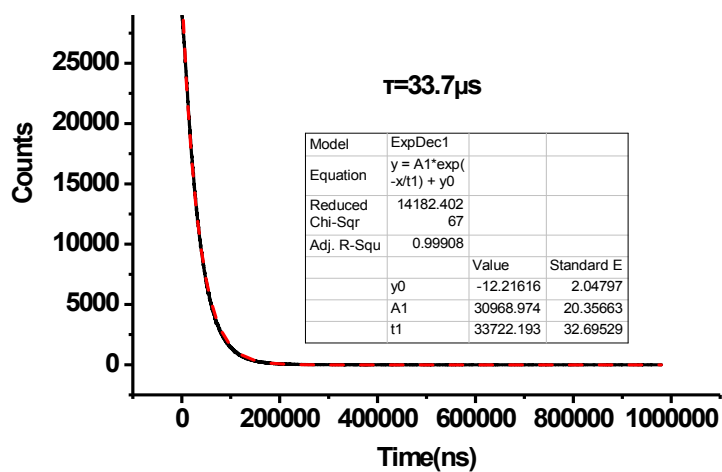


Figure S90. Phosphorescence decay profiles of C3 in the solid state at 298K.

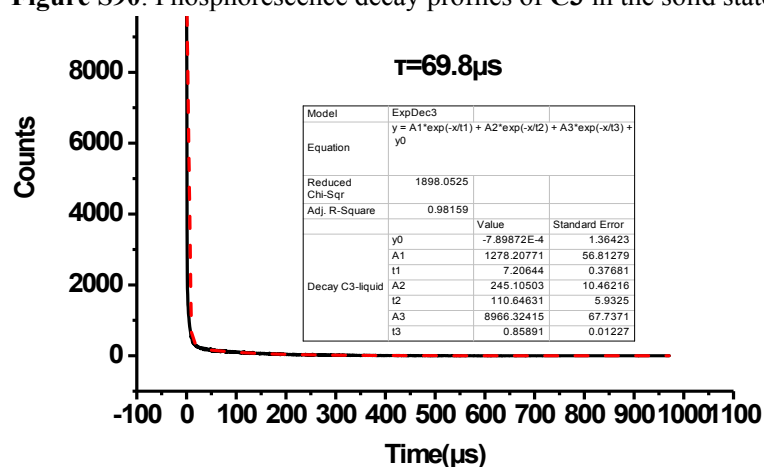


Figure S91. Phosphorescence decay profiles of C3 in CH<sub>3</sub>CN solution ( $1 \times 10^{-5}$  mol/L).

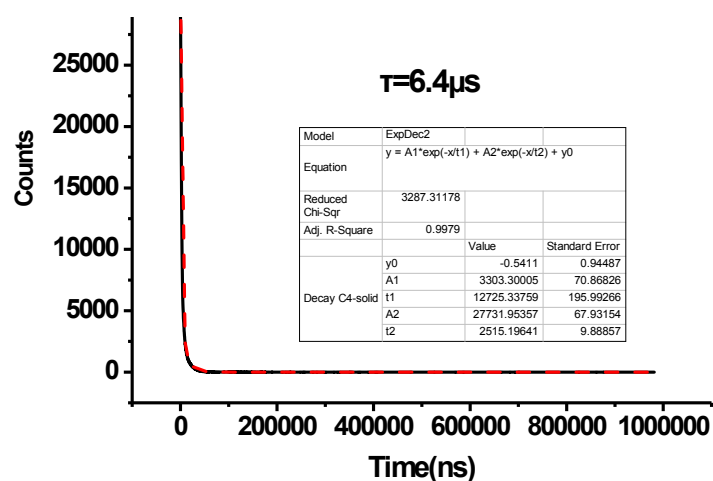


Figure S92. Phosphorescence decay profiles of C4 in the solid state at 298K.

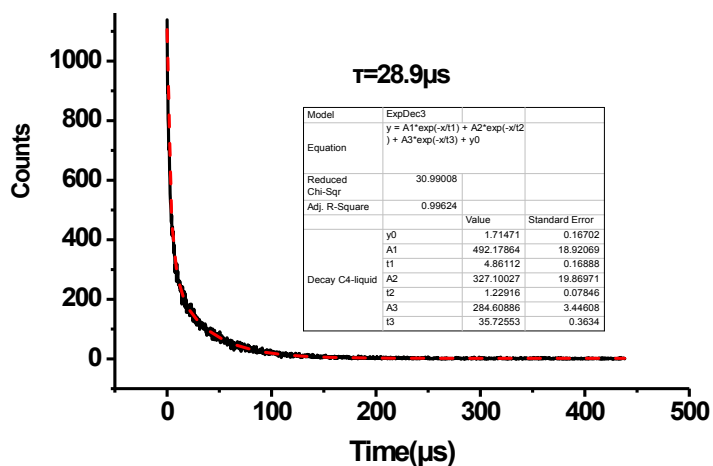


Figure S93. Phosphorescence decay profiles of C4 in CH<sub>3</sub>CN solution ( $1 \times 10^{-5}$  mol/L).

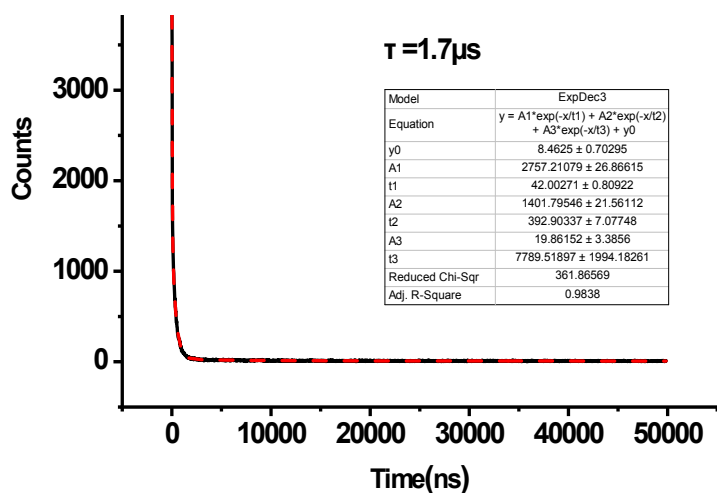


Figure S94. Phosphorescence decay profiles of C5 in the solid state at 298K.

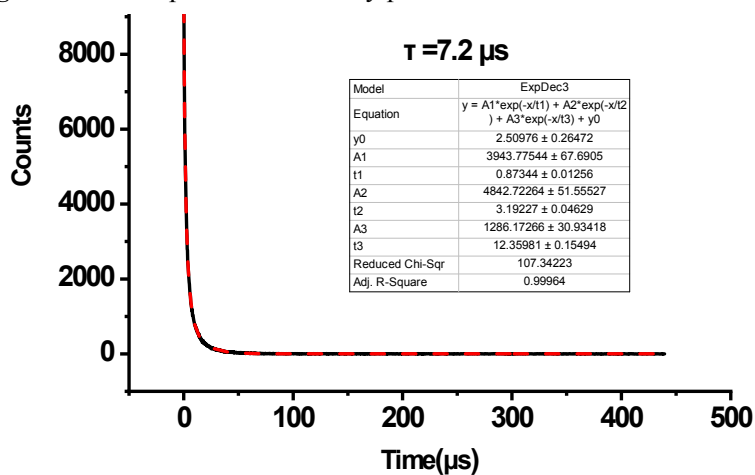


Figure S95. Phosphorescence decay profiles of C5 in CH<sub>3</sub>CN solution ( $1 \times 10^{-5}$  mol/L),

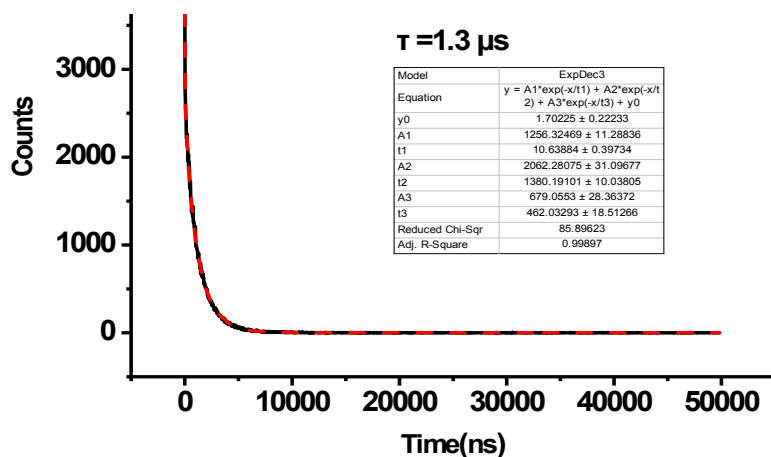


Figure S96. Phosphorescence decay profiles of C6 in the solid state at 298K.

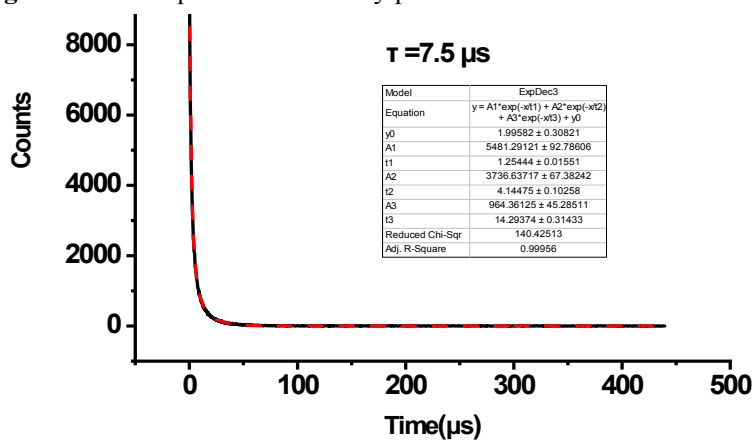


Figure S97. Phosphorescence decay profiles of C6 in CH<sub>3</sub>CN solution ( $1 \times 10^{-5}$  mol/L),

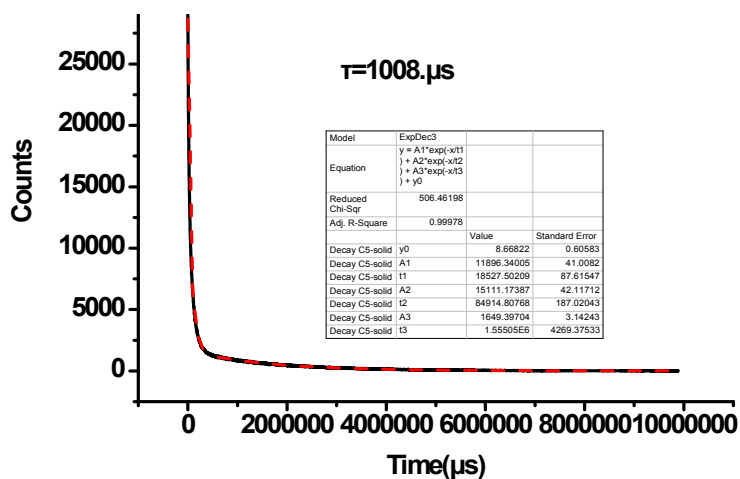


Figure S98. Phosphorescence decay profiles of C7 in the solid state at 298K.



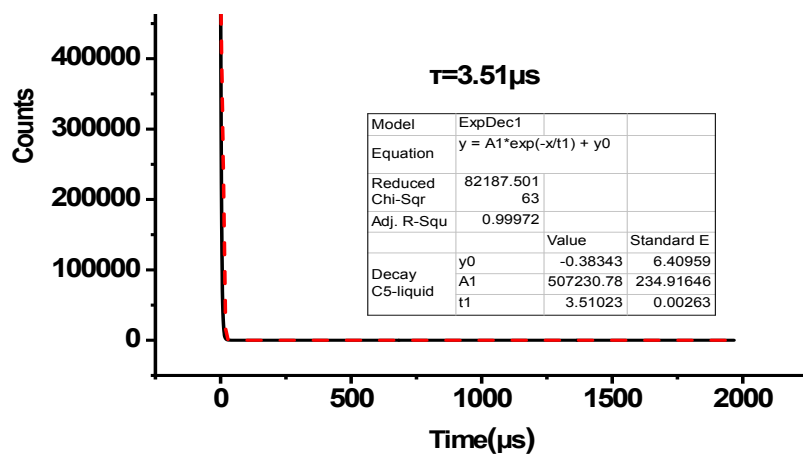


Figure S99. Phosphorescence decay profiles of C7 in CH<sub>3</sub>CN solution ( $1 \times 10^{-5}$  mol/L).

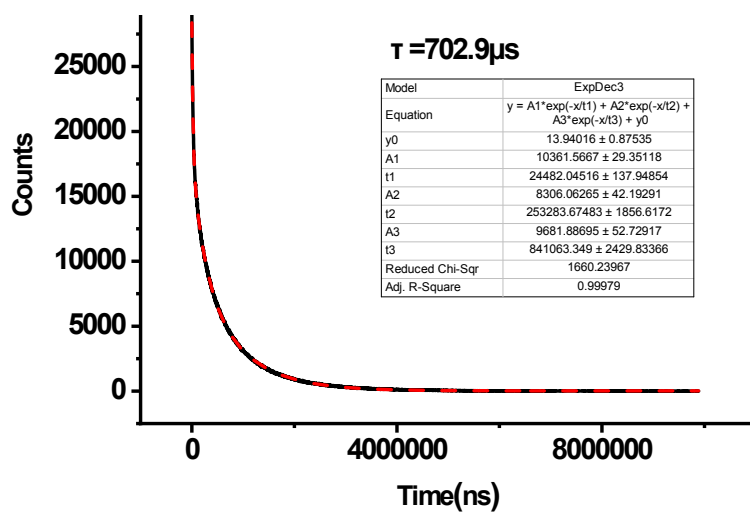


Figure S100. Phosphorescence decay profiles of C8 in the solid state at 298K.

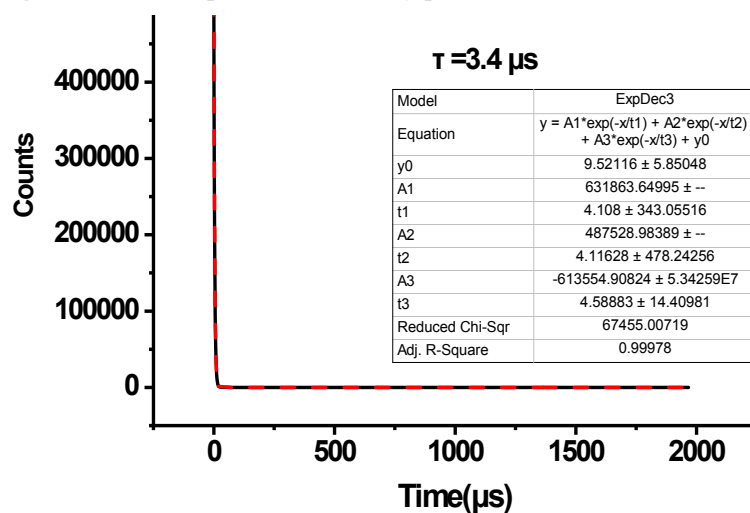


Figure S101. Phosphorescence decay profiles of C8 in CH<sub>3</sub>CN solution ( $1 \times 10^{-5}$  mol/L).

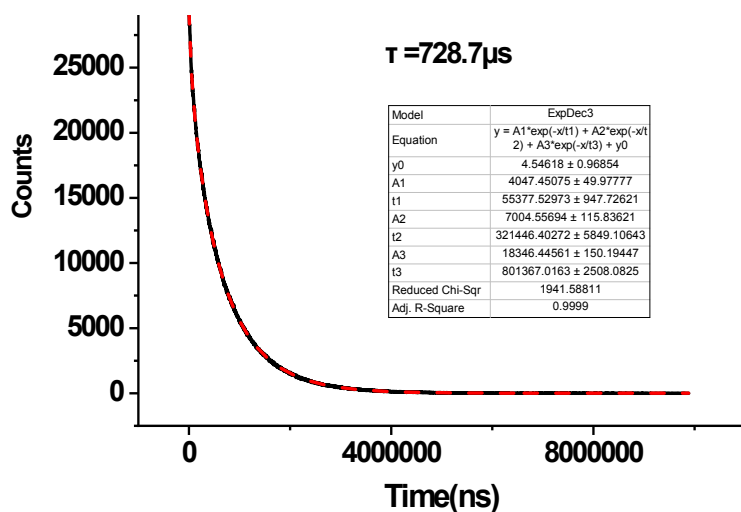


Figure S102. Phosphorescence decay profiles of C9 in the solid state at 298K.

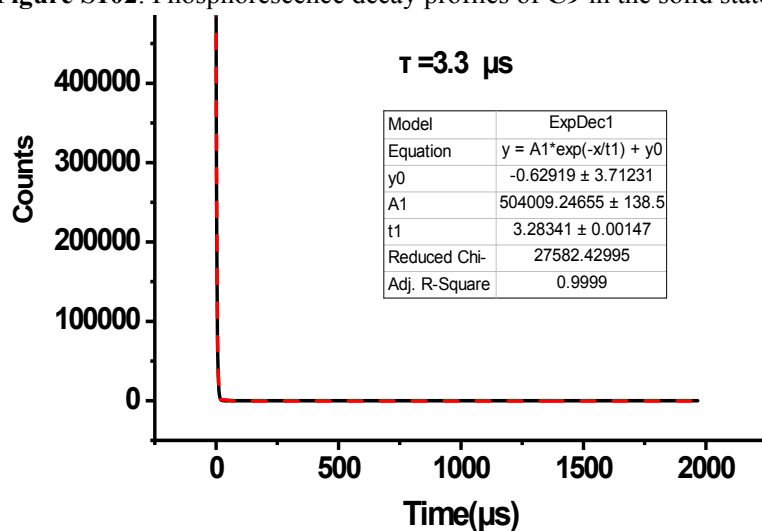


Figure S103. Phosphorescence decay profiles of C9 in CH<sub>3</sub>CN solution ( $1 \times 10^{-5}$  mol/L).

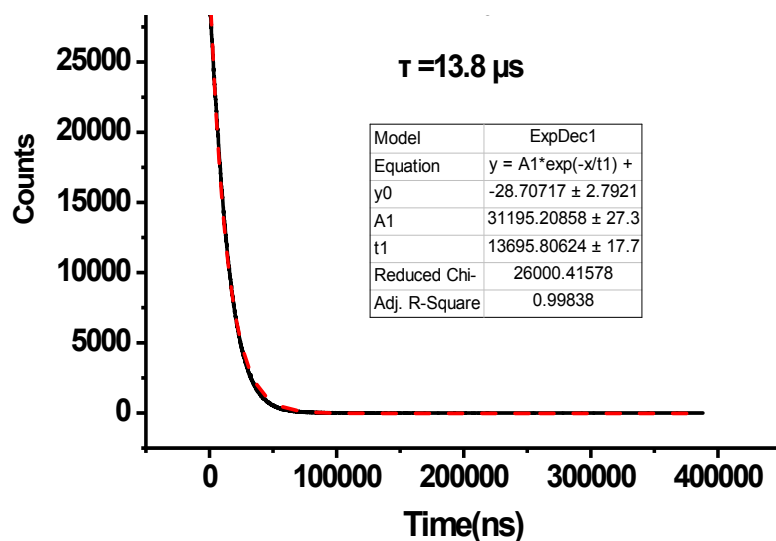
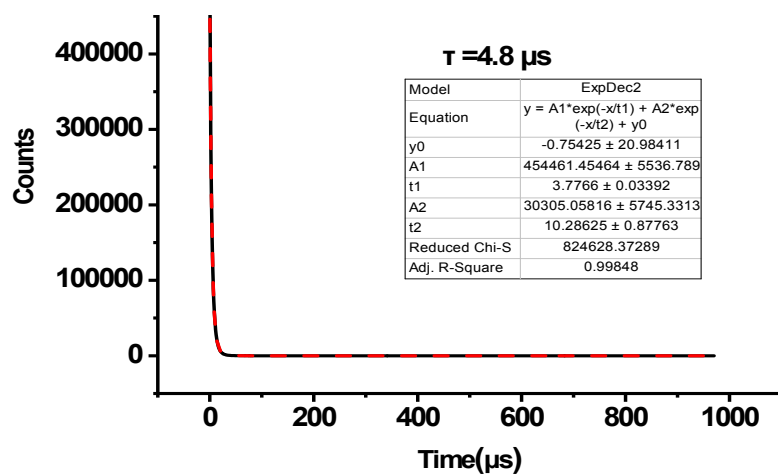
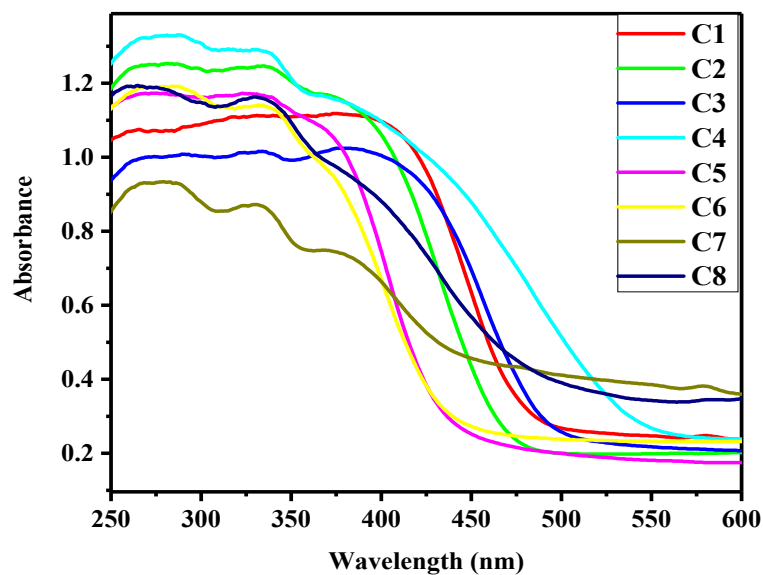


Figure S104. Phosphorescence decay profiles of C10 in the solid state at 298K.



**Figure S105.** Phosphorescence decay profiles of **C10** in  $\text{CH}_3\text{CN}$  solution ( $1 \times 10^{-5}$  mol/L),



**Figure S106.** UV-Vis absorption spectrum of complexes **C1-C8** in the solid state at 298K.

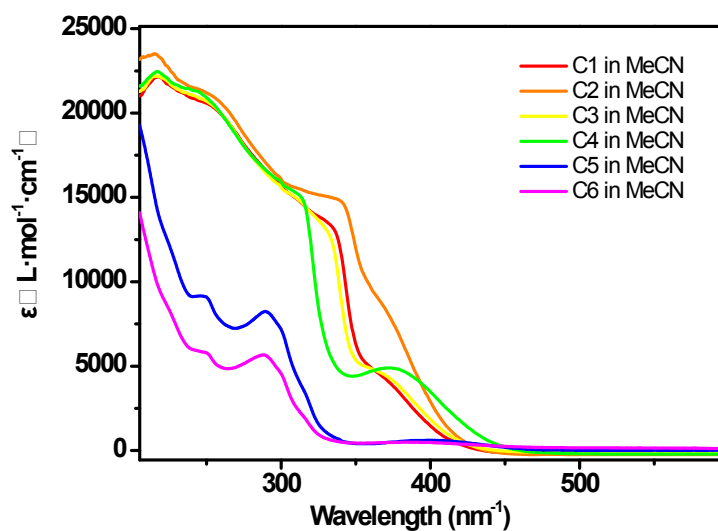


Figure S107. UV-Vis absorption spectrum of complexes **C1-C6** (MeCN  $2.5 \times 10^{-5} \text{M}$ ) at 298k.

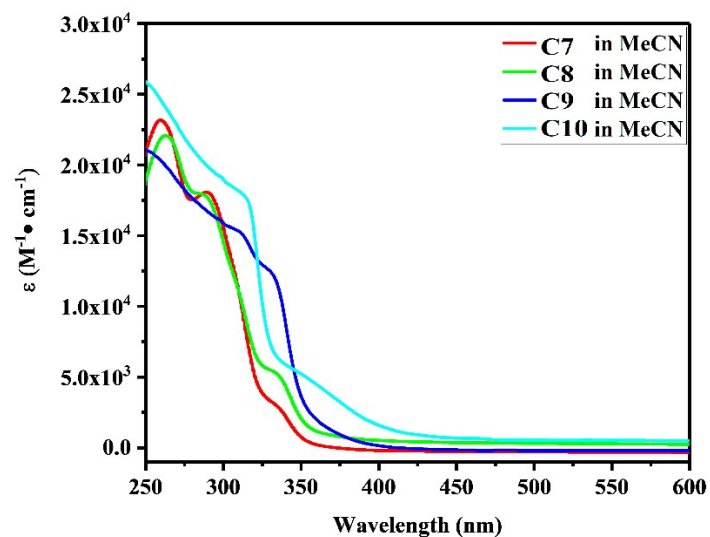


Figure S108. UV-Vis absorption spectrum of complexes **C5-C8** (MeCN  $2.5 \times 10^{-5} \text{M}$ ) at 298k.

Table S9. The calculated LUMO and HOMO energy (eV) of Cu(I) complexes **C1**, **C6** and **C10**.

Complexes	(charge, spin multiplicity)	Orbital	LUMO (eV)	HOMO (eV)	Gap (eV)
<b>C1</b>	(1, 2)	$\alpha$	-4.01	-4.57	0.56
		$\beta$	-3.52	-7.54	4.02
<b>C6</b>	(1, 2)	$\alpha$	-4.51	-7.89	3.38
		$\beta$	-5.09	-7.89	2.80

C8	(2,3)	$\alpha$	-6.19	-6.93	0.74
		$\beta$	-9.12	-10.12	1.00
	(2,1)		-6.06	-9.87	3.81

S6. Luminescent sensing experiments for silver ions of Cu(I)-POP Complexes C1-C4 in solution.

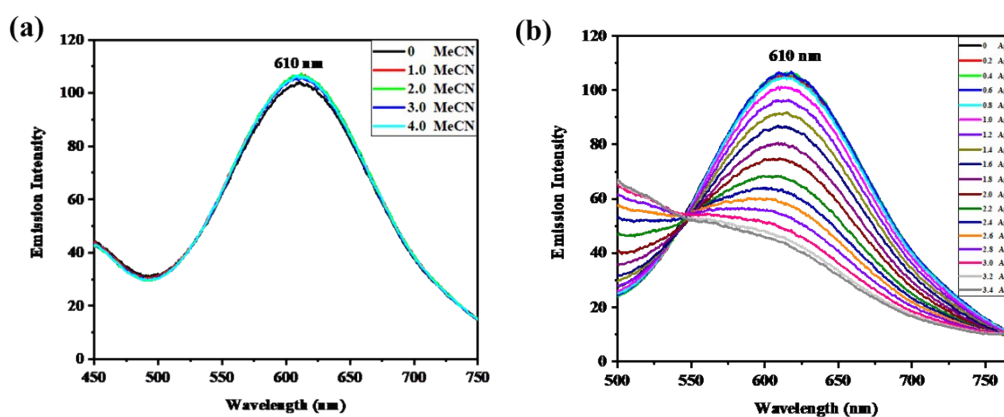


Figure S109. Emission spectra of complexes C1 in  $\text{CH}_2\text{Cl}_2$  solution ( $1 \times 10^{-6}\text{M}$ ) at 298k.

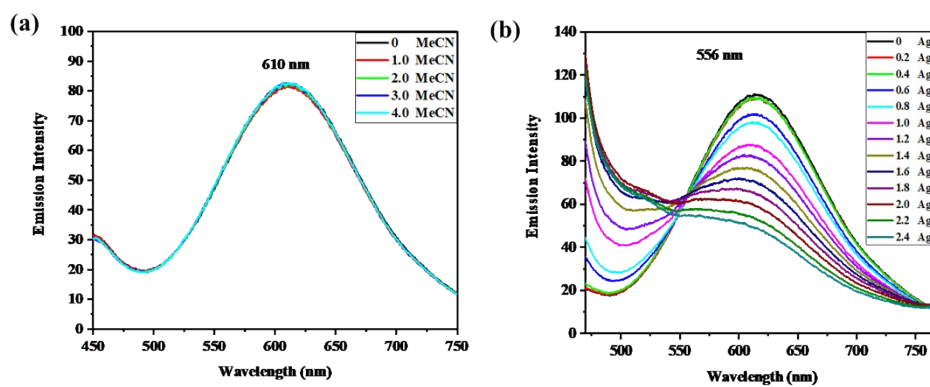


Figure S110. Emission spectra of complexes C2 in  $\text{CH}_2\text{Cl}_2$  solution ( $1 \times 10^{-6}\text{M}$ ) at 298k.

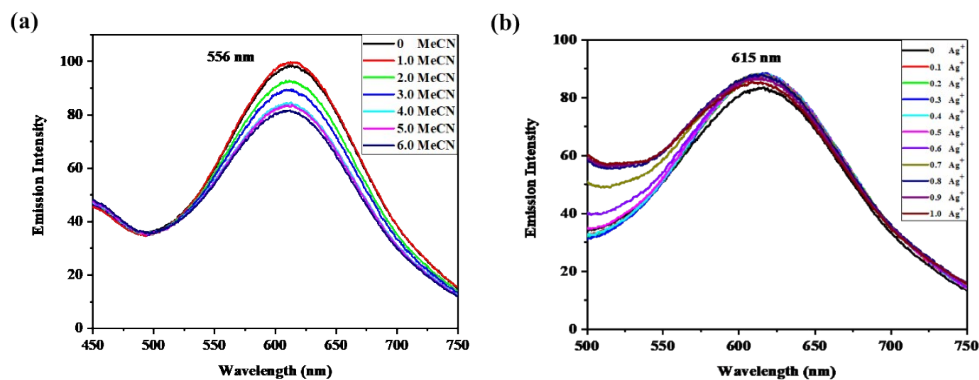


Figure S111. Emission spectra of complexes C3 in  $\text{CH}_2\text{Cl}_2$  solution ( $1 \times 10^{-6}\text{M}$ ) at 298k.

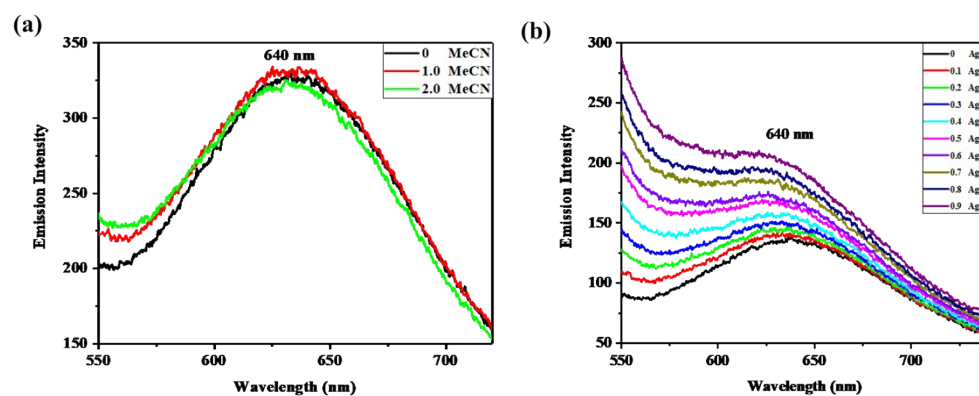


Figure S112. Emission spectra of complexes C4 in  $\text{CH}_2\text{Cl}_2$  solution ( $1 \times 10^{-6}\text{M}$ ) at 298k.

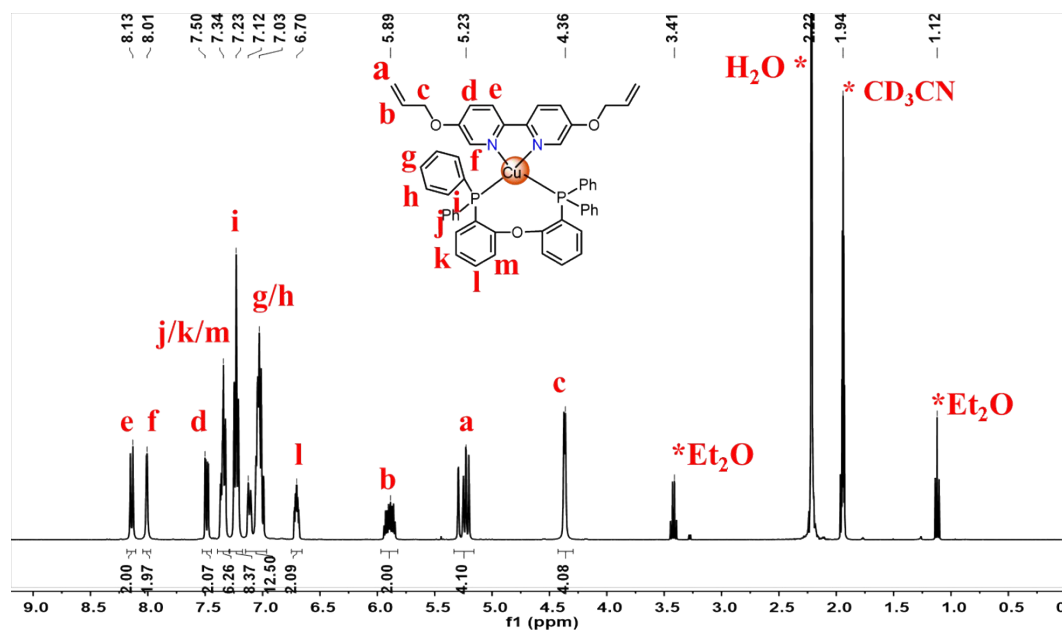
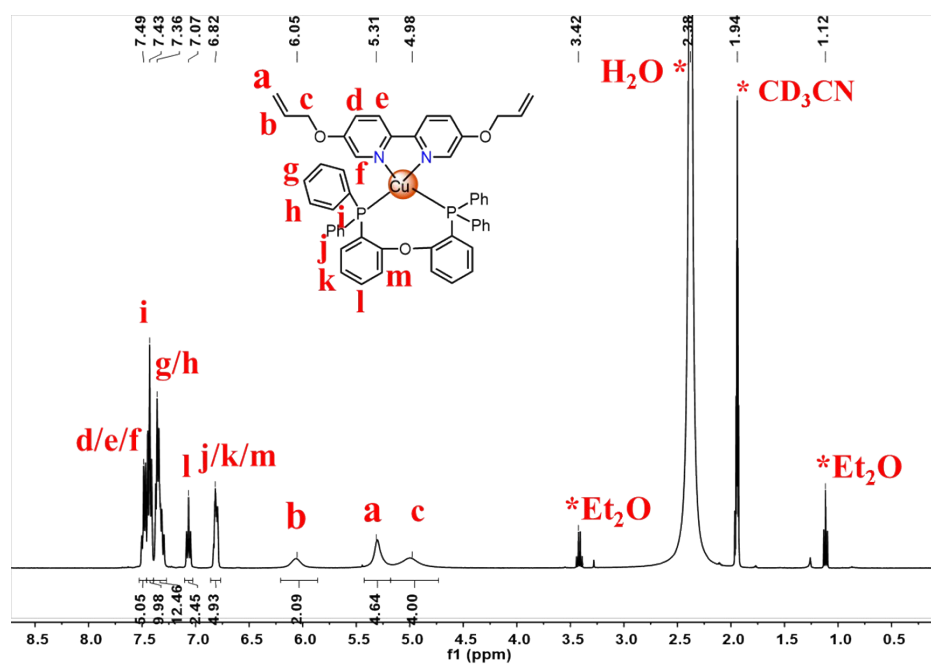


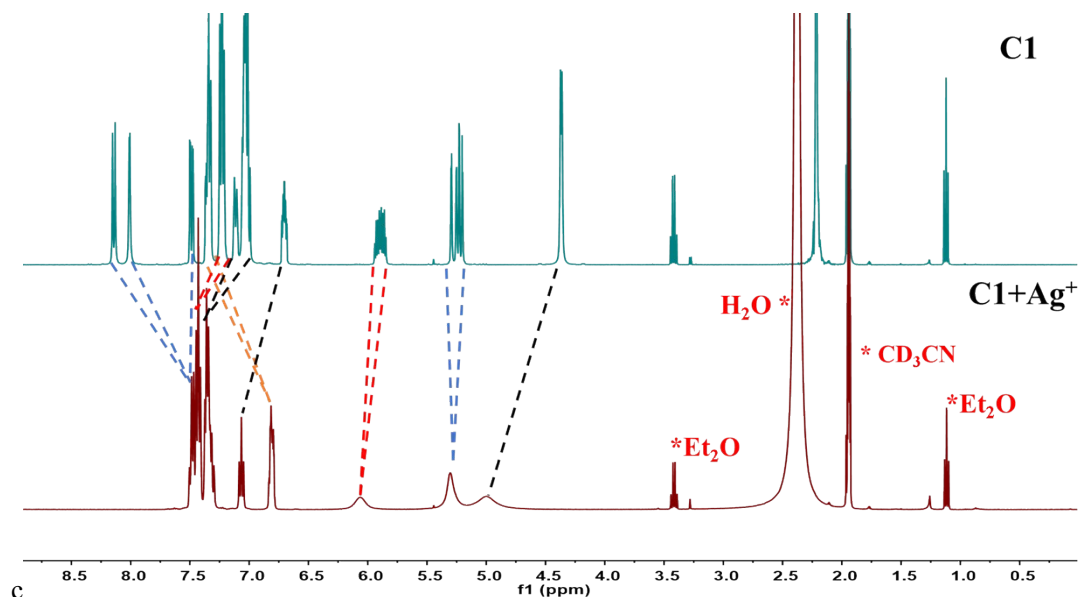
Figure S113.  $^1\text{H}$  NMR spectrum (400 MHz, Acetonitrile- $d_3$ ) of C1 recorded at 298 K.

$^1\text{H}$  NMR (400 MHz, Acetonitrile- $d_3$ )  $\delta$  8.24 (d,  $J = 9.0$  Hz, 2H, H<sup>e</sup>), 7.82 (s, 2H, H<sup>f</sup>), 7.46 (d,  $J =$

11.7 Hz, 2H, H<sup>d</sup>), 7.24 (m, 6H, H<sup>i/k/m</sup>), 7.13 (m, 8H, H<sup>i</sup>), 6.91 (m, 12H, H<sup>g/h</sup>), 6.68 (m, 2H, H<sup>l</sup>), 5.82 (m, 2H, H<sup>b</sup>), 5.19 (m, 4H, H<sup>a</sup>), 4.26 (d, J = 5.3 Hz, 4H, H<sup>c</sup>).



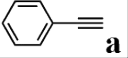
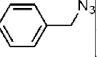
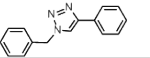
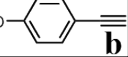
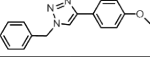
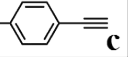
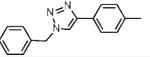
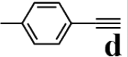
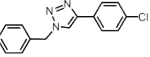
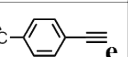
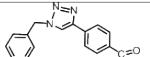
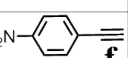
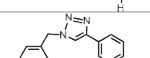
**Figure S114.** <sup>1</sup>H NMR spectrum (400 MHz, Acetonitrile-*d*<sub>3</sub>) of C1+Ag<sup>+</sup> recorded at 298 K. <sup>1</sup>H NMR (400 MHz, Acetonitrile-*d*<sub>3</sub>) δ 7.49 (m, 5H, H<sup>d/e/f</sup>), 7.43 (m, 8H, H<sup>i</sup>), 7.36 (m, 12H, H<sup>g/h</sup>), 7.07 (m, 2H, H<sup>l</sup>), 6.82 (m, 6H, H<sup>j/k/m</sup>), 6.05 (s, 2H, H<sup>b</sup>), 5.31 (s, 4H, H<sup>a</sup>), 4.98 (s, 4H, H<sup>c</sup>).



**Figure S115.** <sup>1</sup>H-NMR spectra of C1 and silver ions in CD<sub>3</sub>CN, with dashed lines showing the symmetry change before and after complexation.

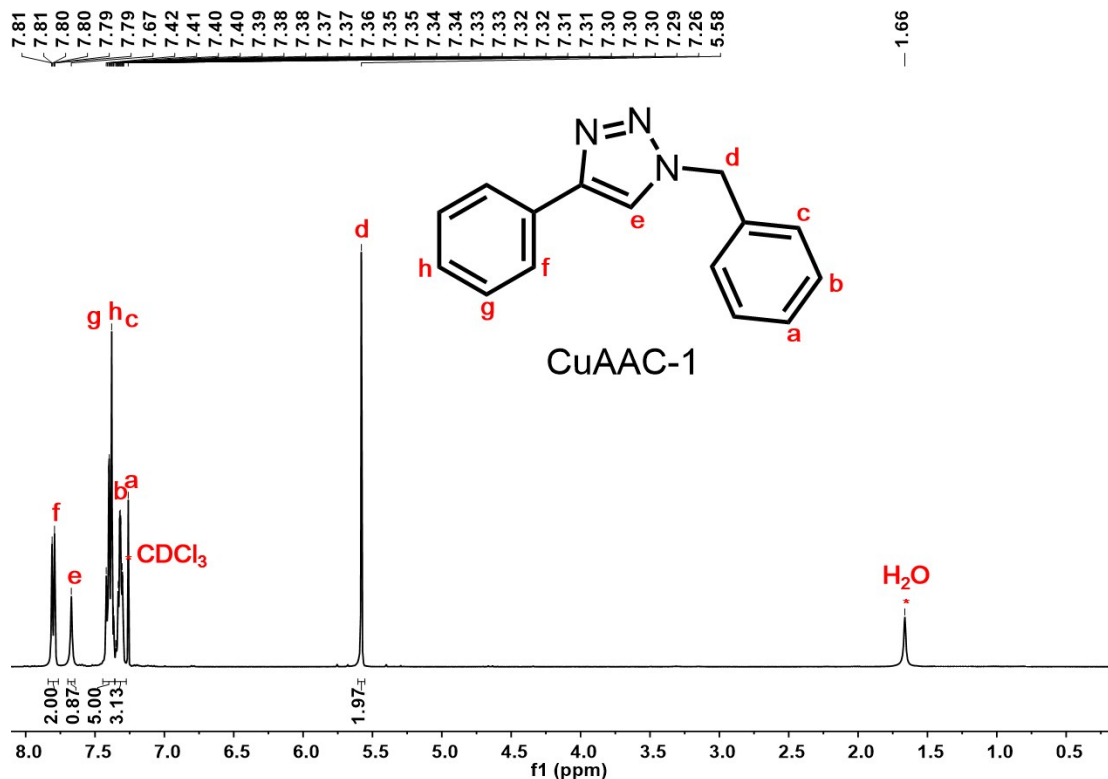
**S7. The experimental procedures and catalytic performance of C1-C10 for CuAAC reaction in water solution.**

**Table S10.** Substrate scope of CuAAC reactions between Benzyl Azides and various Alkynes using C1-C10 as catalyst at 80°C in water.

Entry	Alkyne	Azide	Product	Yield (C2)	Yield (C3)	Yield (C4)	Yield (C5)	Yield (C6)	Yield (C7)	Yield (C8)	Yield (C9)	Yield (C10)
CuAAC-1				93%	98%	58%	79%	81%	98%	85%	85%	91%
CuAAC-2						93%	91%	95%	90%	94%	96%	97%
CuAAC-3						94%	89%	95%	93%	92%	95%	83%
CuAAC-5				81%	98%	70%	43%	42%	64%	52%	75%	76%
CuAAC-6				95%	96%							
CuAAC-7				89%	97%							

[a] Reaction conditions: azide (0.1 mmol), alkyne (0.11 mmol), C1-C8 catalyst (1%, 0.001 mmol), water (2mL), CH<sub>3</sub>CN(1mL), 80°C,8h;

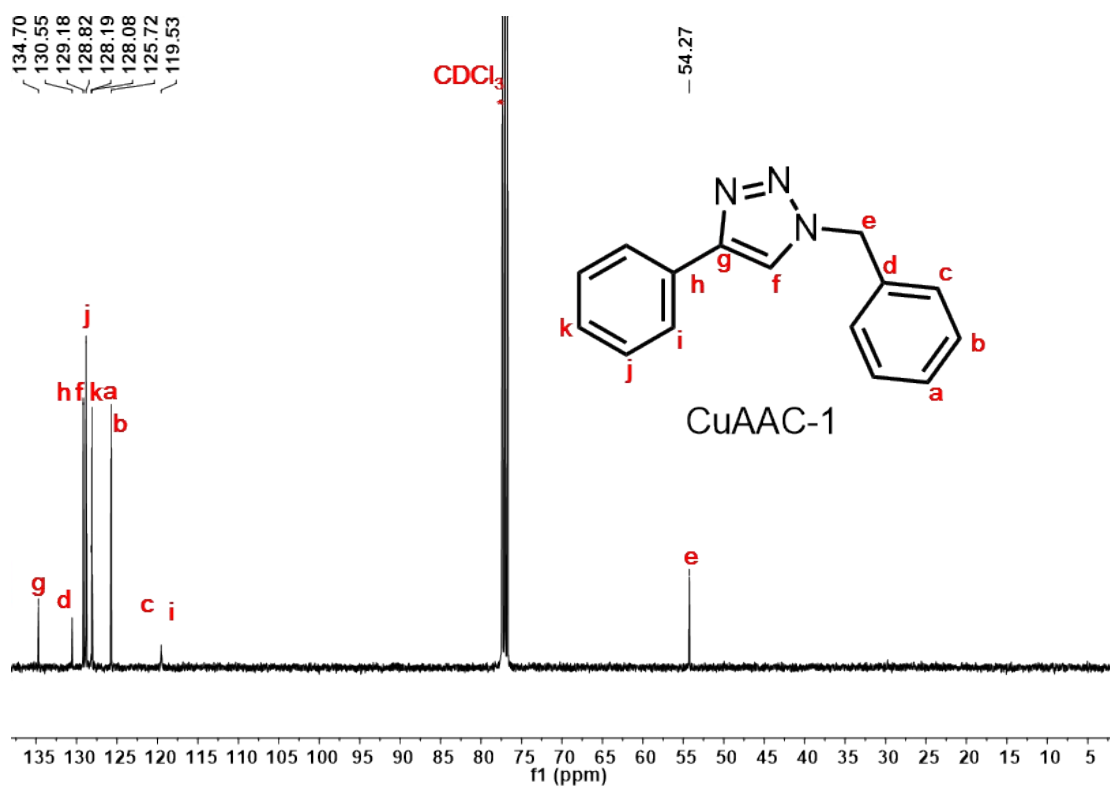
[b] The yeild of product isolated was calculated through crystallization, NMR and MS analysis.



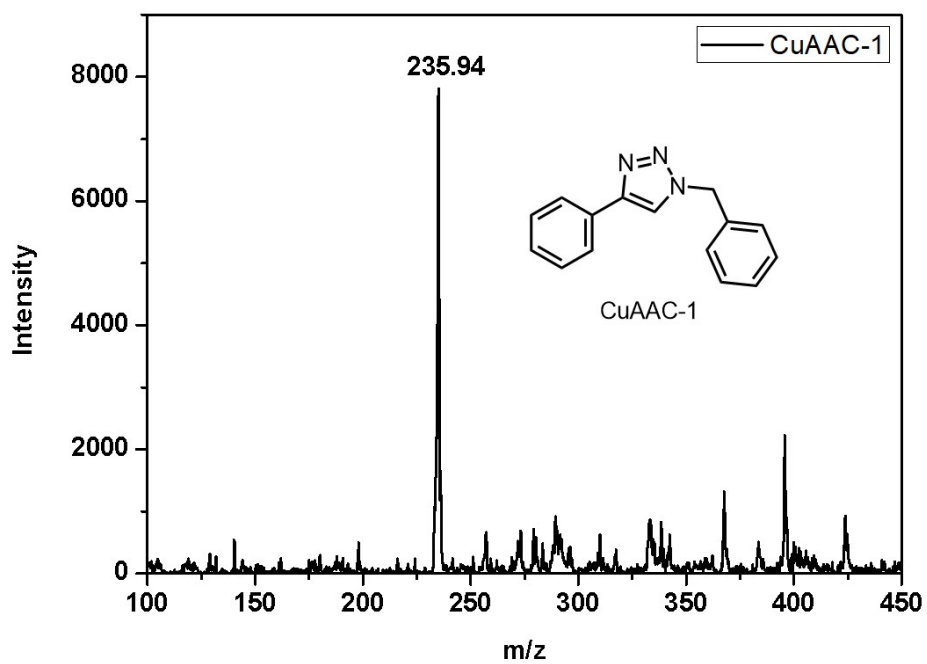
**Figure S116.** <sup>1</sup>H NMR (400 MHz, CDCl<sub>3</sub>) for triazole-based compound **3a** (1-benzyl-4-phenyl-1H-



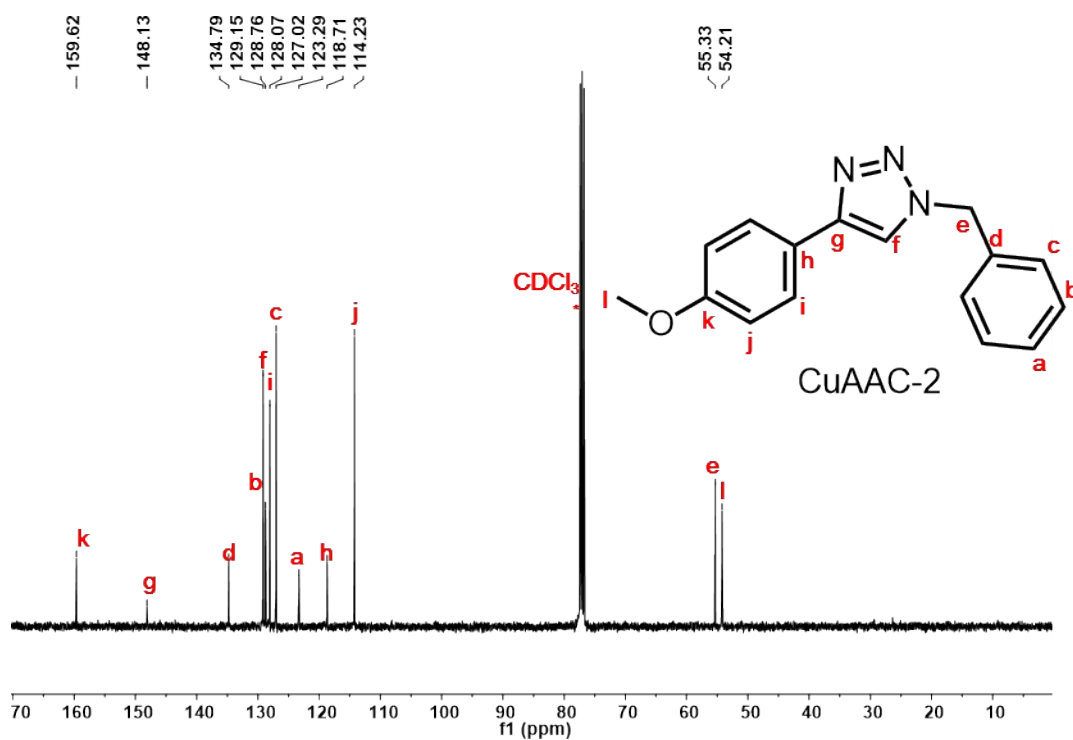
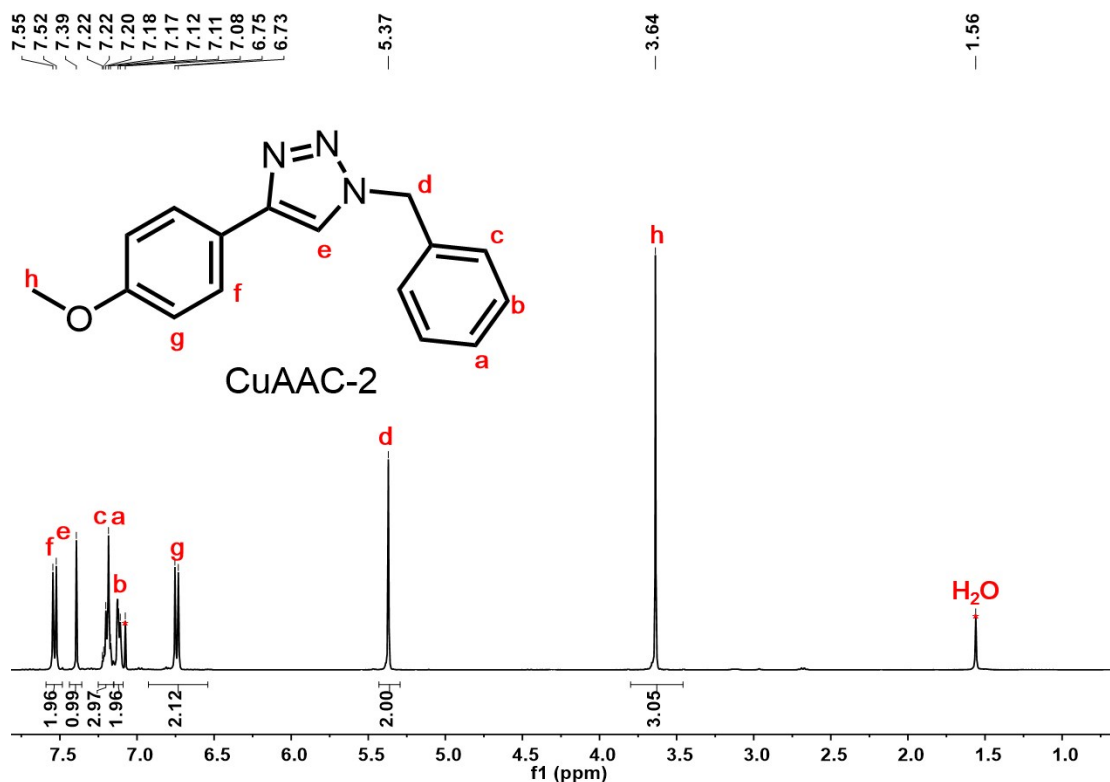
1,2,3-triazole):  $\delta = 7.84 - 7.76$  (m, 2H), 7.67 (s, 1H), 7.44 - 7.36 (m, 5H), 7.36 - 7.28 (m, 3H), 5.58 (s, 2H).



**Figure S117.**  $^{13}\text{C}$  NMR (100 MHz,  $\text{CDCl}_3$ ) for triazole-based compound **3a** (CuAAC-1, 1-benzyl-4-phenyl-1H-1,2,3-triazole):  $\delta = 129.18$ , 128.82, 128.19, 128.08, 125.72, 119.53, 54.27.

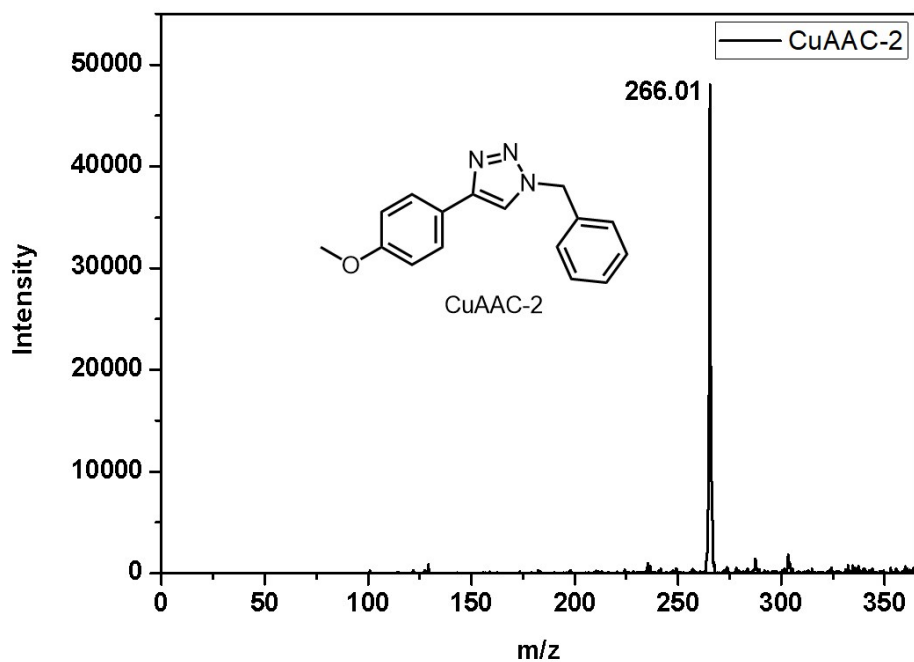


**Figure S118.** ESI-MS spectrum of triazole-based compound **3a** (1-benzyl-4-phenyl-1H-1,2,3-triazole). ESI-MS ( $\text{CH}_2\text{Cl}_2$ , m/z):  $[\text{CuAAC-1}+\text{H}]^+$ , calcd for 236.11, found, 235.94.

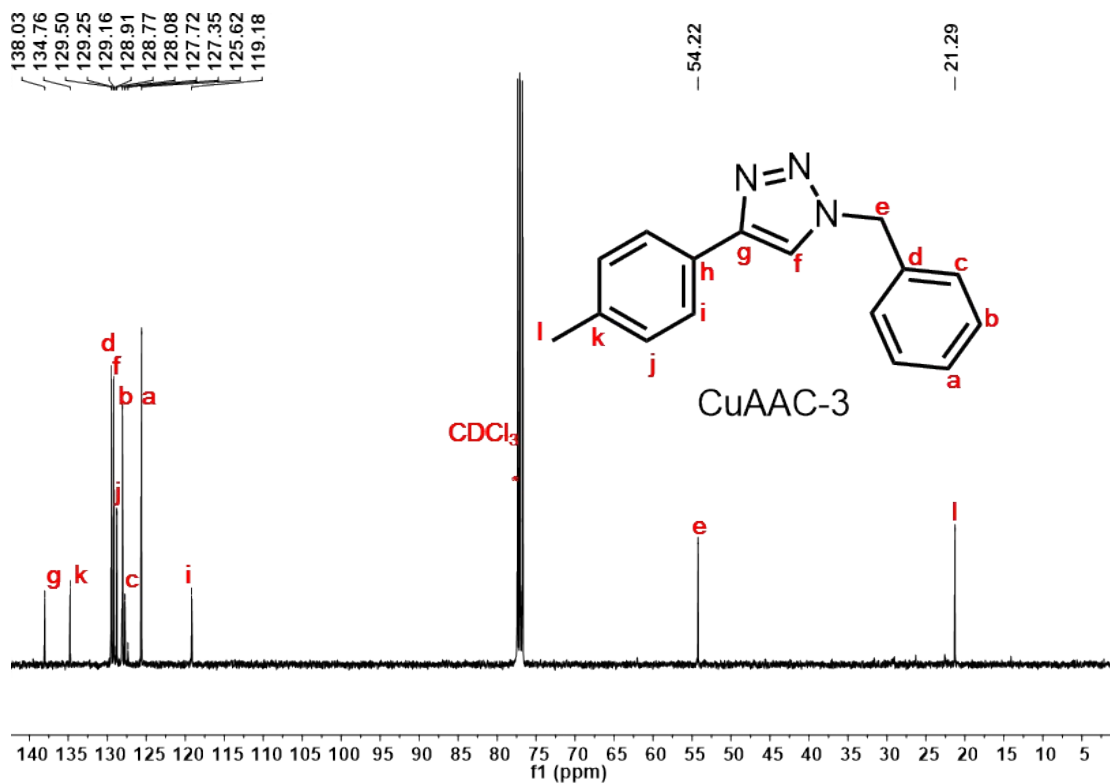
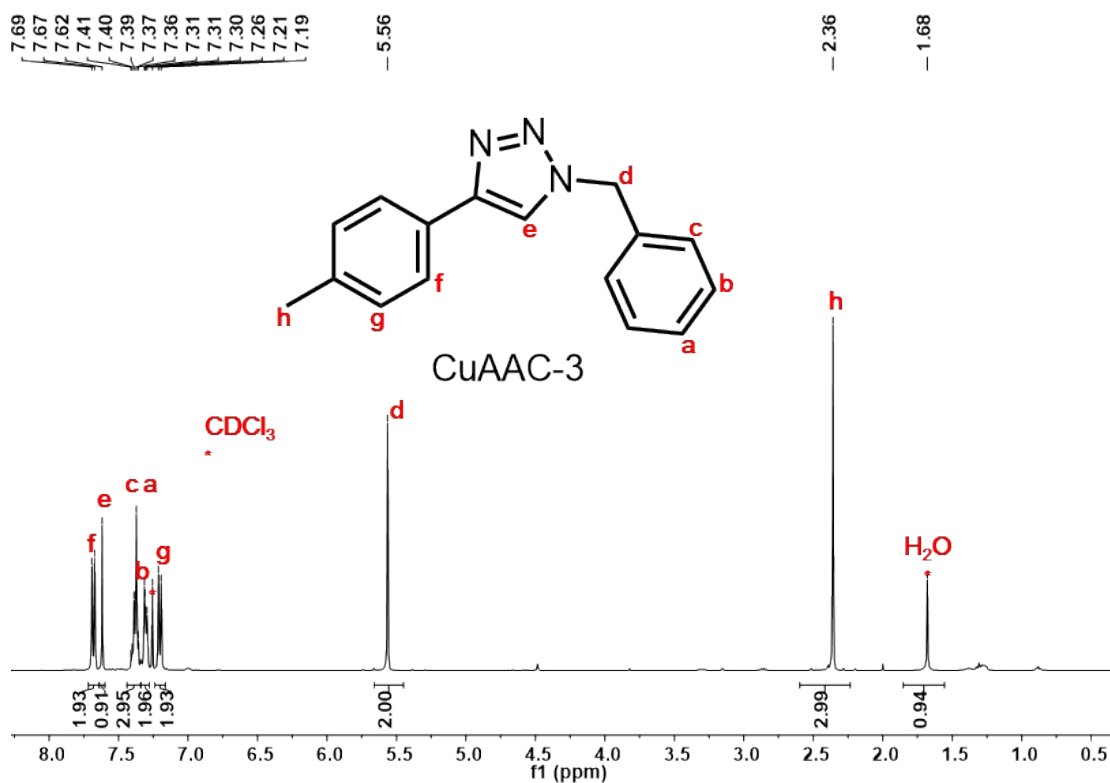


**Figure S120.**  $^{13}\text{C}$  NMR (100 MHz,  $\text{CDCl}_3$ ) for triazole-based compound **3b** (benzyl-4-(4-methoxyphenyl)-1H-1,2,3-triazole):  $\delta$  = 159.62, 148.13, 129.15, 128.76, 128.07, 127.02, 123.29

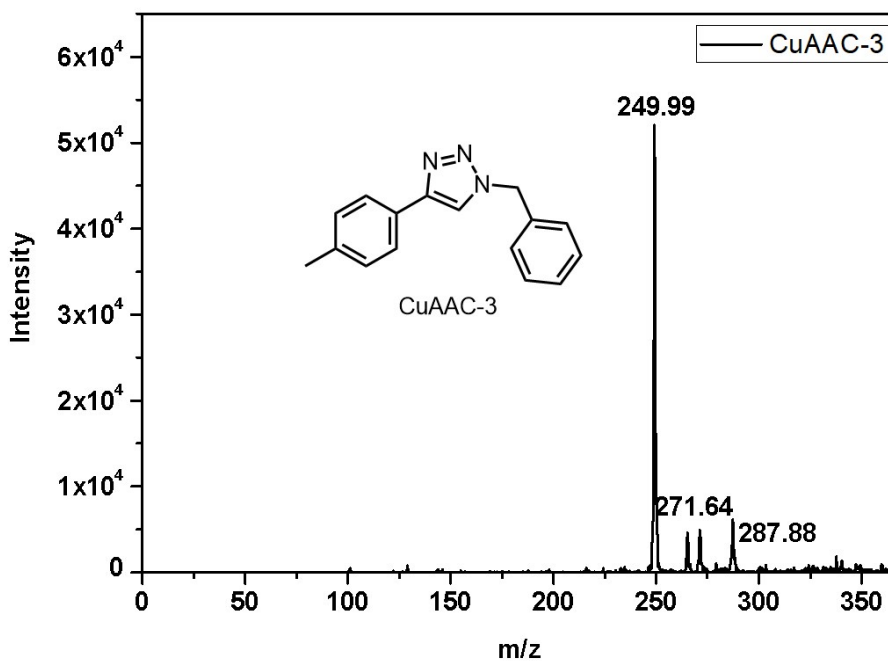
, 118.71 , 114.23 , 55.33 , 54.21.



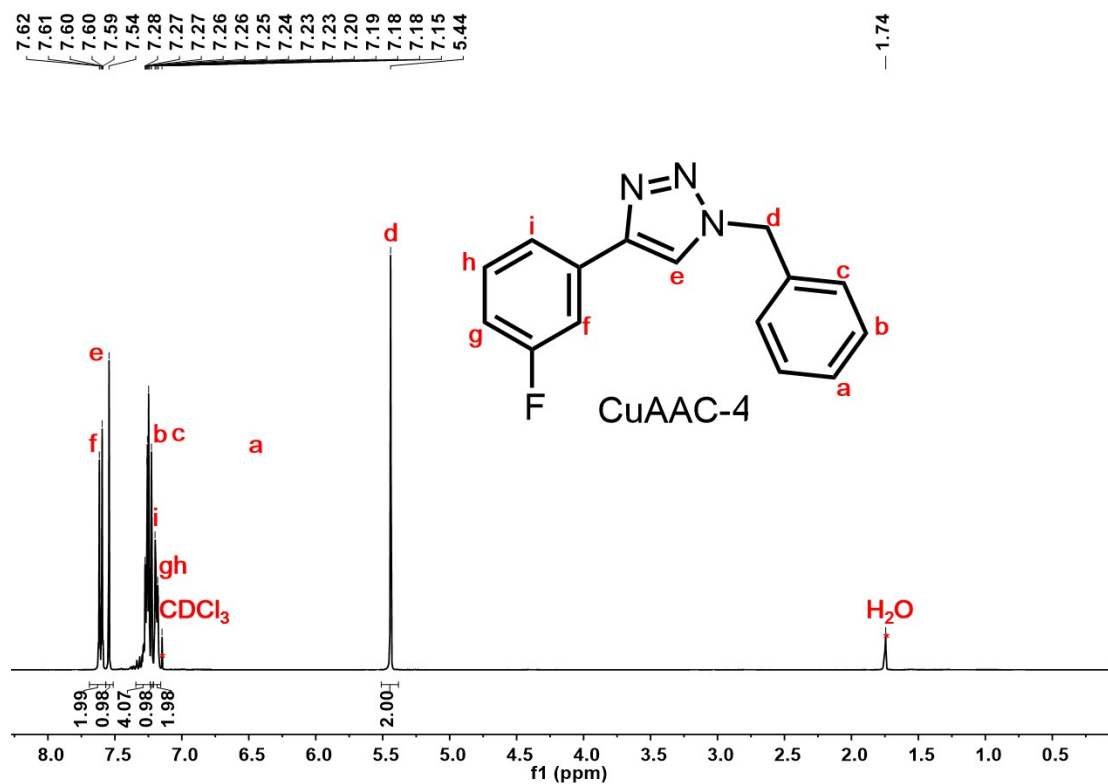
**Figure S121.** ESI-MS spectrum of triazole-based compound **3b** (benzyl-4-(4-methoxyphenyl)-1H-1,2,3-triazole). ESI-MS ( $\text{CH}_2\text{Cl}_2$ , m/z):  $[\text{CuAAC-2}+\text{H}]^+$ , calcd for 266.12, found,266.01.



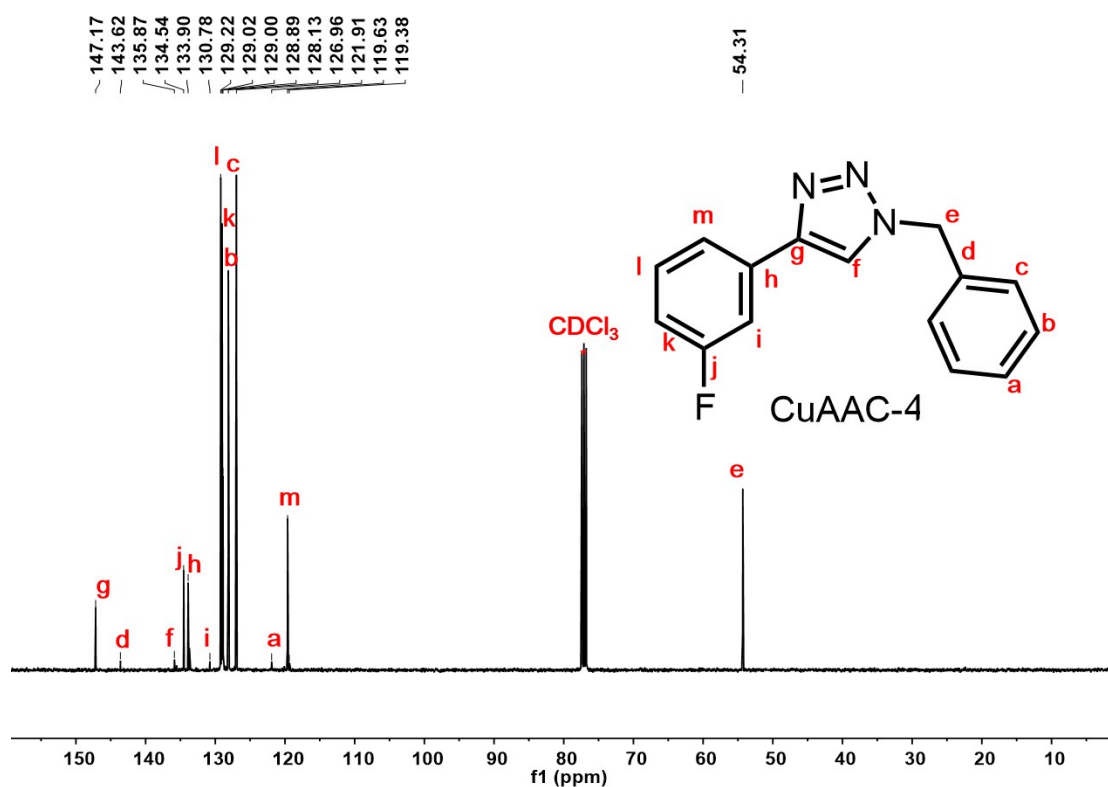
**Figure S123.**  $^{13}\text{C}$  NMR (100 MHz,  $\text{CDCl}_3$ ) for triazole-based compound **3c** (1-benzyl-4-p-tolyl-1H-1,2,3-triazole):  $\delta=148.33$  ,  $138.03$  ,  $134.76$  ,  $129.50$  ,  $129.16$  ,  $128.77$  ,  $128.08$  ,  $127.72$  ,  $125.62$  ,  $119.18$  ,  $54.22$  ,  $21.29$  .



**Figure S124.** ESI-MS spectrum of triazole-based compound **3c** (1-benzyl-4-p-tolyl-1H-1,2,3-triazole). ESI-MS ( $\text{CH}_2\text{Cl}_2$ ,  $m/z$ ): [**CuAAC-3**+H] $^+$ , calcd for 250.13, found,249.99; [**CuAAC-3**+Na] $^+$ , calcd for 272.10, found,271.64; [**CuAAC-3**+K] $^+$ , calcd for 288.22, found,287.88.

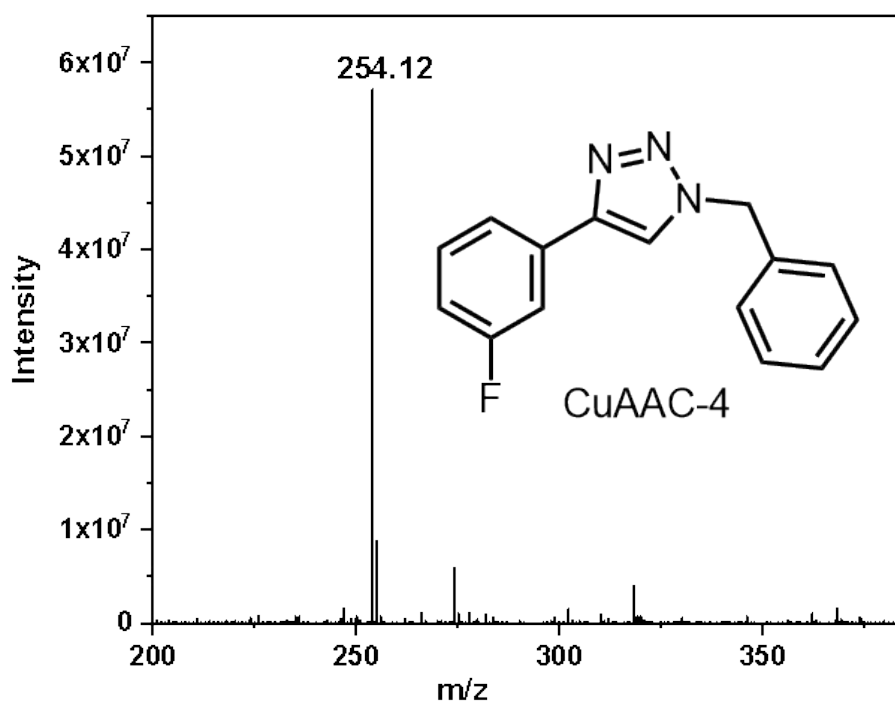


**Figure S125.** <sup>1</sup>H NMR (400 MHz, CDCl<sub>3</sub>) for triazole-based compound **3d** (CuAAC-4, 1-benzyl-4-(3-fluorophenyl)-1H-1,2,3-triazole): δ = 7.54 (s, 1H), 7.49 – 7.35 (m, 2H), 7.33 – 7.16 (m, 6H), 6.87 (m, 1H), 5.45 (s, 2H).



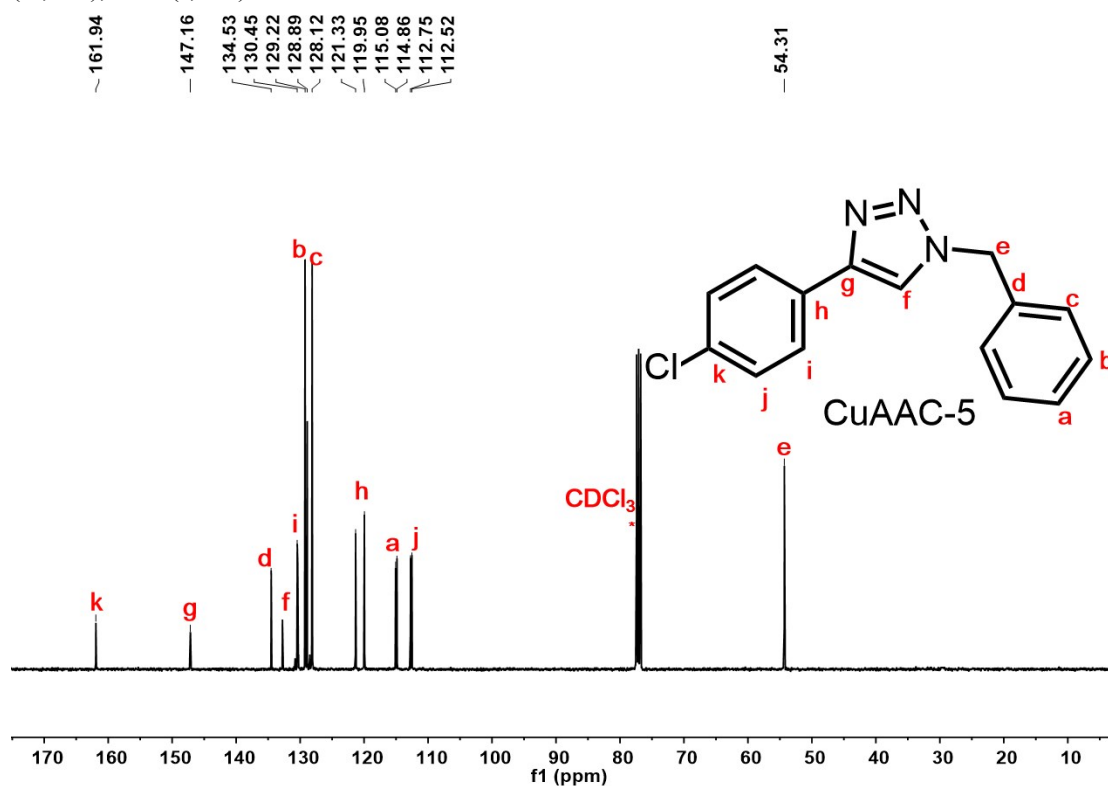
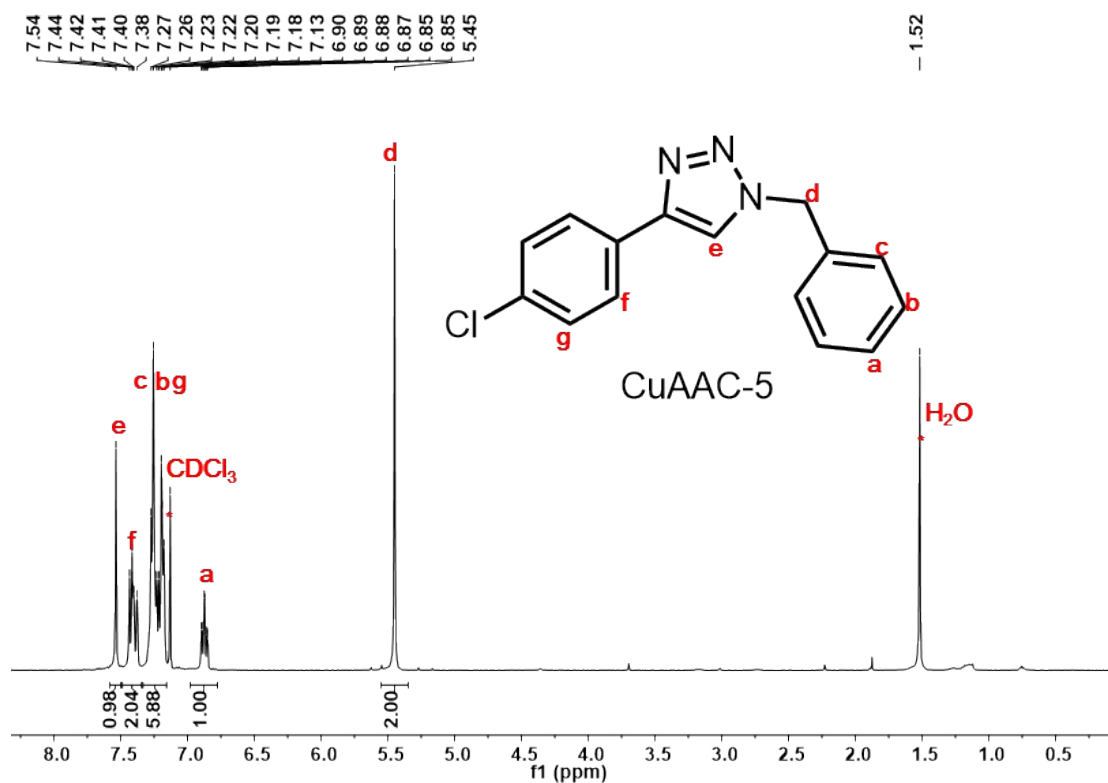
**Figure S126.** <sup>13</sup>C NMR (100 MHz, CDCl<sub>3</sub>) for triazole-based compound **3d** (1-benzyl-4-(3-

fluorophenyl)-1H-1,2,3-triazole):  $\delta$  =134.53 , 130.45 , 129.22 , 128.89 , 128.12 , 121.33 , 119.95 , 115.08 , 114.86 , 112.75 , 112.52, 54.31 .



**Figure S127.** MALDI-TOF-MS spectrum of triazole-based compound **3d** (1-benzyl-4-(3-fluorophenyl)-1H-1,2,3-triazole). MALDI-TOF-MS (CH<sub>2</sub>Cl<sub>2</sub>, m/z): [CuAAC-4+H]<sup>+</sup>, calcd for 254.10, found, 254.12 .





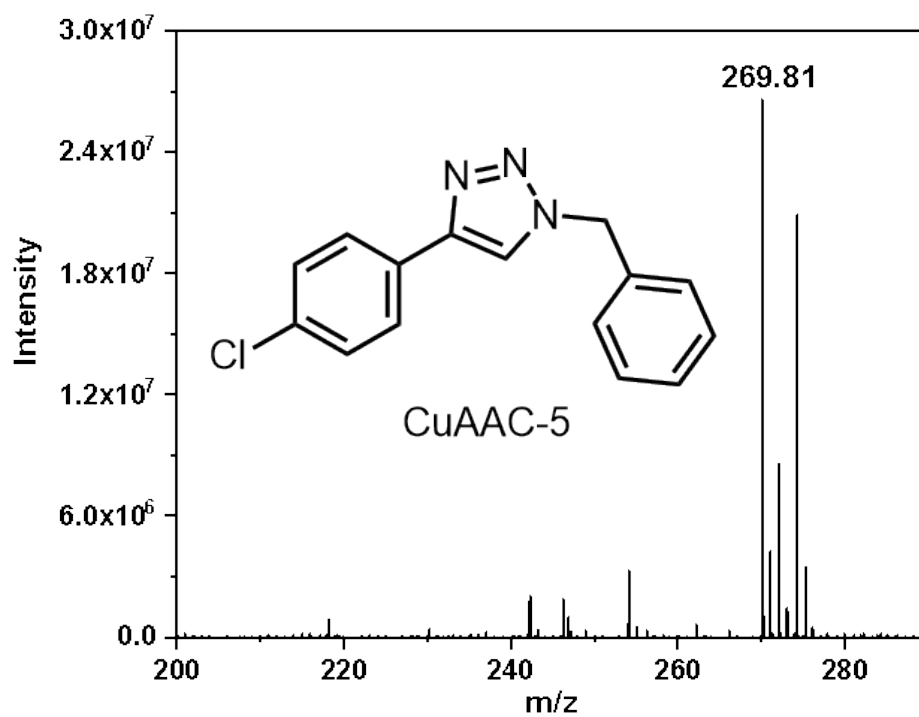


**Figure S130.** MALDI-TOF-MS spectrum of triazole-based compound **3e** (1-benzyl-4-(4-chlorophenyl)-1H-1,2,3-triazole). MALDI-TOF-MS (CH<sub>2</sub>Cl<sub>2</sub>, m/z): [CuAAC-5+H]<sup>+</sup>, calcd for 270.07, found, 269.81.

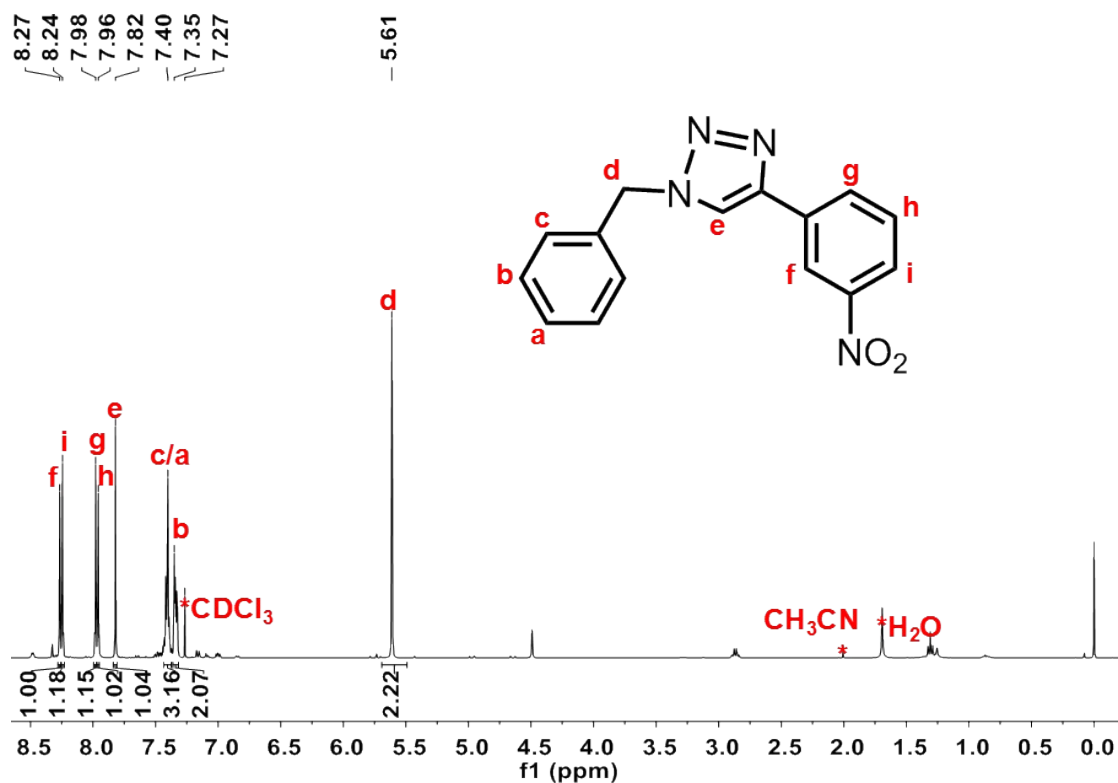


**Figure S131.** <sup>1</sup>H NMR (400 MHz, CDCl<sub>3</sub>) for triazole-based compound **3f** (1-benzyl-4-(3-nitrophenyl)-1H-1,2,3-triazole): δ 8.27 (s, 1H), 8.24 (s, 1H), 7.98 (s, 1H), 7.96 (s, 1H), 7.82 (s, 1H), 7.40 (s, 3H), 7.35 (s, 2H), 5.61 (s, 2H).

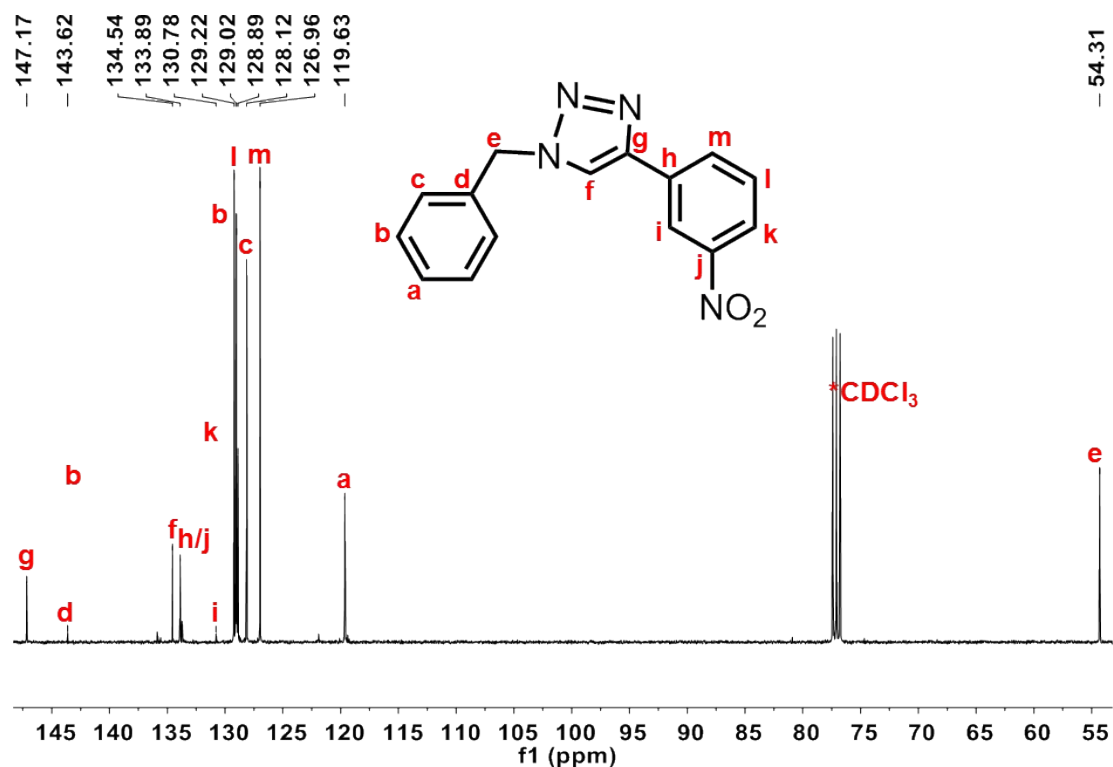


**Figure S132.** <sup>13</sup>C NMR (100 MHz, CDCl<sub>3</sub>) for triazole-based compound **3f** (1-benzyl-4-(3-nitrophenyl)-1H-1,2,3-triazole): δ = <sup>13</sup>C NMR (101 MHz, Chloroform-d) δ 147.17, 134.54, 133.89

, 129.22 , 129.02 , 128.89 , 128.12 , 126.96 , 119.63 , 54.31 .

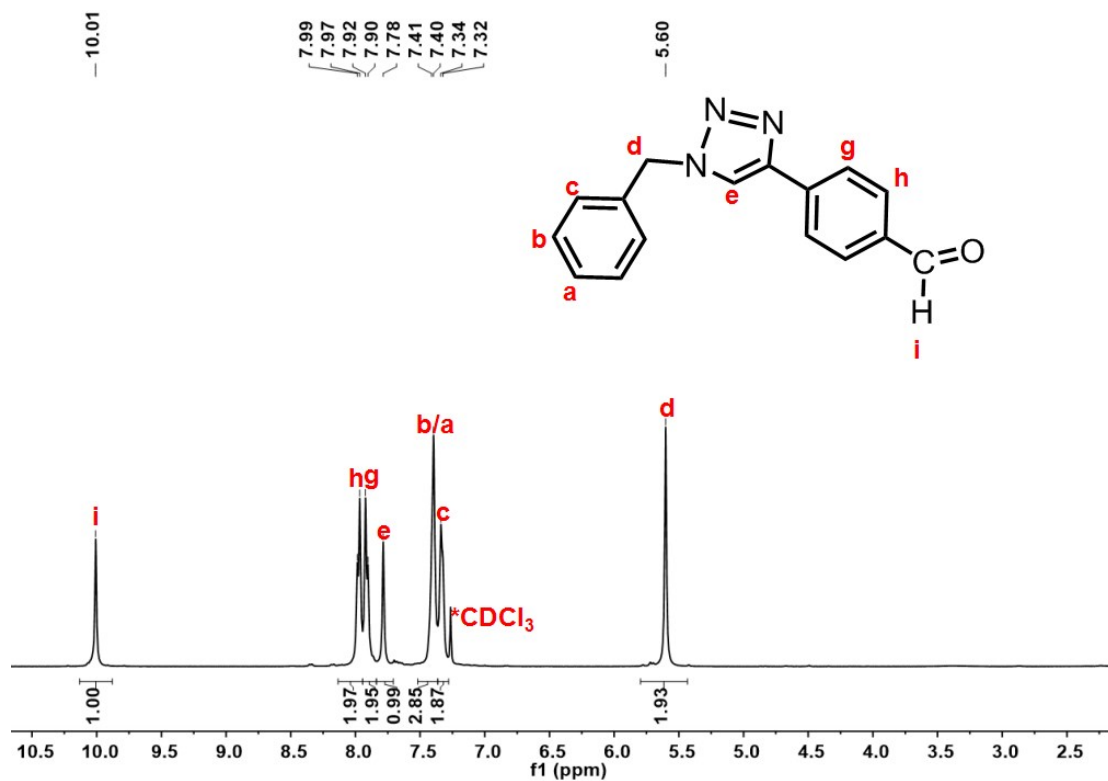


**Figure S133.**  $^1\text{H}$  NMR (400 MHz,  $\text{CDCl}_3$ ) for compound **3g** (1-benzyl-4-(3-chlorophenyl)-1H-1,2,3-triazole):  $\delta$  = 10.01 (s, 1H), 7.98 (d,  $J$  = 7.9 Hz, 2H), 7.91 (d,  $J$  = 8.0 Hz, 2H), 7.78 (s, 1H), 7.40 (d,  $J$  = 6.5 Hz, 3H), 7.33 (d,  $J$  = 6.7 Hz, 2H), 5.60 (s, 2H).

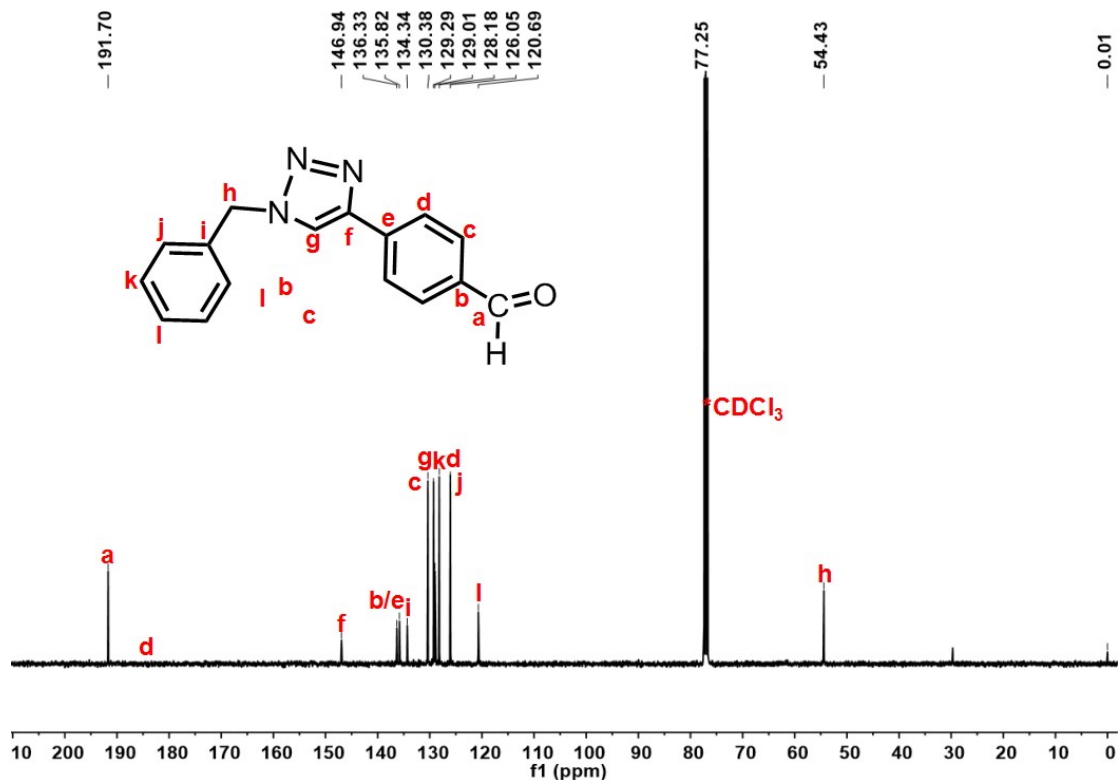


**Figure S134.**  $^{13}\text{C}$  NMR (100 MHz,  $\text{CDCl}_3$ ) for triazole-based compound **3g** (4-(1-benzyl-1H-1,2,3-triazol-4-yl)benzaldehyde) :  $\delta$  = 191.70, 146.94, 136.33, 135.82, 134.34, 130.38, 129.29, 129.01,

128.18, 126.05, 120.69, 54.43.

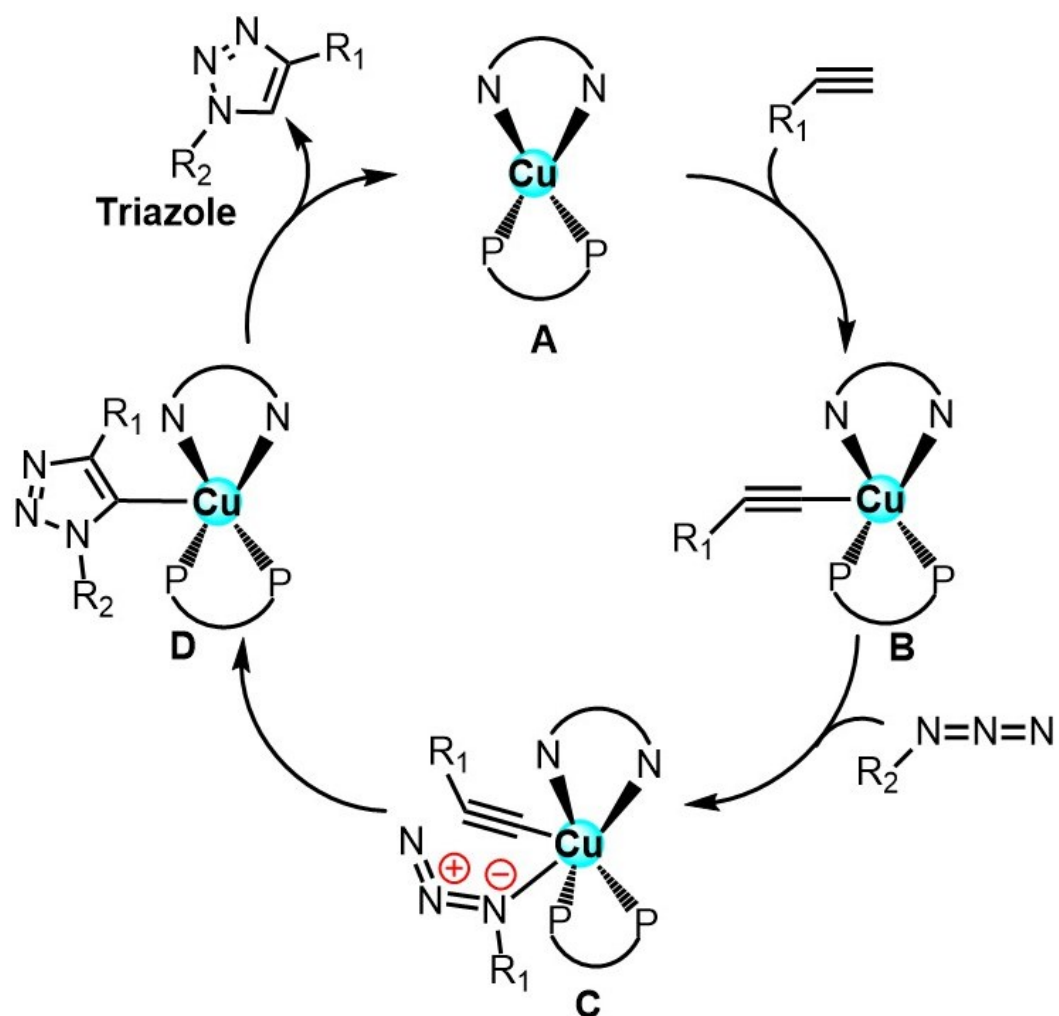


**Figure S135.** Proposed mechanistic pathways of CuAAC reaction catalyzed by heteroleptic complexes C1-C10.